

## **Distribution Agreement**

In presenting this thesis or dissertation as a partial fulfillment of the requirements for an advanced degree from Emory University, I hereby grant to Emory University and its agents the non-exclusive license to archive, make accessible, and display my thesis or dissertation in whole or in part in all forms of media, not or hereafter known, including display on the world wide web. I understand that I may select some access restrictions as part of the online submission of this thesis or dissertation. I retain all ownership rights to the copyright of the thesis or dissertation. I also retain the right to use in future works (such as articles or books) all or part of this thesis or dissertation.

Signature:

---

Sarah E. Michalets

---

Date

Impact of Respiratory Tract Resident Memory CD8 T Cells on Viral Transmission

By

Sarah E. Michalets  
Doctor of Philosophy

Graduate Division of Biological and Biomedical Sciences  
Immunology and Molecular Pathogenesis

---

Jacob E. Kohlmeier, Ph.D.  
Advisor

---

Haydn Kissick, Ph.D.  
Committee Member

---

Christopher LaRock, Ph.D.  
Committee Member

---

Anice Lowen, Ph.D.  
Committee Member

---

Christopher Scharer, Ph.D.  
Committee Member

Accepted

---

Kimberly Jacob Arriola, Ph.D., MPH  
Dean of the James T. Laney School of Graduate Studies

---

Date

Impact of Respiratory Tract Resident Memory CD8 T Cells on Viral Transmission

By

Sarah E. Michalets  
B.S., North Carolina State University, 2020

Advisor: Jacob E. Kohlmeier, Ph.D.

An abstract of  
A dissertation submitted to the Faculty of the  
Jame T. Laney School of Graduate Studies of Emory University  
in partial fulfillment of the requirements for the degree of  
Doctor of Philosophy  
in Graduate Division of Biological and Biomedical Science  
Immunology and Molecular Pathogenesis  
2024

## **Abstract**

### **Impact of Respiratory Tract Resident Memory CD8 T Cells on Viral Transmission**

By Sarah E. Michalets

Respiratory virus-specific T cells recognize internal, conserved viral epitopes, enabling protection against drifted and antigenically novel viral variants. One memory T cell subset, tissue resident memory T cells (TRM), remain within nonlymphoid tissues where they persist, poised to rapidly initiate effector functions upon exposure to their cognate antigen. Numerous studies have demonstrated that respiratory tract CD8 TRM can substantially reduce viral burdens upon heterosubtypic influenza virus infection and prevent immunopathology. However, these studies often rely upon intranasal challenge models where large viral doses are deposited uniformly throughout the respiratory tract. In nature, respiratory virus infection occurs by transmission; small numbers of virions deposit along the respiratory mucosa and replicate to form an initial foci of infection. Prior to the work presented in this thesis, it was unknown whether respiratory tract CD8 TRM were capable of preventing infection caused by natural respiratory virus transmission.

This thesis defines and characterizes the ability of respiratory tract CD8 TRM to protect against natural respiratory virus transmission. Using Sendai virus as a model of respiratory virus transmission, we show that antigen-specific CD8 TRM not only significantly reduce viral burdens upon breakthrough infection but can prevent detectable infection entirely, in correlation with the quantity of CD8 TRM in the respiratory tract. This protection elicited by CD8 TRM proved long-lasting for at least six months upon intranasal immunization with a recombinant adenoviral vector vaccine. Furthermore, we evaluated the CD8 TRM effector mechanisms responsible for preventing viral transmission and learned that IFN- $\gamma$  signaling was essential. Rapid IFN- $\gamma$  secretion caused nasal cavity epithelial cells to adopt antiviral transcriptional states, increase antigen presentation, and secrete lymphocyte attractant chemokines. We assessed the respiratory tract localization of the CD8 TRM response to viral transmission and noted that TRM in the upper respiratory tract, but not lower respiratory tract, become activated, proliferate, and establish antiviral effector transcriptional programs in response to transmitted virus. Finally, we demonstrated that nasal cavity CD8 TRM alone are sufficient to protect against respiratory virus transmission.

The findings presented in this thesis provide critical insights for vaccine design aimed to prevent viral transmission and spread among populations.

Impact of Respiratory Tract Resident Memory CD8 T Cells on Viral Transmission

By

Sarah E. Michalets  
B.S., North Carolina State University, 2020

Advisor: Jacob E. Kohlmeier, Ph.D.

A dissertation submitted to the Faculty of the  
Jame T. Laney School of Graduate Studies of Emory University  
in partial fulfillment of the requirements for the degree of  
Doctor of Philosophy  
in Graduate Division of Biological and Biomedical Science  
Immunology and Molecular Pathogenesis  
2024

## Table of Contents

<b>CHAPTER I: Introduction .....</b>	<b>1</b>
<b>References .....</b>	<b>23</b>
<b>CHAPTER II: Tissue resident memory CD8 T cells provide durable protection against respiratory virus transmission through IFN-<math>\gamma</math> .....</b>	<b>61</b>
<b>Abstract .....</b>	<b>62</b>
<b>Introduction .....</b>	<b>63</b>
<b>Materials and Methods .....</b>	<b>65</b>
<b>Results .....</b>	<b>71</b>
<b>Discussion .....</b>	<b>77</b>
<b>Main Figures .....</b>	<b>81</b>
Figure 1 .....	81
Figure 2 .....	83
Figure 3 .....	85
<b>Supplementary Information .....</b>	<b>88</b>
Extended Data Figure 1 .....	88
Extended Data Figure 2 .....	90
Extended Data Figure 3 .....	91
Extended Data Figure 4 .....	93
Extended Data Figure 5 .....	94
Extended Data Figure 6 .....	96
Extended Data Figure 7 .....	97
Extended Data Figure 8 .....	99
<b>Acknowledgements &amp; Author Contributions .....</b>	<b>100</b>
<b>References .....</b>	<b>101</b>
<b>CHAPTER III: Vaccine-induced upper respiratory tract resident memory CD8 T cells are sufficient to inhibit productive infection after viral transmission.....</b>	<b>111</b>
<b>Abstract .....</b>	<b>112</b>
<b>Introduction .....</b>	<b>113</b>
<b>Materials and Methods .....</b>	<b>115</b>
<b>Results .....</b>	<b>121</b>

<b>Discussion</b> .....	1288
<b>Main Figures</b> .....	132
Figure 1 .....	132
Figure 2 .....	134
Figure 3 .....	136
Figure 4 .....	137
<b>Supplementary Information</b> .....	139
Extended Data Figure 1 .....	139
Extended Data Figure 2 .....	141
Extended Data Figure 3 .....	142
<b>Acknowledgements &amp; Author Contributions</b> .....	143
<b>References</b> .....	144
<b>CHAPTER IV: Discussion</b> .....	<b>156</b>
<b>References</b> .....	168

## **CHAPTER I: Introduction**

### ***Global Burden of Respiratory Viruses***

Millions of individuals globally contract respiratory virus infections annually, including influenza viruses, coronaviruses such as SARS-CoV-2, rhinoviruses, adenoviruses, parainfluenza virus, respiratory syncytial virus (RSV), and others. At the time of writing, the Centers for Disease Control and Prevention reports approximately 1.2 million deaths in the United States since the initiation of the SARS-CoV-2 global pandemic in January 2020<sup>1</sup>. Between the years 2010 and 2023, influenza cases in the United States have ranged from 9 to 41 million with up to 700,000 hospitalization and 50,000 deaths annually<sup>2</sup>. Some respiratory viruses, such as RSV and parainfluenza virus, disproportionately impact children, the elderly, and other immune compromised populations. RSV causes around 4 million pediatric cases and 100,000 hospitalizations each year, while around 3 million infections and 29,000 hospitalizations can be attributed to parainfluenza virus<sup>3</sup>. Symptoms for respiratory virus infections can range from sore throat, runny nose, cough, headache, fever, and occasionally progress to bronchitis or pneumonia which may require hospitalization in severe cases<sup>3,4</sup>. Although vaccines are available for influenza and SARS-CoV-2, they vary in effectiveness due to seasonal differences in circulating vaccine strains and frequently require updating to match new strains. Furthermore, traditional vaccine formats often fail to provide immune protection against potentially pandemic viruses and place the population at risk for future outbreaks. As evidenced by the SARS-CoV-2 pandemic, respiratory viruses can cause major burdens not only on health care infrastructure, but on businesses, schools, and the economy due to loss of consumer revenue, missed time at work, and demoralized attitudes. There is a significant need for more effective vaccines against respiratory viruses that can provide

cross protection against virus strains and limit viral transmission throughout populations to help mitigate the impact of novel, potentially pandemic strains.

### ***Routes of Respiratory Virus Transmission***

An infected individual can spread a respiratory virus to another individual through contact with respiratory secretions. There are four primary modes through which respiratory virus transmission occurs, including direct contact, indirect contact, droplet, and aerosol transmission<sup>5</sup>.<sup>6</sup> Transmission by direct contact occurs when an infected individual has physical contact with a susceptible individual, predominately through contact with unwashed hands and subsequent touching of mucosal membranes. Indirect contact transmission, also referred to as fomite transmission, occurs when an infected individual touches a surface, such as a cell phone, door handle, or light switch and leaves infectious virions behind. A susceptible individual then touches that surface, comes in contact with the viral particles, and touches their own mucous membranes to initiate an infection<sup>7, 8</sup>. These two modes of transmission are often targeted in public health campaigns to reduce viral transmission, with suggested measures including decontamination of surfaces and proper hand washing hygiene. In contrast to forms of contact transmission, aerosol and droplet transmission involve the spread of viral particles through the air. Although there is some debate about the molecular size determination that differentiates a droplet from an aerosol, many researchers use a 5  $\mu\text{m}$  size cut off, where particles larger than 5  $\mu\text{m}$  are considered droplets and those smaller are considered aerosols<sup>5, 9, 10</sup>. Larger sized droplet particles are typically generated by coughing or sneezing, while aerosols can originate from exhaled breath. Some studies have shown that respiratory viruses can also become aerosolized after flushing toilets with infected feces<sup>11, 12</sup>. Because of droplets' larger size, they tend to stay suspended in air for briefer periods of

time, less than 15 minutes, and remain localized near their site of expulsion<sup>5, 13-15</sup>. On the other hand, aerosols can be found over 1 meter away from their generation and can remain in the air for long periods of time. Another important difference between aerosol and droplet transmission is their location of deposition along the respiratory tract of susceptible hosts. Aerosol's smaller size allows them to penetrate deeper within the respiratory tract, pass the nasal turbinates, and settle within alveolar and lung tissue<sup>5, 6, 10, 13, 16, 17</sup>. It is well established that when respiratory viruses infect lung tissue, they can cause significant immunopathology and often lead to pneumonia, which may necessitate hospitalization. Contrastingly, droplets deposit within the upper respiratory tract and nasal cavity where they may more easily be cleared by mucus production<sup>5, 6, 10, 13, 15, 17, 18</sup>. Thus, the mode of transmission can have significant ramifications on the location, duration, and symptoms of subsequent infections.

### ***Models Used to Study Respiratory Virus Transmission***

To study modes and immunological determinants of transmission, it is critical to have clear, consistent, and reproducible animal models. The most common animals used in transmission studies are mice, ferrets, guinea pigs, hamsters, rabbits, and non-human primates. Different animals are more suitable for modeling pathogenesis and transmission of different viruses. For example, ferrets have been shown to support direct contact transmission of SARS-CoV-2, but do not show obvious signs of disease or pathology<sup>19</sup>. In contrast, Syrian golden hamsters show respiratory distress and disease upon intranasal SARS-CoV-2 infection and more effectively model droplet or aerosol transmission<sup>20</sup>. Due to their more effective recapitulation of COVID-19 disease, the majority of SARS-CoV-2 studies utilize the Syrian golden hamster as their model organism<sup>21</sup>. To model influenza induced respiratory disease, mice are frequently used due to their relatively

low cost, ease of breeding, and the availability of transgenic mouse strains and immunological reagents. Due to differences in sialic acid linkages frequently found in the airways of human and mice, most human influenza A isolates do not cause disease upon inoculation in mice without previous host adaptation through serial passaging<sup>22, 23</sup>. A few exceptions to this exist, as the 1918 pandemic flu strain, some H5N1, and H7 influenza strains do not need lab adaptation to cause symptoms of disease and replicate within mice<sup>24</sup>. Most influenza virus studies are conducted using lab adapted PR8 (H1N1) or X31 (H3N2) influenza strains which cause most inbred mouse strains to exhibit signs of clinical disease such as weight loss, lethargy, lung lesions, pulmonary edema, and in some cases, death<sup>24</sup>. Furthermore, influenza disease in mice is contingent upon deactivation or lack of an *Mx1* gene allele. The Mx1 protein has been shown to be induced after interferon signaling (an interferon-stimulated gene) and encodes an antiviral protein that is a potent inhibitor of influenza virus replication<sup>25</sup>. In wild mice or Mx1 competent mice, infection with a highly pathogenic H5N1 influenza virus resulted in minimal weight loss or viral titers in the lungs when compared to Mx1 deficient mice<sup>26</sup>.

Although mice are useful to model influenza virus disease upon intranasal inoculation, they fail to support efficient transmission among cage mates and produce consistent results between research groups and facilities. Historical studies on influenza transmission from the 1960s demonstrated that influenza transmitted with varying efficiencies depending on subtype, with PR8 influenza in particular only transmitting to 5% of contacts<sup>27, 28</sup>. Follow up studies in the 2000s were unable to reproduce these findings, with neither H1N1, H3N2, H5N1, or the 1918 pandemic flu strain transmitting to cage mates, as evidenced by a lack of seroconversion<sup>29</sup>. Another study demonstrated that H1N1 influenza virus was unable to transmit between mice, while a few H3N2 strains, namely A/Udorn, were able to transmit by contact transmission only, albeit in varying

efficiencies<sup>30</sup>. Contrastingly, a different study found that A/Udorn was able to transmit between mice by contact and aerosol routes<sup>31</sup>. Infant mice may serve as a model for x31 H3N2 influenza virus transmission due to their immunocompromised state and difficulty to control viral replication, but do not support H1N1 influenza transmission<sup>32</sup>. It is possible that the discrepancies in results regarding H3N2 influenza transmission between research groups could be due to differences in infection doses, age of mice, time of contact between index mice and susceptible cage mates, and animal facility housing conditions, as relative humidity and temperature significantly impact influenza transmission<sup>33</sup>. Ultimately, mice are poor models of influenza virus transmission because they do not support H1N1 influenza virus transmission and results on H3N2 transmission have proved inconsistent and not reproducible.

Ferrets and guinea pigs are the most popular models used to study influenza virus transmission, as they readily support transmission of all subtypes and recapitulate clinical symptoms of disease. Upon intranasal inoculation with influenza virus, ferrets display symptoms resembling those seen during human infection such as fever, nasal discharge, lethargy, and sneezing<sup>24</sup>. Furthermore, infection in ferrets is predominately limited to the upper respiratory tract, as in humans, while lower respiratory tract infection is seen in the majority of mouse influenza infections<sup>34</sup>. Additionally, human influenza virus isolates do not require lab adaptation to infect ferrets<sup>24</sup>. Dating back to studies in the 1930s, ferrets have been used as the main animal model to study influenza virus transmission using PR8 H1N1 influenza<sup>35</sup>. In years since, ferrets have widely been used to study mechanisms of transmission<sup>14, 36, 37</sup>, influenza virology and reassortment in transmission<sup>38, 39</sup>, pandemic potential of novel influenza viruses<sup>40-42</sup>, and assess the effect of antiviral drugs and vaccines on transmission<sup>43-46</sup>. Similar to ferrets, guinea pigs can support viral replication of human influenza virus isolates without lab adaptation, exhibit upper respiratory tract

infections, and support influenza transmission by airborne and contact modes<sup>24, 29</sup>. However, transmission efficiencies varied between strains tested and were lower than those seen in ferret studies<sup>24</sup>. Additionally, guinea pigs do not display clinical symptoms of disease similar to those seen in mice, ferrets, or humans<sup>47, 48</sup>. Because of this, guinea pigs are not widely used to assess antiviral drugs or vaccine candidates. Although guinea pigs and ferrets are useful models of influenza virus transmission, experiments are limited to lower group sizes due to cost and housing concerns, and immunological tools such as antibodies, tetramers, and genetic engineering are rudimentary.

Human parainfluenza viruses are capable of infecting many species such as ferrets, guinea pigs, cotton rats, and hamsters, but do not cause signs of disease or pathology<sup>49-53</sup>. Furthermore, mouse species are not permissive to human parainfluenza virus infections<sup>49</sup>. Because of this, Sendai virus, a murine parainfluenza virus, is frequently used to model parainfluenza infection in mice. Sendai virus and human parainfluenza virus exhibit high levels of sequence homology with 86% amino acid sequence overlap in the large protein, 72% with the HN protein, 61% with the matrix protein, and 83% with the nucleoprotein<sup>54-57</sup>. Additionally, Sendai virus and human parainfluenza virus infection generate cross-reactive CD8 T cells and exhibit similar replication kinetics<sup>58, 59</sup>. Sendai virus infection in non-human primates generated long-lived neutralizing antibody responses that constituted protection against a human parainfluenza virus challenge<sup>60</sup>. Unlike mouse-adapted influenza viruses, Sendai virus transmits naturally between mice. In order to study the kinetics, effect of inoculum dose, and tissue tropism of Sendai virus transmission, Burke et. al. generated a luciferase expressing Sendai virus, which enabled tracking of viral replication and transmission efficiency through bioluminescent *in vivo* imaging<sup>61</sup>. This mutant virus demonstrated similar kinetics, antibody titers, and lymphocyte infiltrates found in

bronchoalveolar lavage to wildtype Sendai virus<sup>61</sup>. Furthermore, bioluminescence flux measurements were identified as a substitute for viral titers, as bioluminescence in the nasopharynx, trachea, and lung regions strongly correlated with viral titers from corresponding tissues<sup>61</sup>. Overall, the luciferase expressing Sendai virus demonstrated higher levels of infection in the nasopharynx and trachea compared to the lung<sup>61</sup>. The Sendai-luciferase virus was then used to analyze transmission dynamics by both contact and aerosol transmission. Contact transmission caused infection to initiate in the nasopharynx region and spread to the lung, which corresponded with high viral titers in the nasal cavity of mice<sup>17</sup>. In contrast, airborne transmission occurred around 2 days later than contact dependent transmission and initiated in the trachea<sup>17</sup>. This coincides with the understanding that droplet particle size contributes to localization and deposition of virions along the respiratory tract, with aerosols establishing infection deeper in the respiratory tract than larger sized droplets. When analyzing viral titers throughout the respiratory tract of Sendai-luciferase infected mice, viral loads in the lung did not correlate with airborne transmission efficiency<sup>17</sup>. This suggests that titers in the nasopharynx of index mice may be responsible for transmission efficiency, which aligns with results from a recent study demonstrating that viral replication within the nasal respiratory epithelium of ferrets is the source of infectious virions that spread during influenza virus A transmission<sup>36</sup>. Another interesting finding regarding Sendai virus transmission was that mice who had previously been infected with Sendai-luciferase by contact transmission, as opposed to airborne transmission, were better protected against reinfection with the same virus<sup>17</sup>. Overall, these studies demonstrate that Sendai virus represents a useful substitute to study respiratory virus transmission in mice. The use of Sendai virus circumvents the inconsistencies seen in influenza virus transmission in mice, while

enabling utilization of immunological resources that are currently unavailable to ferret and guinea pig models.

### ***Initiation of Infection in Respiratory Epithelium***

Following transmission of a respiratory virus, infectious virions deposit on locations along the respiratory tract and initiate infection by binding to entry receptors on target cells. Influenza virus infection initiates by binding the viral glycoprotein hemagglutinin to sialic acid receptors on respiratory epithelium<sup>62</sup>. These sialic acid linkages have been identified on epithelial cells within the trachea, nasal mucosa, paranasal sinuses, bronchi, and alveoli within the lung<sup>62, 63</sup>. Similarly, Sendai virus enters cells through binding to sialic acid receptors present throughout the upper and lower respiratory tract<sup>64, 65</sup>. Consequently, it is critical to understand the epithelial cell composition throughout the respiratory tract and antiviral mechanisms which may prevent productive infection. There are several main types of epithelial cells present in respiratory epithelium, including goblet cells, club cells, tuft cells, basal cells, and ciliated cells. Basal cells are located directly beneath the epithelial layer exposed to the external environment and serve as stem cells which give rise to ciliated and secretory cells, enabling regeneration and repair of the epithelial barrier<sup>66-68</sup>. Club cells and goblet cells are responsible for the secretion of mucins, proteases, and antimicrobial peptides, which form a thick mucus layer covering the underlying epithelium<sup>67, 69</sup>. Virions that find their way onto the airway epithelial surface can become trapped by this mucus layer, swept upwards by ciliated cells, and ultimately expelled by sneezing or nasal discharge<sup>67, 69</sup>. A rarer epithelial cell population, termed tuft or brush cells, express a variety of immune and metabolic receptors that enable them to promote innate immune activation<sup>66</sup>. It is important to note that epithelial cell composition differs between locations along the respiratory tract and between species. For

example, basal cells are located throughout the respiratory tract in humans but are strictly found within trachea and proximal bronchi in mice<sup>68</sup>. Alveolar epithelial cells are only located within the lung alveoli and have specialized functions for gas exchange and pulmonary surfactant secretion that helps maintain structural integrity and function of the lung<sup>66, 69</sup>. Epithelial cell types are best defined through transcription factor analysis, as different transcription factors are expressed or downregulated at various stages throughout cell development and activation. Ultimately, the composition of the epithelial barrier is highly heterogenous, and recent single cell RNA sequencing studies have enabled identification of rare cell types, whose functions are still being discerned. Because the airway epithelium is constantly exposed to both infectious and innocuous particles present in the air, its role in antiviral defense is critical to protecting against and limiting respiratory virus transmission.

### ***Innate Immune Response***

Besides the production of mucus and antimicrobial peptides, epithelial cells express pattern recognition receptors (PRRs), which enable rapid detection and response to invading pathogens. Stimulation of PRRs triggers signaling cascades that lead to the production of cytokines and chemokines that help activate an antiviral state in nearby cells and recruit other cells to the site of infection. The main types of PRRs that respond to viral infections are the Toll-like receptors (TLRs) and retinoic acid-inducible gene 1-like receptors (RLRs). TLRs 3, 7, and 9 respond to double stranded DNA, single stranded DNA, and unmethylated CpG, respectively within the endosomal compartment<sup>70-72</sup>. Of the known RLRs, retinoic acid-inducible gene I (RIG-I) detects unmethylated 5'-triphosphate ends on single stranded RNA and melanoma differentiation associated gene 5 (MDA5) recognizes double stranded RNA found in the cytoplasmic compartment<sup>73, 74</sup>. The cyclic GMP-AMP synthase (cGAS)- stimulator of interferon genes

(STING) pathway is invoked by sensing of double stranded DNA within the cytoplasm<sup>75</sup>. Genomic material is normally not found within the cytoplasm or endosomal compartments of cells but can often be detected during viral fusion with the cell membrane and endosome formation or viral replication in the cytoplasm. Stimulation of these receptors leads to activation of nuclear factor - $\kappa$ B (NF- $\kappa$ B) and interferon regulatory factors (IRFs)<sup>76</sup>. Expression of these antiviral transcription factors leads to production of type I interferons, IFN- $\alpha$  and IFN- $\beta$ , along with type III interferons, IFN- $\lambda$ s<sup>77</sup>. Interferons signal through their respective receptors to induce interferon stimulated genes (ISGs) which encode antiviral functions such as apoptosis, termination of translation, enhanced antigen presentation, and inhibition of viral membrane fusion<sup>78-80</sup>. The Mx1 gene, previously mentioned, is one such ISG<sup>25</sup>. In addition to the interferon response, stimulation of epithelial cells through their PRRs can initiate production of many pro-inflammatory cytokines. TNF- $\alpha$ , IL-1 $\beta$ , and IL-6 promote inflammation by causing fever, increasing expression of adhesion molecules, and increasing vascular permeability to ultimately cause leukocyte influx to the site of infection<sup>81,82</sup>. CCL2 and IL-8 are chemokines that recruit inflammatory monocytes, dendritic cells, and neutrophils<sup>83-85</sup>. Additionally, NK cells are recruited from the bloodstream and can be found in the lung 3 days after influenza virus infection<sup>86</sup>. All of these innate immune responses are intended to initiate the adaptive immune response and hold viral replication at bay until an effective antigen specific lymphocyte response can be mounted to clear the infection.

### ***Development of Adaptive Immune Response***

During a respiratory virus infection, dendritic cells either resident or recently recruited into the airways recognize antigen and undergo maturation. Dendritic cells (DCs) can acquire antigen by either becoming directly infected with virus themselves or phagocytosing an infected cell<sup>87, 88</sup>.

Once a DC encounters antigen, their PRRs will become stimulated, invoking expression of molecules involved in antigen presentation such as MHC Class II and co-stimulatory molecules required for naïve T cell priming including CD80, CD86, and CD40<sup>89</sup>. Additionally, the chemokine receptor CCR7 becomes upregulated which guides DCs to the nearest tissue draining lymph node along a CCL21 and CCL19 gradient<sup>90</sup>. In the case of influenza infection in the lung, this is the mediastinal lymph node, while the nasal cavity, turbinates, and nasopharynx drain into the pharyngeal and retropharyngeal lymph nodes in humans<sup>91, 92</sup>. Upon migration into lymph nodes, DCs can enter into T cell zones and present their antigen on MHC Class I and II to CD8 and CD4 T cell respectively<sup>93</sup>. In the context of influenza infection, CD103+ cDC1s in the lung are critical for cross-priming and activation of CD8 T cells<sup>94</sup>. This initial dendritic cell – T cell interaction is referred to as T cell priming and is the first step in activating an antigen specific immune response, designed to eliminate infected cells.

### ***T Cell Response to Respiratory Viruses***

Once a naïve T cell recognizes its antigen presented by MHC on a dendritic cell, they form stable contacts that persist for multiple hours<sup>95</sup>. During this time, T cells undergo massive amounts of proliferation, generating a large number of virus-specific T cells<sup>96</sup>. Co-stimulatory molecules including CD28, CD27, 4-1BB, and OX40 expressed by dendritic cells are needed to generate effective T cell responses, and reduced effector and memory T cell responses have been reported in the absence of these molecules<sup>97, 98</sup>. Cytokines secreted by dendritic cells or other cells in the local microenvironment can influence T cell differentiation, particularly for CD4 T cell polarization<sup>99</sup>. These recently activated effect T cells then follow an S1P gradient via S1PR1 to exit the lymph nodes, enter the bloodstream, and ultimately enter the infected nonlymphoid

tissue<sup>100</sup>. Influenza specific effector CD8 T cells can first be seen in the lung around 4-5 days after infection<sup>101</sup>. A variety of chemokines are involved in the trafficking of T cells into infected lung tissue, as chemokine receptors are often redundant in their roles and ligands. In the case of influenza infection, CCR4 and CXCR3 help guide antigen specific CD4 T cells into the lung<sup>102</sup>,<sup>103</sup>. Effector and memory CD8 T cell trafficking into the lung depends at least partially on CXCR3 and CCR5<sup>104-106</sup>. CXCL12 secreted by neutrophils within the lung can also attract influenza-specific CD8 T cells into the lung by CXCR4<sup>107</sup>. Memory CD8 T cells have also been shown to traffic from the lung parenchyma into the airways by CXCR6 expression, along a CXCL16 gradient<sup>108</sup>. Furthermore, expression of adhesion molecules such as VLA-4 and LFA-1, which bind to VCAM-1 and ICAM-1 respectively, are necessary for CD8 T cell recruitment and retention in the lung<sup>109</sup>. While T cell trafficking into the nasopharynx region and nasal associated lymphoid tissue (NALT) has not been as widely studied as trafficking into the lung, one study suggests that the presence of CXCL10 in influenza infected NALT tissue recruits CXCR3+ effector and memory CD8 T cells<sup>110</sup>. Expression of the adhesion molecules MadCam-1 and PNAd within the NALT further enables lymphocyte homing<sup>110, 111</sup>.

Effector CD8 T cells can eliminate infected target cells in a variety of ways. Perhaps the most well characterized, cytotoxic T lymphocytes (CTLs) can secrete pre-formed cytotoxic granules containing granzyme, perforin, and granulysin. Perforin created a pore-like channel in target cells that enables proteases, namely granzyme B, to enter the cell and initiate caspase-3 and caspase-8 mediated cell death<sup>112</sup>. Granzymes A and K have also been demonstrated to play cytotoxic roles, albeit to a lesser extent than granzyme B<sup>113</sup>. CTLs can also kill target cells through FAS ligand binding to the death receptor FAS (CD95) on the surface of an infected cell, leading to caspase-8 activation and apoptosis<sup>114</sup>. Effector CD8 T cells can also secrete cytokines including

IFN- $\gamma$ , TNF- $\alpha$ , and IL-2, which help activate other innate cells at the site of infection, generate an antiviral state in neighboring cells, and promote additional T cell proliferation<sup>115, 116</sup>. Secretion of pro-inflammatory cytokines from T cells and other innate cells can cause significant damage to the respiratory tract. To mitigate this, effector CD8 T cells exclusively produce large amounts of IL-10 in the lungs during respiratory virus infections such as influenza<sup>117</sup>. All of these effector mechanisms ultimately lead to viral clearance.

### ***T Cell Memory Formation and Subsets***

Following viral clearance and removal of antigen, the effector T cell population retracts and 90-95% of viral-specific T cells die by apoptosis<sup>118</sup>. The surviving cells constitute the virus specific memory T cell pool and remain relatively stable over time. Cells that are fated to become memory T cells, termed memory precursor effector cells (MPECs), can be identified by their expression of CD127 (IL-7R $\alpha$ ) and lack of KLRG1. Contrastingly, SLECs (short lived effector cells) do not express CD127 but gain KLRG1<sup>119-121</sup>. While it was well known that IL-7 was required for lymphocyte maintenance, more recent studies have demonstrated that KLRG1 is a marker of terminal differentiation. Expression of this marker indicates that a cell no longer has the capacity to alter its transcriptional programming into a memory T cell signature and phenotype. Additionally, high levels of Tbet and Blimp1 transcription factors indicate terminally differentiated effector cells (SLECs)<sup>122</sup>. The MPECs ultimately transition into one of the three memory T cell subsets: central memory (TCM), effector memory (TEM), or tissue resident memory (TRM). TCM cells are retained in or near the bone marrow and secondary lymphoid organs where they are poised to rapidly proliferate and produce IL-2, mounting an antigen-specific T cell and B cell response upon re-encounter of their antigen. In contrast, TEM can be found in

circulation and home to peripheral nonlymphoid tissues upon challenge, where they are prone to cytokine secretion and cytolytic activity. Both of these subsets can be defined by their expression patterns of CCR7 and CD62L; TCM express both of these markers for lymphoid organ retention, while TEM express neither of these markers<sup>122-124</sup>.

### ***CD8 Tissue Resident Memory T Cells***

Unlike central or effector memory T cell subsets, tissue resident memory T cells are unique in that they remain within the previously infected tissue and do not re-circulate through the blood or lymphoid organs. Because of this, TRM can primarily be found in tissues that are exposed to the external microenvironment, such as the skin, gut, respiratory tract, and genital tract<sup>125-129</sup>. CD8 TRM generally establish residence within epithelial barriers, where they are positioned to rapidly respond to and eliminate their cognate antigens. On the other hand, CD4 TRM are often found deeper within the lamina propria of the tissue<sup>130</sup>. TRM can be identified based on their surface expression of both CD69 and CD103, markers that enable retention within the tissue. As previously mentioned, activated lymphocytes exit lymphoid and non-lymphoid organs into the bloodstream following an S1P (sphingolipid-1 phosphate) gradient using S1PR1<sup>100</sup>. During T cell activation within the lymph node, CD69 is transiently expressed to enable clonal expansion and stable cell-cell contacts with dendritic cells and B cells<sup>131</sup>. CD69 prevents tissue egress by binding to S1PR1 post-translationally, causing its internalization and degradation. In the case of TRM, permanent expression of CD69 allows long-term residence within nonlymphoid tissue. CD103 binds to E-cadherin on epithelial cells and allows anchoring onto epithelial surfaces. While both CD103 and CD69 expression has canonically been used to define TRM, many studies have identified TRM that lack CD103 expression. Some CD4 TRM lack CD103 expression, as they do

not reside in the epithelium<sup>132</sup>. This applies for CD4 TRM in the lung, where CD103 expression cannot be found on any of these cells<sup>133</sup>. Specific tissue microenvironments can influence the requirement for CD103 expression. For example, virtually all CD8 TRM in the skin express CD103 and CD69, while those within the liver express only CD69<sup>129</sup>. CD8 TRM in airways have lower levels of CD103 expression compared to lung TRM, although the reason and functional implications behind this have not been delineated<sup>134</sup>. Other phenotypic markers that have been associated with CD8 TRM in the respiratory tract include CD49a and CD11a. CD49a complexes with CD29 to form VLA-1, an  $\alpha 1\beta 1$  integrin, which binds to collagen types I and IV<sup>135</sup>. Expression of this marker helps TRM in the lung attach to the extracellular matrix and establish residency. The majority of influenza specific CD8 T cells express VLA-1 and deficiency in this marker reduces the number of CD8 TRM in the airways and lung, which corresponds with a decrease in protection against heterosubtypic influenza challenge<sup>135</sup>. Both CD4 and CD8 TRM express CD11a, which binds with CD18 to form the integrin LFA-1, a critical adhesion molecule involved in lymphocyte extravasation and tissue migration. Although CD8 memory T cells in the lung express CD11a, airway TRM downregulate CD11a expression within 40 hours of their migration to the airways<sup>136</sup>. Many studies use CD11a expression as a marker to identify TRM that have recently been recruited into the airways. The chemokine receptors CXCR6 and CXCR3 are also associated with CD8 TRM in the respiratory tract, as these molecules are involved in trafficking to the lung and airways<sup>106, 108</sup>. A variety of adhesion molecules, chemokine receptors, and markers involved in tissue retention can be used to characterize and define TRM in the respiratory tract.

While TRM can be identified based on phenotypic markers, they also exhibit distinct transcriptional programming. The transcription factor KLF2 encodes genes involved in secondary lymphoid organ circulation such as S1PR1 and is downregulated in TRM<sup>124</sup>. Blimp and Hobit are

also expressed by TRM, and Hobit may have a role in promoting KLF2 downregulation<sup>124, 137</sup>. High levels of expression of T-bet have been shown to prevent CD103 expression; thus, T-bet is downregulated in TRM<sup>138</sup>. However, intermediate levels of T-bet are needed to maintain IL-15R $\beta$  (CD122) expression, as IL-15 signaling is required for memory T cell survival<sup>139</sup>. The T-box transcription factor Eomes is also downregulated in TRM to enable TGF- $\beta$  signaling, which in turn induces CD103 expression<sup>139</sup>. Interestingly, it has recently been reported that S1PR5 may play an underappreciated role in tissue retention. Although S1PR5 is not encoded by KLF2 and does not bind to CD69, its downregulation is required for CD8 TRM differentiation<sup>140</sup>. Downregulation of transcription factors Zeb2 and Tbx21 promoted S1PR5 downregulation and was induced by TGF- $\beta$  signaling<sup>140</sup>. One recent study demonstrated that CD8 TRM require Runx3 expression for residence within epithelial surfaces and that Runx3 enhanced the chromatin accessibility of TGF- $\beta$  related genes needed for CD103 expression. Furthermore, this same study showed that while CD8 TRM depend on Runx3 expression, it is dispensable for CD4 TRM development, and CD4 TRM instead rely on Runx1<sup>130</sup>.

### ***Techniques for Studying TRM***

Historically, one powerful technique used for identifying tissue resident memory lymphocytes is parabiotic surgery. In this procedure, two congenically distinct mice are surgically conjoined at the flank region to allow for shared circulation between partners. Within around two weeks after surgery, blood in each mouse contains an equal number of cells originating from themselves and their partner. Resident cells can be identified by their absence of recirculation or equilibration in the partner mouse. Although difficult to execute, this technique allows tracking of circulating cellular populations over the course of many weeks and recapitulates natural migration

patterns *in vivo*<sup>124</sup>. A simpler, yet equally effective technique that is widely used to identify resident cells is intravascular staining. Before euthanasia, mice are injected intravenously (i.v.) with an anti-CD3 or anti-CD45 antibody conjugated to a fluorescent fluorophore. With this method, cells in the vasculature will be labeled with the antibody, while those within nonlymphoid tissue and lymph nodes will not be exposed to the antibody. In the lung, a portion of cells that lacked the intravascular label also expressed the surface markers CD103 and CD69. These cells were identified as tissue resident memory lymphocytes<sup>141</sup>. One caveat with this method is that effector memory T cells may migrate into the tissue transiently and will not be labelled with the intravital antibody. However, the likelihood of these cells expressing both CD69 and CD103 is low. Nonetheless, this should be taken into consideration when analyzing and interpreting data involving i.v. labeling. To date, the combination of i.v. labelling and phenotypic expression of CD69 and CD103 is used as the gold standard to identify tissue resident memory T cells.

### ***Generation and Maintenance of TRM in the Respiratory Tract***

Following respiratory virus infections, tissue resident memory T cells can be found in the nasal tissue, airways, and lungs<sup>126, 142-144</sup>. Developmental requirements for TRM differ based on the local tissue microenvironment, and variations can be seen even within the respiratory tract. In tissues such as the skin and gut, effector T cells can be recruited to the tissue by pro-inflammatory signals such as IL-12 and type I interferons and differentiate into CD69 and/or CD103 positive tissue resident memory T cells, in the absence of cognate antigen<sup>145, 146</sup>. One study sought to test whether this was the case in the lung, and developed a strategy where mice were infected with influenza by the intramuscular route with CpG and influenza peptide intranasal dosing or by the intranasal route alone<sup>147</sup>. Although intramuscular infection with inflammatory stimuli delivered to

the respiratory tract was able to draw effector CD8 T cells into the lung, CD103<sup>+</sup> CD69<sup>+</sup> CD8 TRM were only found in the group given intranasal infections<sup>147</sup>. These results demonstrated that CD8 TRM in the lung are unique in that they require local recognition of their cognate antigen for development. Another study assessed the requirement for antigen in the development of nasal cavity TRM by infecting mice with x31 influenza wildtype or x31 influenza conjugated to ovalbumin (OVA)<sup>126</sup>. Transgenic CD8 OT-I T cells specific for the OVA protein were then transferred to these cohorts and their nasal cavity responses were assessed. CD103<sup>+</sup> CD69<sup>+</sup> OT-I T cells were found in the nasal cavities of mice who received wildtype influenza infections, although significantly fewer were present compared to the x31-OVA infection group<sup>126</sup>. These results suggested that nasal cavity CD8 TRM can form in the absence of localized antigen, albeit in lower numbers.

TGF- $\beta$  signaling is required for the development of CD8 TRM in many tissues including the gut, skin, and salivary glands<sup>129, 148</sup>. Studies have assessed the requirement for TGF- $\beta$  signaling in the generation of lung and nasal cavity CD8 TRM by seeding mice with OT-I T cells that lack expression of the TGF- $\beta$  receptor. When infected with an OVA expressing influenza virus, these cells failed to develop into CD103<sup>+</sup> TRM in the lung, but moderate numbers of CD103<sup>+</sup> TRM were seen in the nasal cavity<sup>126, 149</sup>. It was further shown that the likely source of TGF- $\beta$  in the lung was cross-presenting CD103<sup>+</sup> lung dendritic cells<sup>149</sup>. In addition to TGF- $\beta$ , IL-15 produced by macrophages and dendritic cells in the lung contributes to the survival of CD8 lung TRM<sup>139</sup>. Although it has been shown that nasal cavity CD8 TRM can develop in the absence of cognate antigen and TGF- $\beta$ , which signals can substitute in driving TRM differentiation in this site has not yet been thoroughly investigated.

CD8 TRM populations are relatively stable over time in the skin and gut<sup>148, 150</sup>. However, TRM within the lung and airways decline over time, corresponding with a loss in heterosubtypic immunity to influenza<sup>151-154</sup>. As virus is cleared and the antigen is removed, the loss in antigen stimulation leads to the loss of key survival signals needed by lung TRM. This was demonstrated using a model of recombinant adenoviral vector vaccination, where intranasal vaccination with an adenoviral vector expressing the influenza virus nucleoprotein was able to induce lung and airway CD8 TRM populations that persisted up to one year post vaccination<sup>154</sup>. Using Nur77 GFP reporter mice and EdU incorporation, it was shown that influenza nucleoprotein antigen remaining in the lung from the adenoviral vector vaccination stimulated TRM in an antigen specific manner, leading to their continued proliferation and survival, as well as recruitment of circulating effector cells into the TRM pool<sup>154</sup>. Ultimately, the source of this persistent antigen was shown to be long lived alveolar macrophages in the lungs<sup>155</sup>. CD4 T cell help also likely contributes to the enhanced longevity of lung CD8 TRM in this vaccination scenario<sup>155</sup>. Other mechanisms may contribute to the decline of CD8 lung TRM including environmental stress and metabolic factors. For example, airway influenza specific CD8 TRM have been shown to decline at a more rapid rate than interstitial lung TRM<sup>151</sup>. RNA and ATAC sequencing of airway and lung TRM elucidated distinct transcriptional profiles, where genes associated with cell stress and apoptosis were upregulated in airway TRM with increased chromatin accessibility<sup>151</sup>. Due to the unique microenvironment of the trachea and airways where nutrients are scarce during homeostasis to limit unnecessary immune infiltration and immunopathology, airway TRM undergo amino acid starvation and an integrated cellular stress response, leading to their apoptosis<sup>151</sup>. Despite the decline in lung and airway TRM over time, nasal cavity TRM are stable for at least 120 days and maintain protection against heterosubtypic strains of influenza<sup>126</sup>. The underlying mechanisms behind the stability of nasal

cavity TRM has not yet been explored but may be related to their ability to form in the absence of localized antigen stimulation.

### ***CD8 TRM in Respiratory Virus Infections and Vaccinations***

CD8 TRM elicit protective immunity against respiratory infections through effector functions including cytotoxic killing of target cells and secretion of cytokines and chemokines that result in recruitment of circulating immune cells<sup>122, 124, 127, 142, 143, 156</sup>. For example, CD8 TRM in the airways primarily act through production of antiviral cytokines, namely IFN- $\gamma$ . Despite airway CD8 TRM's poorly cytolytic capacity, they are able to confer significant immune protection against x31 influenza and Sendai virus by secretion of IFN- $\gamma$ <sup>143, 157</sup>. This was demonstrated through intra-tracheal transfer of antigen specific CD8 airway TRM to influenza infected mice, where TRM transferred from IFN- $\gamma$  knockout mice were unable to limit viral replication to the same extent as TRM from wildtype mice<sup>143</sup>. Although many studies of CD8 TRM in the respiratory tract have utilized mouse models, similar results have been corroborated in tissues from human donors. CD8 TRM from healthy human lungs retain the capacity to secrete IFN- $\gamma$ , TNF- $\alpha$ , and IL-2 in a polyfunctional manner and express CD107a, granzyme B, and perforin, markers of cytotoxic activity<sup>158, 159</sup>.

Respiratory tract resident CD8 memory T cells have been shown to mediate cross-protection against strains of influenza<sup>152, 153, 160</sup>. Unlike neutralizing antibodies which target viral surface proteins subject to immune escape, CD8 T cells and CD8 TRM recognize internal viral epitopes, that are conserved across viral strains<sup>161</sup>. In the case of influenza, the nucleoprotein, matrix protein, and polymerase subunits are often targeted by CD8 T cells<sup>162-164</sup>. Because of this, T cell based vaccines have the potential to provide protection against a wide variety of virus strains

in addition to potentially pandemic variants. Recent vaccine development efforts, particularly in response to the SARS-CoV-2 pandemic, have evaluated the ability of different vaccine vectors and platforms to elicit CD8 TRM. As previously mentioned, recombinant adenoviral vector based vaccines have been shown to generate stable CD8 TRM populations against influenza virus<sup>154, 155</sup>. One study immunized non-human primates with Ad26.COV2.S, the Johnson & Johnson adenoviral vector SARS-CoV-2 vaccine, administered a CD8 depleting monoclonal antibody, and then challenged animals with high titers of the SARS-CoV-2 B.1.617.2 (Delta) variant. Animals who received the CD8 T cell depleting antibody had significantly higher viral loads in the nasal mucosa and bronchoalveolar lavage than those who did not receive antibody depletion, further suggesting a critical role for CD8 T cells, and potentially CD8 TRM, in adenoviral vector vaccine mediated immune protection<sup>165</sup>. Another recent study compared immune responses to the Astra-Zeneca chimpanzee adenoviral vector based SARS-CoV-2 vaccine, ChAdOx1-S. Significantly higher numbers of spike protein specific CD8 TRM were found in the lungs of mice following intranasal vaccine administration when compared to intramuscular immunization<sup>166</sup>. In a model of influenza virus transmission, vaccination with an adenoviral vector based influenza vaccine was shown to limit viral transmission from vaccinated to unvaccinated contact mice, independently of neutralizing antibodies<sup>31, 167</sup>. However, the mechanisms behind this phenomena and potential role for CD8 TRM has not been investigated. As the first mRNA vaccines were developed in 2020 for SARS-CoV-2, numerous groups investigated the CD8 T cell response to both Pfizer and Moderna vaccine platforms. One group identified CD8 TRM in the nasal mucosa of humans following immunization with the Pfizer-BioNTech COVID-10 vaccine and observed the expression of cytokines and degranulation markers on these cells following antigen stimulation<sup>168</sup>. Another study developed an mRNA-based vaccine encoding the influenza nucleoprotein and demonstrated that

intramuscular prime and boost immunization was able to generate lung CD8 TRM, but intranasal boosting or initial intranasal immunization was needed for elicit a maximal response<sup>169</sup>. These results are in line with the requirement for localized antigen in lung CD8 TRM formation and highlight the importance of future research and development into intranasally administered vaccines. Live attenuated influenza vaccine (LAIV), which is FDA approved under the name FluMist and administered intranasally, has also been shown to generate CD8 TRM in the respiratory tract<sup>170-172</sup>. However, LAIV vaccination has proved most effective in children due to pre-existing influenza immunity in adults that results in neutralization or clearance of the viral vaccine strain<sup>173-175</sup>.

In the modern era of globalization and urbanization, the risk of zoonotic events and pandemic outbreaks is continually increasing. Thus, there is a critical need for effective vaccine platforms capable of providing immune protection across viral subtypes and potentially pandemic variants. As CD8 TRM can control respiratory virus infections, provide heterologous protection against influenza strains, and form at mucosal barriers that are often the first sites of pathogen exposure, vaccines which focus on the induction of CD8 TRM pose a promising alternative to traditional vaccine platforms. Prior to the work outlined in the remainder of this dissertation, no studies had evaluated the ability of respiratory tract CD8 TRM to control viral transmission. The research henceforth presented will cast light on the cellular immune pathways underlying respiratory virus transmission and help inform more effective vaccine design that limits the spread of respiratory viruses.

## References

1. United States COVID-19 Cases, Deaths, and Laboratory Testing (NAATs) by State, Territory, and Jurisdiction: Centers for Disease Control and Prevention; 2024. Available from: [https://covid.cdc.gov/covid-data-tracker/#cases\\_casesper100k](https://covid.cdc.gov/covid-data-tracker/#cases_casesper100k).
2. Estimated U.S. Flu Burden, By Season: Centers for Disease Control and Prevention; 2024. Available from: [https://www.cdc.gov/flu-burden/php/about/index.html?CDC\\_AAref\\_Val=https://www.cdc.gov/flu/about/burden/index.html](https://www.cdc.gov/flu-burden/php/about/index.html?CDC_AAref_Val=https://www.cdc.gov/flu/about/burden/index.html).
3. Lee MS, Walker RE, Mendelman PM. Medical burden of respiratory syncytial virus and parainfluenza virus type 3 infection among US children. Implications for design of vaccine trials. *Hum Vaccin*. 2005;1(1):6-11. Epub 20050110. doi: 10.4161/hv.1.1.1424. PubMed PMID: 17038832.
4. Signs and Symptoms of Flu: Centers for Disease Control and Prevention; 2024. Available from: <https://www.cdc.gov/flu/signs-symptoms/index.html>.
5. Leung NHL. Transmissibility and transmission of respiratory viruses. *Nat Rev Microbiol*. 2021;19(8):528-45. Epub 20210322. doi: 10.1038/s41579-021-00535-6. PubMed PMID: 33753932; PMCID: PMC7982882.

6. Kutter JS, Spronken MI, Fraaij PL, Fouchier RA, Herfst S. Transmission routes of respiratory viruses among humans. *Curr Opin Virol.* 2018;28:142-51. Epub 20180117. doi: 10.1016/j.coviro.2018.01.001. PubMed PMID: 29452994; PMCID: PMC7102683.
7. Bridges CB, Kuehnert MJ, Hall CB. Transmission of influenza: implications for control in health care settings. *Clin Infect Dis.* 2003;37(8):1094-101. Epub 20030919. doi: 10.1086/378292. PubMed PMID: 14523774.
8. Szablewski C. DM, Azziz-Baumgartner E. *CDC Yellow Book 2024: Influenza: Centers for Disease Control and Prevention; 2024.*
9. Cowling BJ, Ip DK, Fang VJ, Suntarattiwong P, Olsen SJ, Levy J, Uyeki TM, Leung GM, Malik Peiris JS, Chotpitayasunondh T, Nishiura H, Mark Simmerman J. Aerosol transmission is an important mode of influenza A virus spread. *Nat Commun.* 2013;4:1935. doi: 10.1038/ncomms2922. PubMed PMID: 23736803; PMCID: PMC3682679.
10. Jayaweera M, Perera H, Gunawardana B, Manatunge J. Transmission of COVID-19 virus by droplets and aerosols: A critical review on the unresolved dichotomy. *Environ Res.* 2020;188:109819. Epub 20200613. doi: 10.1016/j.envres.2020.109819. PubMed PMID: 32569870; PMCID: PMC7293495.

11. Johnson D, Lynch R, Marshall C, Mead K, Hirst D. Aerosol Generation by Modern Flush Toilets. *Aerosol Sci Technol*. 2013;47(9):1047-57. doi: 10.1080/02786826.2013.814911. PubMed PMID: 26635429; PMCID: PMC4666014.
12. Chan MC, Lee N, Chan PK, To KF, Wong RY, Ho WS, Ngai KL, Sung JJ. Seasonal influenza A virus in feces of hospitalized adults. *Emerg Infect Dis*. 2011;17(11):2038-42. doi: 10.3201/eid1711.110205. PubMed PMID: 22099092; PMCID: PMC3310558.
13. Wang CC, Prather KA, Sznitman J, Jimenez JL, Lakdawala SS, Tufekci Z, Marr LC. Airborne transmission of respiratory viruses. *Science*. 2021;373(6558). doi: 10.1126/science.abd9149. PubMed PMID: 34446582; PMCID: PMC8721651.
14. Zhou J, Wei J, Choy KT, Sia SF, Rowlands DK, Yu D, Wu CY, Lindsley WG, Cowling BJ, McDevitt J, Peiris M, Li Y, Yen HL. Defining the sizes of airborne particles that mediate influenza transmission in ferrets. *Proc Natl Acad Sci U S A*. 2018;115(10):E2386-E92. Epub 20180220. doi: 10.1073/pnas.1716771115. PubMed PMID: 29463703; PMCID: PMC5877994.
15. Duguid JP. The size and the duration of air-carriage of respiratory droplets and droplet-nuclei. *J Hyg (Lond)*. 1946;44(6):471-9. doi: 10.1017/s0022172400019288. PubMed PMID: 20475760; PMCID: PMC2234804.
16. Wedel J, Steinmann P, Strakl M, Hribersek M, Cui Y, Ravnik J. Anatomy matters: The role of the subject-specific respiratory tract on aerosol deposition - A CFD study. *Comput*

Methods Appl Mech Eng. 2022;401:115372. Epub 20220728. doi: 10.1016/j.cma.2022.115372.  
PubMed PMID: 35919629; PMCID: PMC9333481.

17. Burke CW, Bridges O, Brown S, Rahija R, Russell CJ. Mode of parainfluenza virus transmission determines the dynamics of primary infection and protection from reinfection. PLoS Pathog. 2013;9(11):e1003786. Epub 20131121. doi: 10.1371/journal.ppat.1003786. PubMed PMID: 24278024; PMCID: PMC3836739.

18. Stilianakis NI, Drossinos Y. Dynamics of infectious disease transmission by inhalable respiratory droplets. J R Soc Interface. 2010;7(50):1355-66. Epub 20100217. doi: 10.1098/rsif.2010.0026. PubMed PMID: 20164087; PMCID: PMC2894888.

19. Schlottau K, Rissmann M, Graaf A, Schon J, Sehl J, Wylezich C, Hoper D, Mettenleiter TC, Balkema-Buschmann A, Harder T, Grund C, Hoffmann D, Breithaupt A, Beer M. SARS-CoV-2 in fruit bats, ferrets, pigs, and chickens: an experimental transmission study. Lancet Microbe. 2020;1(5):e218-e25. Epub 20200707. doi: 10.1016/S2666-5247(20)30089-6. PubMed PMID: 32838346; PMCID: PMC7340389.

20. Sia SF, Yan LM, Chin AWH, Fung K, Choy KT, Wong AYL, Kaewpreedee P, Perera R, Poon LLM, Nicholls JM, Peiris M, Yen HL. Pathogenesis and transmission of SARS-CoV-2 in golden hamsters. Nature. 2020;583(7818):834-8. Epub 20200514. doi: 10.1038/s41586-020-2342-5. PubMed PMID: 32408338; PMCID: PMC7394720.

21. de Vries RD, Rockx B, Haagmans BL, Herfst S, Koopmans MP, de Swart RL. Animal models of SARS-CoV-2 transmission. *Curr Opin Virol.* 2021;50:8-16. Epub 20210629. doi: 10.1016/j.coviro.2021.06.007. PubMed PMID: 34256352; PMCID: PMC8238653.
22. Ibricevic A, Pekosz A, Walter MJ, Newby C, Battaile JT, Brown EG, Holtzman MJ, Brody SL. Influenza virus receptor specificity and cell tropism in mouse and human airway epithelial cells. *J Virol.* 2006;80(15):7469-80. doi: 10.1128/JVI.02677-05. PubMed PMID: 16840327; PMCID: PMC1563738.
23. Glaser L, Conenello G, Paulson J, Palese P. Effective replication of human influenza viruses in mice lacking a major alpha2,6 sialyltransferase. *Virus Res.* 2007;126(1-2):9-18. Epub 20070220. doi: 10.1016/j.virusres.2007.01.011. PubMed PMID: 17313986.
24. Bouvier NM, Lowen AC. Animal Models for Influenza Virus Pathogenesis and Transmission. *Viruses.* 2010;2(8):1530-63. doi: 10.3390/v20801530. PubMed PMID: 21442033; PMCID: PMC3063653.
25. Jin HK, Yamashita T, Ochiai K, Haller O, Watanabe T. Characterization and expression of the Mx1 gene in wild mouse species. *Biochem Genet.* 1998;36(9-10):311-22. doi: 10.1023/a:1018741312058. PubMed PMID: 9919357.
26. Tumpey TM, Szretter KJ, Van Hoeven N, Katz JM, Kochs G, Haller O, Garcia-Sastre A, Staeheli P. The Mx1 gene protects mice against the pandemic 1918 and highly lethal human

H5N1 influenza viruses. *J Virol.* 2007;81(19):10818-21. Epub 20070725. doi: 10.1128/JVI.01116-07. PubMed PMID: 17652381; PMCID: PMC2045488.

27. Schulman JL. The use of an animal model to study transmission of influenza virus infection. *Am J Public Health Nations Health.* 1968;58(11):2092-6. doi: 10.2105/ajph.58.11.2092. PubMed PMID: 5748875; PMCID: PMC1229043.

28. Schulman JL. Experimental transmission of influenza virus infection in mice. IV. Relationship of transmissibility of different strains of virus and recovery of airborne virus in the environment of infector mice. *J Exp Med.* 1967;125(3):479-88. doi: 10.1084/jem.125.3.479. PubMed PMID: 6016901; PMCID: PMC2138293.

29. Lowen AC, Mubareka S, Tumpey TM, Garcia-Sastre A, Palese P. The guinea pig as a transmission model for human influenza viruses. *Proc Natl Acad Sci U S A.* 2006;103(26):9988-92. Epub 20060619. doi: 10.1073/pnas.0604157103. PubMed PMID: 16785447; PMCID: PMC1502566.

30. Edenborough KM, Gilbertson BP, Brown LE. A mouse model for the study of contact-dependent transmission of influenza A virus and the factors that govern transmissibility. *J Virol.* 2012;86(23):12544-51. Epub 20120905. doi: 10.1128/JVI.00859-12. PubMed PMID: 22951824; PMCID: PMC3497676.

31. Price GE, Lo CY, Mispion JA, Epstein SL. Mucosal immunization with a candidate universal influenza vaccine reduces virus transmission in a mouse model. *J Virol*. 2014;88(11):6019-30. Epub 20140312. doi: 10.1128/JVI.03101-13. PubMed PMID: 24623430; PMCID: PMC4093854.
  
32. Ortigoza MB, Blaser SB, Zafar MA, Hammond AJ, Weiser JN. An Infant Mouse Model of Influenza Virus Transmission Demonstrates the Role of Virus-Specific Shedding, Humoral Immunity, and Sialidase Expression by Colonizing *Streptococcus pneumoniae*. *mBio*. 2018;9(6). Epub 20181218. doi: 10.1128/mBio.02359-18. PubMed PMID: 30563897; PMCID: PMC6299224.
  
33. Lowen AC, Mubareka S, Steel J, Palese P. Influenza virus transmission is dependent on relative humidity and temperature. *PLoS Pathog*. 2007;3(10):1470-6. doi: 10.1371/journal.ppat.0030151. PubMed PMID: 17953482; PMCID: PMC2034399.
  
34. Matsuoka Y, Lamirande EW, Subbarao K. The ferret model for influenza. *Curr Protoc Microbiol*. 2009;Chapter 15:Unit 15G 2. doi: 10.1002/9780471729259.mc15g02s13. PubMed PMID: 19412910.
  
35. Francis T, Magill TP. Immunological Studies with the Virus of Influenza. *J Exp Med*. 1935;62(4):505-16. doi: 10.1084/jem.62.4.505. PubMed PMID: 19870430; PMCID: PMC2133289.

36. Richard M, van den Brand JMA, Bestebroer TM, Lexmond P, de Meulder D, Fouchier RAM, Lowen AC, Herfst S. Influenza A viruses are transmitted via the air from the nasal respiratory epithelium of ferrets. *Nat Commun.* 2020;11(1):766. Epub 20200207. doi: 10.1038/s41467-020-14626-0. PubMed PMID: 32034144; PMCID: PMC7005743.
37. Karlsson EA, Meliopoulos VA, Savage C, Livingston B, Mehle A, Schultz-Cherry S. Visualizing real-time influenza virus infection, transmission and protection in ferrets. *Nat Commun.* 2015;6:6378. Epub 20150306. doi: 10.1038/ncomms7378. PubMed PMID: 25744559; PMCID: PMC4366512.
38. Maines TR, Chen LM, Matsuoka Y, Chen H, Rowe T, Ortin J, Falcon A, Nguyen TH, Mai le Q, Sedyaningsih ER, Harun S, Tumpey TM, Donis RO, Cox NJ, Subbarao K, Katz JM. Lack of transmission of H5N1 avian-human reassortant influenza viruses in a ferret model. *Proc Natl Acad Sci U S A.* 2006;103(32):12121-6. Epub 20060731. doi: 10.1073/pnas.0605134103. PubMed PMID: 16880383; PMCID: PMC1567706.
39. Kimble JB, Angel M, Wan H, Sutton TC, Finch C, Perez DR. Alternative reassortment events leading to transmissible H9N1 influenza viruses in the ferret model. *J Virol.* 2014;88(1):66-71. Epub 20131016. doi: 10.1128/JVI.02677-13. PubMed PMID: 24131710; PMCID: PMC3911707.
40. Belser JA, Blixt O, Chen LM, Pappas C, Maines TR, Van Hoeven N, Donis R, Busch J, McBride R, Paulson JC, Katz JM, Tumpey TM. Contemporary North American influenza H7

viruses possess human receptor specificity: Implications for virus transmissibility. *Proc Natl Acad Sci U S A*. 2008;105(21):7558-63. Epub 20080527. doi: 10.1073/pnas.0801259105. PubMed PMID: 18508975; PMCID: PMC2396559.

41. Munster VJ, de Wit E, van den Brand JM, Herfst S, Schrauwen EJ, Bestebroer TM, van de Vijver D, Boucher CA, Koopmans M, Rimmelzwaan GF, Kuiken T, Osterhaus AD, Fouchier RA. Pathogenesis and transmission of swine-origin 2009 A(H1N1) influenza virus in ferrets. *Science*. 2009;325(5939):481-3. Epub 20090702. doi: 10.1126/science.1177127. PubMed PMID: 19574348; PMCID: PMC4814155.

42. Zhu H, Wang D, Kelvin DJ, Li L, Zheng Z, Yoon SW, Wong SS, Farooqui A, Wang J, Banner D, Chen R, Zheng R, Zhou J, Zhang Y, Hong W, Dong W, Cai Q, Roehrl MH, Huang SS, Kelvin AA, Yao T, Zhou B, Chen X, Leung GM, Poon LL, Webster RG, Webby RJ, Peiris JS, Guan Y, Shu Y. Infectivity, transmission, and pathology of human-isolated H7N9 influenza virus in ferrets and pigs. *Science*. 2013;341(6142):183-6. Epub 20130523. doi: 10.1126/science.1239844. PubMed PMID: 23704376.

43. Lee LYY, Zhou J, Frise R, Goldhill DH, Koszalka P, Mifsud EJ, Baba K, Noda T, Ando Y, Sato K, Yuki AI, Shishido T, Uehara T, Wildum S, Zwanziger E, Collinson N, Kuhlbusch K, Clinch B, Hurt AC, Barclay WS. Baloxavir treatment of ferrets infected with influenza A(H1N1)pdm09 virus reduces onward transmission. *PLoS Pathog*. 2020;16(4):e1008395. Epub 20200415. doi: 10.1371/journal.ppat.1008395. PubMed PMID: 32294137; PMCID: PMC7159184.

44. Herlocher ML, Truscon R, Elias S, Yen HL, Roberts NA, Ohmit SE, Monto AS. Influenza viruses resistant to the antiviral drug oseltamivir: transmission studies in ferrets. *J Infect Dis.* 2004;190(9):1627-30. Epub 20040928. doi: 10.1086/424572. PubMed PMID: 15478068.
45. Pearce MB, Belser JA, Houser KV, Katz JM, Tumpey TM. Efficacy of seasonal live attenuated influenza vaccine against virus replication and transmission of a pandemic 2009 H1N1 virus in ferrets. *Vaccine.* 2011;29(16):2887-94. Epub 20110221. doi: 10.1016/j.vaccine.2011.02.014. PubMed PMID: 21338676.
46. Le Sage V, Jones JE, Kormuth KA, Fitzsimmons WJ, Nturibi E, Padovani GH, Arevalo CP, French AJ, Avery AJ, Manivanh R, McGrady EE, Bhagwat AR, Luring AS, Hensley SE, Lakdawala SS. Pre-existing heterosubtypic immunity provides a barrier to airborne transmission of influenza viruses. *PLoS Pathog.* 2021;17(2):e1009273. Epub 20210218. doi: 10.1371/journal.ppat.1009273. PubMed PMID: 33600489; PMCID: PMC7891786.
47. Kwon YK, Lipatov AS, Swayne DE. Bronchointerstitial pneumonia in guinea pigs following inoculation with H5N1 high pathogenicity avian influenza virus. *Vet Pathol.* 2009;46(1):138-41. doi: 10.1354/vp.46-1-138. PubMed PMID: 19112127.
48. Van Hoeven N, Belser JA, Szretter KJ, Zeng H, Staeheli P, Swayne DE, Katz JM, Tumpey TM. Pathogenesis of 1918 pandemic and H5N1 influenza virus infections in a guinea

pig model: antiviral potential of exogenous alpha interferon to reduce virus shedding. *J Virol.* 2009;83(7):2851-61. Epub 20090114. doi: 10.1128/JVI.02174-08. PubMed PMID: 19144714; PMCID: PMC2655560.

49. Henrickson KJ. Parainfluenza viruses. *Clin Microbiol Rev.* 2003;16(2):242-64. doi: 10.1128/CMR.16.2.242-264.2003. PubMed PMID: 12692097; PMCID: PMC153148.

50. Johnson DP, Green RH. Viremia during parainfluenza type 3 virus infection of hamsters. *Proc Soc Exp Biol Med.* 1973;144(3):745-8. doi: 10.3181/00379727-144-37673. PubMed PMID: 4358238.

51. Mascoli CC, Metzgar DP, Larson EJ, Fuscaldo AA, Gower TA. An animal model for studying infection and immunity to and attenuation of human parainfluenza viruses. *Dev Biol Stand.* 1975;28:414-21. PubMed PMID: 165121.

52. Murphy TF, Dubovi EJ, Clyde WA, Jr. The cotton rat as an experimental model of human parainfluenza virus type 3 disease. *Exp Lung Res.* 1981;2(2):97-109. doi: 10.3109/01902148109052306. PubMed PMID: 6268401.

53. Rijsbergen LC, Schmitz KS, Begeman L, Drew-Bear J, Gommers L, Lamers MM, Greninger AL, Haagmans BL, Porotto M, de Swart RL, Moscona A, de Vries RD. Modeling Infection and Tropism of Human Parainfluenza Virus Type 3 in Ferrets. *mBio.*

2021;13(1):e0383121. Epub 20220215. doi: 10.1128/mbio.03831-21. PubMed PMID: 35164568; PMCID: PMC8844927.

54. Galinski MS, Mink MA, Lambert DM, Wechsler SL, Pons MW. Molecular cloning and sequence analysis of the human parainfluenza 3 virus gene encoding the matrix protein. *Virology*. 1987;157(1):24-30. doi: 10.1016/0042-6822(87)90309-6. PubMed PMID: 3029963.

55. Takimoto T, Bousse T, Coronel EC, Scroggs RA, Portner A. Cytoplasmic domain of Sendai virus HN protein contains a specific sequence required for its incorporation into virions. *J Virol*. 1998;72(12):9747-54. doi: 10.1128/JVI.72.12.9747-9754.1998. PubMed PMID: 9811709; PMCID: PMC110485.

56. Takimoto T, Bousse T, Portner A. Molecular cloning and expression of human parainfluenza virus type 1 L gene. *Virus Res*. 2000;70(1-2):45-53. doi: 10.1016/s0168-1702(00)00207-0. PubMed PMID: 11074124.

57. Lyn D, Gill DS, Scroggs RA, Portner A. The nucleoproteins of human parainfluenza virus type 1 and Sendai virus share amino acid sequences and antigenic and structural determinants. *J Gen Virol*. 1991;72 ( Pt 4):983-7. doi: 10.1099/0022-1317-72-4-983. PubMed PMID: 1707951.

58. Dave VP, Allan JE, Slobod KS, Smith FS, Ryan KW, Takimoto T, Power UF, Portner A, Hurwitz JL. Viral cross-reactivity and antigenic determinants recognized by human

parainfluenza virus type 1-specific cytotoxic T-cells. *Virology*. 1994;199(2):376-83. doi: 10.1006/viro.1994.1135. PubMed PMID: 7510085.

59. Skiadopoulos MH, Surman SR, Riggs JM, Elkins WR, St Claire M, Nishio M, Garcin D, Kolakofsky D, Collins PL, Murphy BR. Sendai virus, a murine parainfluenza virus type 1, replicates to a level similar to human PIV1 in the upper and lower respiratory tract of African green monkeys and chimpanzees. *Virology*. 2002;297(1):153-60. doi: 10.1006/viro.2002.1416. PubMed PMID: 12083845.

60. Hurwitz JL, Soike KF, Sangster MY, Portner A, Sealy RE, Dawson DH, Coleclough C. Intranasal Sendai virus vaccine protects African green monkeys from infection with human parainfluenza virus-type one. *Vaccine*. 1997;15(5):533-40. doi: 10.1016/s0264-410x(97)00217-x. PubMed PMID: 9160521.

61. Burke CW, Mason JN, Surman SL, Jones BG, Dalloneau E, Hurwitz JL, Russell CJ. Illumination of parainfluenza virus infection and transmission in living animals reveals a tissue-specific dichotomy. *PLoS Pathog*. 2011;7(7):e1002134. Epub 20110707. doi: 10.1371/journal.ppat.1002134. PubMed PMID: 21750677; PMCID: PMC3131265.

62. Couceiro JN, Paulson JC, Baum LG. Influenza virus strains selectively recognize sialyloligosaccharides on human respiratory epithelium; the role of the host cell in selection of hemagglutinin receptor specificity. *Virus Res*. 1993;29(2):155-65. doi: 10.1016/0168-1702(93)90056-s. PubMed PMID: 8212857.

63. Shinya K, Ebina M, Yamada S, Ono M, Kasai N, Kawaoka Y. Avian flu: influenza virus receptors in the human airway. *Nature*. 2006;440(7083):435-6. doi: 10.1038/440435a. PubMed PMID: 16554799.
64. Markwell MA, Paulson JC. Sendai virus utilizes specific sialyloligosaccharides as host cell receptor determinants. *Proc Natl Acad Sci U S A*. 1980;77(10):5693-7. doi: 10.1073/pnas.77.10.5693. PubMed PMID: 6255459; PMCID: PMC350135.
65. Yonemitsu Y, Kitson C, Ferrari S, Farley R, Griesenbach U, Judd D, Steel R, Scheid P, Zhu J, Jeffery PK, Kato A, Hasan MK, Nagai Y, Masaki I, Fukumura M, Hasegawa M, Geddes DM, Alton EW. Efficient gene transfer to airway epithelium using recombinant Sendai virus. *Nat Biotechnol*. 2000;18(9):970-3. doi: 10.1038/79463. PubMed PMID: 10973218.
66. Hewitt RJ, Lloyd CM. Regulation of immune responses by the airway epithelial cell landscape. *Nat Rev Immunol*. 2021;21(6):347-62. Epub 20210113. doi: 10.1038/s41577-020-00477-9. PubMed PMID: 33442032; PMCID: PMC7804588.
67. Whitsett JA. Airway Epithelial Differentiation and Mucociliary Clearance. *Ann Am Thorac Soc*. 2018;15(Suppl 3):S143-S8. doi: 10.1513/AnnalsATS.201802-128AW. PubMed PMID: 30431340; PMCID: PMC6322033.

68. Rock JR, Onaitis MW, Rawlins EL, Lu Y, Clark CP, Xue Y, Randell SH, Hogan BL. Basal cells as stem cells of the mouse trachea and human airway epithelium. *Proc Natl Acad Sci U S A*. 2009;106(31):12771-5. Epub 20090722. doi: 10.1073/pnas.0906850106. PubMed PMID: 19625615; PMCID: PMC2714281.
69. Denney L, Ho LP. The role of respiratory epithelium in host defence against influenza virus infection. *Biomed J*. 2018;41(4):218-33. Epub 20180910. doi: 10.1016/j.bj.2018.08.004. PubMed PMID: 30348265; PMCID: PMC6197993.
70. Alexopoulou L, Holt AC, Medzhitov R, Flavell RA. Recognition of double-stranded RNA and activation of NF-kappaB by Toll-like receptor 3. *Nature*. 2001;413(6857):732-8. doi: 10.1038/35099560. PubMed PMID: 11607032.
71. Diebold SS, Kaisho T, Hemmi H, Akira S, Reis e Sousa C. Innate antiviral responses by means of TLR7-mediated recognition of single-stranded RNA. *Science*. 2004;303(5663):1529-31. Epub 20040219. doi: 10.1126/science.1093616. PubMed PMID: 14976261.
72. Lund J, Sato A, Akira S, Medzhitov R, Iwasaki A. Toll-like receptor 9-mediated recognition of Herpes simplex virus-2 by plasmacytoid dendritic cells. *J Exp Med*. 2003;198(3):513-20. doi: 10.1084/jem.20030162. PubMed PMID: 12900525; PMCID: PMC2194085.

73. Hornung V, Ellegast J, Kim S, Brzozka K, Jung A, Kato H, Poeck H, Akira S, Conzelmann KK, Schlee M, Endres S, Hartmann G. 5'-Triphosphate RNA is the ligand for RIG-I. *Science*. 2006;314(5801):994-7. Epub 20061012. doi: 10.1126/science.1132505. PubMed PMID: 17038590.
74. Kato H, Takeuchi O, Sato S, Yoneyama M, Yamamoto M, Matsui K, Uematsu S, Jung A, Kawai T, Ishii KJ, Yamaguchi O, Otsu K, Tsujimura T, Koh CS, Reis e Sousa C, Matsuura Y, Fujita T, Akira S. Differential roles of MDA5 and RIG-I helicases in the recognition of RNA viruses. *Nature*. 2006;441(7089):101-5. Epub 20060409. doi: 10.1038/nature04734. PubMed PMID: 16625202.
75. Decout A, Katz JD, Venkatraman S, Ablasser A. The cGAS-STING pathway as a therapeutic target in inflammatory diseases. *Nat Rev Immunol*. 2021;21(9):548-69. Epub 20210408. doi: 10.1038/s41577-021-00524-z. PubMed PMID: 33833439; PMCID: PMC8029610.
76. Le Goffic R, Pothlichet J, Vitour D, Fujita T, Meurs E, Chignard M, Si-Tahar M. Cutting Edge: Influenza A virus activates TLR3-dependent inflammatory and RIG-I-dependent antiviral responses in human lung epithelial cells. *J Immunol*. 2007;178(6):3368-72. doi: 10.4049/jimmunol.178.6.3368. PubMed PMID: 17339430.

77. Lazear HM, Nice TJ, Diamond MS. Interferon-lambda: Immune Functions at Barrier Surfaces and Beyond. *Immunity*. 2015;43(1):15-28. doi: 10.1016/j.immuni.2015.07.001. PubMed PMID: 26200010; PMCID: PMC4527169.
78. Iwasaki A, Pillai PS. Innate immunity to influenza virus infection. *Nat Rev Immunol*. 2014;14(5):315-28. doi: 10.1038/nri3665. PubMed PMID: 24762827; PMCID: PMC4104278.
79. Everitt AR, Clare S, Pertel T, John SP, Wash RS, Smith SE, Chin CR, Feeley EM, Sims JS, Adams DJ, Wise HM, Kane L, Goulding D, Digard P, Anttila V, Baillie JK, Walsh TS, Hume DA, Palotie A, Xue Y, Colonna V, Tyler-Smith C, Dunning J, Gordon SB, Gen II, Investigators M, Smyth RL, Openshaw PJ, Dougan G, Brass AL, Kellam P. IFITM3 restricts the morbidity and mortality associated with influenza. *Nature*. 2012;484(7395):519-23. Epub 20120325. doi: 10.1038/nature10921. PubMed PMID: 22446628; PMCID: PMC3648786.
80. Plataniias LC. Mechanisms of type-I- and type-II-interferon-mediated signalling. *Nat Rev Immunol*. 2005;5(5):375-86. doi: 10.1038/nri1604. PubMed PMID: 15864272.
81. Kalliolias GD, Ivashkiv LB. TNF biology, pathogenic mechanisms and emerging therapeutic strategies. *Nat Rev Rheumatol*. 2016;12(1):49-62. Epub 20151210. doi: 10.1038/nrrheum.2015.169. PubMed PMID: 26656660; PMCID: PMC4809675.

82. Dinarello CA. Immunological and inflammatory functions of the interleukin-1 family. *Annu Rev Immunol.* 2009;27:519-50. doi: 10.1146/annurev.immunol.021908.132612. PubMed PMID: 19302047.
83. Herold S, von Wulffen W, Steinmueller M, Pleschka S, Kuziel WA, Mack M, Srivastava M, Seeger W, Maus UA, Lohmeyer J. Alveolar epithelial cells direct monocyte transepithelial migration upon influenza virus infection: impact of chemokines and adhesion molecules. *J Immunol.* 2006;177(3):1817-24. doi: 10.4049/jimmunol.177.3.1817. PubMed PMID: 16849492.
84. Bickel M. The role of interleukin-8 in inflammation and mechanisms of regulation. *J Periodontol.* 1993;64(5 Suppl):456-60. PubMed PMID: 8315568.
85. Palomino-Segura M, Perez L, Farsakoglu Y, Virgilio T, Latino I, D'Antuono R, Chatziandreou N, Pizzagalli DU, Wang G, Garcia-Sastre A, Sallusto F, Carroll MC, Neyrolles O, Gonzalez SF. Protection against influenza infection requires early recognition by inflammatory dendritic cells through C-type lectin receptor SIGN-R1. *Nat Microbiol.* 2019;4(11):1930-40. Epub 20190729. doi: 10.1038/s41564-019-0506-6. PubMed PMID: 31358982; PMCID: PMC6817362.
86. Gazit R, Gruda R, Elboim M, Arnon TI, Katz G, Achdout H, Hanna J, Qimron U, Landau G, Greenbaum E, Zakay-Rones Z, Porgador A, Mandelboim O. Lethal influenza infection in the absence of the natural killer cell receptor gene *Ncr1*. *Nat Immunol.* 2006;7(5):517-23. Epub 20060326. doi: 10.1038/ni1322. PubMed PMID: 16565719.

87. Albert ML, Sauter B, Bhardwaj N. Dendritic cells acquire antigen from apoptotic cells and induce class I-restricted CTLs. *Nature*. 1998;392(6671):86-9. doi: 10.1038/32183. PubMed PMID: 9510252.
88. Hargadon KM, Zhou H, Albrecht RA, Dodd HA, Garcia-Sastre A, Braciale TJ. Major histocompatibility complex class II expression and hemagglutinin subtype influence the infectivity of type A influenza virus for respiratory dendritic cells. *J Virol*. 2011;85(22):11955-63. Epub 20110914. doi: 10.1128/JVI.05830-11. PubMed PMID: 21917972; PMCID: PMC3209325.
89. Vander Lugt B, Khan AA, Hackney JA, Agrawal S, Lesch J, Zhou M, Lee WP, Park S, Xu M, DeVoss J, Spooner CJ, Chalouni C, Delamarre L, Mellman I, Singh H. Transcriptional programming of dendritic cells for enhanced MHC class II antigen presentation. *Nat Immunol*. 2014;15(2):161-7. Epub 20131222. doi: 10.1038/ni.2795. PubMed PMID: 24362890.
90. Liu J, Zhang X, Cheng Y, Cao X. Dendritic cell migration in inflammation and immunity. *Cell Mol Immunol*. 2021;18(11):2461-71. Epub 20210723. doi: 10.1038/s41423-021-00726-4. PubMed PMID: 34302064; PMCID: PMC8298985.
91. Paik DH, Farber DL. Influenza infection fortifies local lymph nodes to promote lung-resident heterosubtypic immunity. *J Exp Med*. 2021;218(1). doi: 10.1084/jem.20200218. PubMed PMID: 33005934; PMCID: PMC7534905.

92. Pan WR, Suami H, Corlett RJ, Ashton MW. Lymphatic drainage of the nasal fossae and nasopharynx: preliminary anatomical and radiological study with clinical implications. *Head Neck*. 2009;31(1):52-7. doi: 10.1002/hed.20926. PubMed PMID: 18972423.
93. Braun A, Worbs T, Moschovakis GL, Halle S, Hoffmann K, Bolter J, Munk A, Forster R. Afferent lymph-derived T cells and DCs use different chemokine receptor CCR7-dependent routes for entry into the lymph node and intranodal migration. *Nat Immunol*. 2011;12(9):879-87. Epub 20110814. doi: 10.1038/ni.2085. PubMed PMID: 21841786.
94. Ho AW, Prabhu N, Betts RJ, Ge MQ, Dai X, Hutchinson PE, Lew FC, Wong KL, Hanson BJ, Macary PA, Kemeny DM. Lung CD103+ dendritic cells efficiently transport influenza virus to the lymph node and load viral antigen onto MHC class I for presentation to CD8 T cells. *J Immunol*. 2011;187(11):6011-21. Epub 20111031. doi: 10.4049/jimmunol.1100987. PubMed PMID: 22043017.
95. Bousso P, Robey E. Dynamics of CD8+ T cell priming by dendritic cells in intact lymph nodes. *Nat Immunol*. 2003;4(6):579-85. Epub 20030505. doi: 10.1038/ni928. PubMed PMID: 12730692.
96. Burnet FM. A modification of Jerne's theory of antibody production using the concept of clonal selection. *CA Cancer J Clin*. 1976;26(2):119-21. doi: 10.3322/canjclin.26.2.119. PubMed PMID: 816431.

97. Hendriks J, Xiao Y, Borst J. CD27 promotes survival of activated T cells and complements CD28 in generation and establishment of the effector T cell pool. *J Exp Med*. 2003;198(9):1369-80. Epub 20031027. doi: 10.1084/jem.20030916. PubMed PMID: 14581610; PMCID: PMC2194245.
98. Hendriks J, Xiao Y, Rossen JW, van der Sluijs KF, Sugamura K, Ishii N, Borst J. During viral infection of the respiratory tract, CD27, 4-1BB, and OX40 collectively determine formation of CD8+ memory T cells and their capacity for secondary expansion. *J Immunol*. 2005;175(3):1665-76. doi: 10.4049/jimmunol.175.3.1665. PubMed PMID: 16034107.
99. Yamane H, Paul WE. Early signaling events that underlie fate decisions of naive CD4(+) T cells toward distinct T-helper cell subsets. *Immunol Rev*. 2013;252(1):12-23. doi: 10.1111/imr.12032. PubMed PMID: 23405892; PMCID: PMC3578301.
100. Matloubian M, Lo CG, Cinamon G, Lesneski MJ, Xu Y, Brinkmann V, Allende ML, Proia RL, Cyster JG. Lymphocyte egress from thymus and peripheral lymphoid organs is dependent on S1P receptor 1. *Nature*. 2004;427(6972):355-60. doi: 10.1038/nature02284. PubMed PMID: 14737169.
101. Flynn KJ, Belz GT, Altman JD, Ahmed R, Woodland DL, Doherty PC. Virus-specific CD8+ T cells in primary and secondary influenza pneumonia. *Immunity*. 1998;8(6):683-91. doi: 10.1016/s1074-7613(00)80573-7. PubMed PMID: 9655482.

102. Mikhak Z, Strassner JP, Luster AD. Lung dendritic cells imprint T cell lung homing and promote lung immunity through the chemokine receptor CCR4. *J Exp Med*. 2013;210(9):1855-69. Epub 20130819. doi: 10.1084/jem.20130091. PubMed PMID: 23960189; PMCID: PMC3754856.

103. Dhume K, Finn CM, Strutt TM, Sell S, McKinstry KK. T-bet optimizes CD4 T-cell responses against influenza through CXCR3-dependent lung trafficking but not functional programming. *Mucosal Immunol*. 2019;12(5):1220-30. Epub 20190705. doi: 10.1038/s41385-019-0183-z. PubMed PMID: 31278374; PMCID: PMC6717559.

104. Galkina E, Thatte J, Dabak V, Williams MB, Ley K, Braciale TJ. Preferential migration of effector CD8+ T cells into the interstitium of the normal lung. *J Clin Invest*. 2005;115(12):3473-83. Epub 20051123. doi: 10.1172/JCI24482. PubMed PMID: 16308575; PMCID: PMC1288831.

105. Kohlmeier JE, Miller SC, Smith J, Lu B, Gerard C, Cookenham T, Roberts AD, Woodland DL. The chemokine receptor CCR5 plays a key role in the early memory CD8+ T cell response to respiratory virus infections. *Immunity*. 2008;29(1):101-13. doi: 10.1016/j.immuni.2008.05.011. PubMed PMID: 18617426; PMCID: PMC2519120.

106. Slutter B, Pewe LL, Kaech SM, Harty JT. Lung airway-surveilling CXCR3(hi) memory CD8(+) T cells are critical for protection against influenza A virus. *Immunity*. 2013;39(5):939-48. doi: 10.1016/j.immuni.2013.09.013. PubMed PMID: 24238342; PMCID: PMC3872058.
107. Lim K, Hyun YM, Lambert-Emo K, Capece T, Bae S, Miller R, Topham DJ, Kim M. Neutrophil trails guide influenza-specific CD8(+) T cells in the airways. *Science*. 2015;349(6252):aaa4352. doi: 10.1126/science.aaa4352. PubMed PMID: 26339033; PMCID: PMC4809646.
108. Wein AN, McMaster SR, Takamura S, Dunbar PR, Cartwright EK, Hayward SL, McManus DT, Shimaoka T, Ueha S, Tsukui T, Masumoto T, Kurachi M, Matsushima K, Kohlmeier JE. CXCR6 regulates localization of tissue-resident memory CD8 T cells to the airways. *J Exp Med*. 2019;216(12):2748-62. Epub 20190926. doi: 10.1084/jem.20181308. PubMed PMID: 31558615; PMCID: PMC6888981.
109. Thatte J, Dabak V, Williams MB, Braciale TJ, Ley K. LFA-1 is required for retention of effector CD8 T cells in mouse lungs. *Blood*. 2003;101(12):4916-22. Epub 20030306. doi: 10.1182/blood-2002-10-3159. PubMed PMID: 12623847.
110. Pizzolla A, Wang Z, Groom JR, Kedzierska K, Brooks AG, Reading PC, Wakim LM. Nasal-associated lymphoid tissues (NALTs) support the recall but not priming of influenza virus-specific cytotoxic T cells. *Proc Natl Acad Sci U S A*. 2017;114(20):5225-30. Epub 20170501. doi: 10.1073/pnas.1620194114. PubMed PMID: 28461487; PMCID: PMC5441821.

111. Kiyono H, Fukuyama S. NALT- versus Peyer's-patch-mediated mucosal immunity. *Nat Rev Immunol.* 2004;4(9):699-710. doi: 10.1038/nri1439. PubMed PMID: 15343369; PMCID: PMC7097243.
112. Barry M, Bleackley RC. Cytotoxic T lymphocytes: all roads lead to death. *Nat Rev Immunol.* 2002;2(6):401-9. doi: 10.1038/nri819. PubMed PMID: 12093006.
113. Shresta S, Goda P, Wesselschmidt R, Ley TJ. Residual cytotoxicity and granzyme K expression in granzyme A-deficient cytotoxic lymphocytes. *J Biol Chem.* 1997;272(32):20236-44. doi: 10.1074/jbc.272.32.20236. PubMed PMID: 9242702.
114. Rouvier E, Luciani MF, Golstein P. Fas involvement in Ca(2+)-independent T cell-mediated cytotoxicity. *J Exp Med.* 1993;177(1):195-200. doi: 10.1084/jem.177.1.195. PubMed PMID: 7678113; PMCID: PMC2190860.
115. Claassen EA, van der Kant PA, Rychnavska ZS, van Bleek GM, Easton AJ, van der Most RG. Activation and inactivation of antiviral CD8 T cell responses during murine pneumovirus infection. *J Immunol.* 2005;175(10):6597-604. doi: 10.4049/jimmunol.175.10.6597. PubMed PMID: 16272314.
116. Rodrigues LS, Barreto AS, Bomfim LGS, Gomes MC, Ferreira NLC, da Cruz GS, Magalhaes LS, de Jesus AR, Palatnik-de-Sousa CB, Correa CB, de Almeida RP. Multifunctional,

TNF-alpha and IFN-gamma-Secreting CD4 and CD8 T Cells and CD8(High) T Cells Are Associated With the Cure of Human Visceral Leishmaniasis. *Front Immunol.* 2021;12:773983. Epub 20211028. doi: 10.3389/fimmu.2021.773983. PubMed PMID: 34777391; PMCID: PMC8581227.

117. Sun J, Madan R, Karp CL, Braciale TJ. Effector T cells control lung inflammation during acute influenza virus infection by producing IL-10. *Nat Med.* 2009;15(3):277-84. Epub 20090222. doi: 10.1038/nm.1929. PubMed PMID: 19234462; PMCID: PMC2693210.

118. Badovinac VP, Porter BB, Harty JT. CD8+ T cell contraction is controlled by early inflammation. *Nat Immunol.* 2004;5(8):809-17. Epub 20040711. doi: 10.1038/ni1098. PubMed PMID: 15247915.

119. Yuzefpolskiy Y, Baumann FM, Kalia V, Sarkar S. Early CD8 T-cell memory precursors and terminal effectors exhibit equipotent in vivo degranulation. *Cell Mol Immunol.* 2015;12(4):400-8. Epub 20140728. doi: 10.1038/cmi.2014.48. PubMed PMID: 25066419; PMCID: PMC4496536.

120. Kaech SM, Tan JT, Wherry EJ, Konieczny BT, Surh CD, Ahmed R. Selective expression of the interleukin 7 receptor identifies effector CD8 T cells that give rise to long-lived memory cells. *Nat Immunol.* 2003;4(12):1191-8. Epub 20031116. doi: 10.1038/ni1009. PubMed PMID: 14625547.

121. Pizzolla A, Wakim LM. Memory T Cell Dynamics in the Lung during Influenza Virus Infection. *J Immunol*. 2019;202(2):374-81. doi: 10.4049/jimmunol.1800979. PubMed PMID: 30617119.
122. Mueller SN, Gebhardt T, Carbone FR, Heath WR. Memory T cell subsets, migration patterns, and tissue residence. *Annu Rev Immunol*. 2013;31:137-61. Epub 20121203. doi: 10.1146/annurev-immunol-032712-095954. PubMed PMID: 23215646.
123. Sallusto F, Geginat J, Lanzavecchia A. Central memory and effector memory T cell subsets: function, generation, and maintenance. *Annu Rev Immunol*. 2004;22:745-63. doi: 10.1146/annurev.immunol.22.012703.104702. PubMed PMID: 15032595.
124. Masopust D, Soerens AG. Tissue-Resident T Cells and Other Resident Leukocytes. *Annu Rev Immunol*. 2019;37:521-46. Epub 20190206. doi: 10.1146/annurev-immunol-042617-053214. PubMed PMID: 30726153; PMCID: PMC7175802.
125. Gebhardt T, Wakim LM, Eidsmo L, Reading PC, Heath WR, Carbone FR. Memory T cells in nonlymphoid tissue that provide enhanced local immunity during infection with herpes simplex virus. *Nat Immunol*. 2009;10(5):524-30. Epub 20090322. doi: 10.1038/ni.1718. PubMed PMID: 19305395.
126. Pizzolla A, Nguyen THO, Smith JM, Brooks AG, Kedzieska K, Heath WR, Reading PC, Wakim LM. Resident memory CD8(+) T cells in the upper respiratory tract prevent pulmonary

influenza virus infection. *Sci Immunol*. 2017;2(12). doi: 10.1126/sciimmunol.aam6970. PubMed PMID: 28783656.

127. Zheng MZM, Wakim LM. Tissue resident memory T cells in the respiratory tract. *Mucosal Immunol*. 2022;15(3):379-88. Epub 20211020. doi: 10.1038/s41385-021-00461-z. PubMed PMID: 34671115; PMCID: PMC8526531.

128. Kumar BV, Ma W, Miron M, Granot T, Guyer RS, Carpenter DJ, Senda T, Sun X, Ho SH, Lerner H, Friedman AL, Shen Y, Farber DL. Human Tissue-Resident Memory T Cells Are Defined by Core Transcriptional and Functional Signatures in Lymphoid and Mucosal Sites. *Cell Rep*. 2017;20(12):2921-34. doi: 10.1016/j.celrep.2017.08.078. PubMed PMID: 28930685; PMCID: PMC5646692.

129. Christo SN, Evrard M, Park SL, Gandolfo LC, Burn TN, Fonseca R, Newman DM, Alexandre YO, Collins N, Zamudio NM, Souza-Fonseca-Guimaraes F, Pellicci DG, Chisanga D, Shi W, Bartholin L, Belz GT, Huntington ND, Lucas A, Lucas M, Mueller SN, Heath WR, Ginhoux F, Speed TP, Carbone FR, Kallies A, Mackay LK. Discrete tissue microenvironments instruct diversity in resident memory T cell function and plasticity. *Nat Immunol*. 2021;22(9):1140-51. Epub 20210823. doi: 10.1038/s41590-021-01004-1. PubMed PMID: 34426691.

130. Fonseca R, Burn TN, Gandolfo LC, Devi S, Park SL, Obers A, Evrard M, Christo SN, Buquicchio FA, Lareau CA, McDonald KM, Sandford SK, Zamudio NM, Zanluqui NG, Zaid A,

Speed TP, Satpathy AT, Mueller SN, Carbone FR, Mackay LK. Runx3 drives a CD8(+) T cell tissue residency program that is absent in CD4(+) T cells. *Nat Immunol.* 2022;23(8):1236-45. Epub 20220726. doi: 10.1038/s41590-022-01273-4. PubMed PMID: 35882933.

131. Cibrian D, Sanchez-Madrid F. CD69: from activation marker to metabolic gatekeeper. *Eur J Immunol.* 2017;47(6):946-53. doi: 10.1002/eji.201646837. PubMed PMID: 28475283; PMCID: PMC6485631.

132. Oja AE, Piet B, Helbig C, Stark R, van der Zwan D, Blaauwgeers H, Remmerswaal EBM, Amsen D, Jonkers RE, Moerland PD, Nolte MA, van Lier RAW, Hombrink P. Trigger-happy resident memory CD4(+) T cells inhabit the human lungs. *Mucosal Immunol.* 2018;11(3):654-67. Epub 20171115. doi: 10.1038/mi.2017.94. PubMed PMID: 29139478.

133. Lee YT, Suarez-Ramirez JE, Wu T, Redman JM, Bouchard K, Hadley GA, Cauley LS. Environmental and antigen receptor-derived signals support sustained surveillance of the lungs by pathogen-specific cytotoxic T lymphocytes. *J Virol.* 2011;85(9):4085-94. Epub 20110223. doi: 10.1128/JVI.02493-10. PubMed PMID: 21345961; PMCID: PMC3126261.

134. Takamura S, Yagi H, Hakata Y, Motozono C, McMaster SR, Masumoto T, Fujisawa M, Chikaishi T, Komeda J, Itoh J, Umemura M, Kyusai A, Tomura M, Nakayama T, Woodland DL, Kohlmeier JE, Miyazawa M. Specific niches for lung-resident memory CD8+ T cells at the site of tissue regeneration enable CD69-independent maintenance. *J Exp Med.* 2016;213(13):3057-

73. Epub 20161104. doi: 10.1084/jem.20160938. PubMed PMID: 27815325; PMCID: PMC5154946.
135. Ray SJ, Franki SN, Pierce RH, Dimitrova S, Koteliansky V, Sprague AG, Doherty PC, de Fougères AR, Topham DJ. The collagen binding  $\alpha 1\beta 1$  integrin VLA-1 regulates CD8 T cell-mediated immune protection against heterologous influenza infection. *Immunity*. 2004;20(2):167-79. doi: 10.1016/s1074-7613(04)00021-4. PubMed PMID: 14975239.
136. Ely KH, Cookenham T, Roberts AD, Woodland DL. Memory T cell populations in the lung airways are maintained by continual recruitment. *J Immunol*. 2006;176(1):537-43. doi: 10.4049/jimmunol.176.1.537. PubMed PMID: 16365448.
137. Park SL, Mackay LK. Decoding Tissue-Residency: Programming and Potential of Frontline Memory T Cells. *Cold Spring Harb Perspect Biol*. 2021;13(10). Epub 20211001. doi: 10.1101/cshperspect.a037960. PubMed PMID: 33753406; PMCID: PMC8485744.
138. Laidlaw BJ, Zhang N, Marshall HD, Staron MM, Guan T, Hu Y, Cauley LS, Craft J, Kaech SM. CD4<sup>+</sup> T cell help guides formation of CD103<sup>+</sup> lung-resident memory CD8<sup>+</sup> T cells during influenza viral infection. *Immunity*. 2014;41(4):633-45. Epub 20141009. doi: 10.1016/j.immuni.2014.09.007. PubMed PMID: 25308332; PMCID: PMC4324721.
139. Mackay LK, Wynne-Jones E, Freestone D, Pellicci DG, Mielke LA, Newman DM, Braun A, Masson F, Kallies A, Belz GT, Carbone FR. T-box Transcription Factors Combine with the

Cytokines TGF-beta and IL-15 to Control Tissue-Resident Memory T Cell Fate. *Immunity*. 2015;43(6):1101-11. doi: 10.1016/j.immuni.2015.11.008. PubMed PMID: 26682984.

140. Evrard M, Wynne-Jones E, Peng C, Kato Y, Christo SN, Fonseca R, Park SL, Burn TN, Osman M, Devi S, Chun J, Mueller SN, Kannourakis G, Berzins SP, Pellicci DG, Heath WR, Jameson SC, Mackay LK. Sphingosine 1-phosphate receptor 5 (S1PR5) regulates the peripheral retention of tissue-resident lymphocytes. *J Exp Med*. 2022;219(1). Epub 20211022. doi: 10.1084/jem.20210116. PubMed PMID: 34677611; PMCID: PMC8546662.

141. Anderson KG, Sung H, Skon CN, Lefrancois L, Deisinger A, Vezys V, Masopust D. Cutting edge: intravascular staining redefines lung CD8 T cell responses. *J Immunol*. 2012;189(6):2702-6. Epub 20120815. doi: 10.4049/jimmunol.1201682. PubMed PMID: 22896631; PMCID: PMC3436991.

142. Snyder ME, Farber DL. Human lung tissue resident memory T cells in health and disease. *Curr Opin Immunol*. 2019;59:101-8. Epub 20190629. doi: 10.1016/j.coi.2019.05.011. PubMed PMID: 31265968; PMCID: PMC6774897.

143. McMaster SR, Wilson JJ, Wang H, Kohlmeier JE. Airway-Resident Memory CD8 T Cells Provide Antigen-Specific Protection against Respiratory Virus Challenge through Rapid IFN-gamma Production. *J Immunol*. 2015;195(1):203-9. Epub 20150529. doi: 10.4049/jimmunol.1402975. PubMed PMID: 26026054; PMCID: PMC4475417.

144. Lim JME, Tan AT, Le Bert N, Hang SK, Low JGH, Bertoletti A. SARS-CoV-2 breakthrough infection in vaccinees induces virus-specific nasal-resident CD8<sup>+</sup> and CD4<sup>+</sup> T cells of broad specificity. *J Exp Med*. 2022;219(10). Epub 20220816. doi: 10.1084/jem.20220780. PubMed PMID: 35972472; PMCID: PMC9386509.
145. Ariotti S, Beltman JB, Chodaczek G, Hoekstra ME, van Beek AE, Gomez-Eerland R, Ritsma L, van Rheenen J, Maree AF, Zal T, de Boer RJ, Haanen JB, Schumacher TN. Tissue-resident memory CD8<sup>+</sup> T cells continuously patrol skin epithelia to quickly recognize local antigen. *Proc Natl Acad Sci U S A*. 2012;109(48):19739-44. Epub 20121112. doi: 10.1073/pnas.1208927109. PubMed PMID: 23150545; PMCID: PMC3511734.
146. Bergsbaken T, Bevan MJ, Fink PJ. Local Inflammatory Cues Regulate Differentiation and Persistence of CD8(+) Tissue-Resident Memory T Cells. *Cell Rep*. 2017;19(1):114-24. doi: 10.1016/j.celrep.2017.03.031. PubMed PMID: 28380351; PMCID: PMC5444811.
147. McMaster SR, Wein AN, Dunbar PR, Hayward SL, Cartwright EK, Denning TL, Kohlmeier JE. Pulmonary antigen encounter regulates the establishment of tissue-resident CD8 memory T cells in the lung airways and parenchyma. *Mucosal Immunol*. 2018;11(4):1071-8. Epub 20180216. doi: 10.1038/s41385-018-0003-x. PubMed PMID: 29453412; PMCID: PMC6030505.
148. Zhang N, Bevan MJ. Transforming growth factor-beta signaling controls the formation and maintenance of gut-resident memory T cells by regulating migration and retention.

Immunity. 2013;39(4):687-96. Epub 20130926. doi: 10.1016/j.immuni.2013.08.019. PubMed PMID: 24076049; PMCID: PMC3805703.

149. Wakim LM, Smith J, Caminschi I, Lahoud MH, Villadangos JA. Antibody-targeted vaccination to lung dendritic cells generates tissue-resident memory CD8 T cells that are highly protective against influenza virus infection. *Mucosal Immunol.* 2015;8(5):1060-71. Epub 20150114. doi: 10.1038/mi.2014.133. PubMed PMID: 25586557.

150. Jiang X, Clark RA, Liu L, Wagers AJ, Fuhlbrigge RC, Kupper TS. Skin infection generates non-migratory memory CD8<sup>+</sup> T(RM) cells providing global skin immunity. *Nature.* 2012;483(7388):227-31. Epub 20120229. doi: 10.1038/nature10851. PubMed PMID: 22388819; PMCID: PMC3437663.

151. Hayward SL, Scharer CD, Cartwright EK, Takamura S, Li ZT, Boss JM, Kohlmeier JE. Environmental cues regulate epigenetic reprogramming of airway-resident memory CD8(+) T cells. *Nat Immunol.* 2020;21(3):309-20. Epub 20200117. doi: 10.1038/s41590-019-0584-x. PubMed PMID: 31953534; PMCID: PMC7044042.

152. Wu T, Hu Y, Lee YT, Bouchard KR, Benechet A, Khanna K, Cauley LS. Lung-resident memory CD8 T cells (TRM) are indispensable for optimal cross-protection against pulmonary virus infection. *J Leukoc Biol.* 2014;95(2):215-24. Epub 20130904. doi: 10.1189/jlb.0313180. PubMed PMID: 24006506; PMCID: PMC3896663.

153. Slutter B, Van Braeckel-Budimir N, Abboud G, Varga SM, Salek-Ardakani S, Harty JT. Dynamics of influenza-induced lung-resident memory T cells underlie waning heterosubtypic immunity. *Sci Immunol*. 2017;2(7). Epub 20170106. doi: 10.1126/sciimmunol.aag2031. PubMed PMID: 28783666; PMCID: PMC5590757.
154. Uddback I, Cartwright EK, Scholler AS, Wein AN, Hayward SL, Lobby J, Takamura S, Thomsen AR, Kohlmeier JE, Christensen JP. Long-term maintenance of lung resident memory T cells is mediated by persistent antigen. *Mucosal Immunol*. 2021;14(1):92-9. Epub 20200609. doi: 10.1038/s41385-020-0309-3. PubMed PMID: 32518368; PMCID: PMC7726002.
155. Lobby JL, Uddback I, Scharer CD, Mi T, Boss JM, Thomsen AR, Christensen JP, Kohlmeier JE. Persistent Antigen Harbored by Alveolar Macrophages Enhances the Maintenance of Lung-Resident Memory CD8(+) T Cells. *J Immunol*. 2022;209(9):1778-87. Epub 20220926. doi: 10.4049/jimmunol.2200082. PubMed PMID: 36162870; PMCID: PMC9588742.
156. Qian Y, Zhu Y, Li Y, Li B. Legend of the Sentinels: Development of Lung Resident Memory T Cells and Their Roles in Diseases. *Front Immunol*. 2020;11:624411. Epub 20210202. doi: 10.3389/fimmu.2020.624411. PubMed PMID: 33603755; PMCID: PMC7884312.
157. Mintern JD, Guillonneau C, Carbone FR, Doherty PC, Turner SJ. Cutting edge: Tissue-resident memory CTL down-regulate cytolytic molecule expression following virus clearance. *J*

Immunol. 2007;179(11):7220-4. doi: 10.4049/jimmunol.179.11.7220. PubMed PMID: 18025163.

158. Pizzolla A, Nguyen TH, Sant S, Jaffar J, Loudovaris T, Mannering SI, Thomas PG, Westall GP, Kedzierska K, Wakim LM. Influenza-specific lung-resident memory T cells are proliferative and polyfunctional and maintain diverse TCR profiles. *J Clin Invest*. 2018;128(2):721-33. Epub 20180108. doi: 10.1172/JCI96957. PubMed PMID: 29309047; PMCID: PMC5785253.

159. Kumar BV, Kratchmarov R, Miron M, Carpenter DJ, Senda T, Lerner H, Friedman A, Reiner SL, Farber DL. Functional heterogeneity of human tissue-resident memory T cells based on dye efflux capacities. *JCI Insight*. 2018;3(22). Epub 20181115. doi: 10.1172/jci.insight.123568. PubMed PMID: 30429372; PMCID: PMC6302950.

160. McMaster SR, Gabbard JD, Koutsonanos DG, Compans RW, Tripp RA, Tompkins SM, Kohlmeier JE. Memory T cells generated by prior exposure to influenza cross react with the novel H7N9 influenza virus and confer protective heterosubtypic immunity. *PLoS One*. 2015;10(2):e0115725. Epub 20150211. doi: 10.1371/journal.pone.0115725. PubMed PMID: 25671696; PMCID: PMC4324938.

161. Clemens EB, van de Sandt C, Wong SS, Wakim LM, Valkenburg SA. Harnessing the Power of T Cells: The Promising Hope for a Universal Influenza Vaccine. *Vaccines (Basel)*.

2018;6(2). Epub 20180326. doi: 10.3390/vaccines6020018. PubMed PMID: 29587436; PMCID: PMC6027237.

162. Taylor PM, Askonas BA. Influenza nucleoprotein-specific cytotoxic T-cell clones are protective in vivo. *Immunology*. 1986;58(3):417-20. PubMed PMID: 2426185; PMCID: PMC1453480.

163. Terajima M, Cruz J, Leporati AM, Orphin L, Babon JA, Co MD, Pazoles P, Jameson J, Ennis FA. Influenza A virus matrix protein 1-specific human CD8<sup>+</sup> T-cell response induced in trivalent inactivated vaccine recipients. *J Virol*. 2008;82(18):9283-7. Epub 20080709. doi: 10.1128/JVI.01047-08. PubMed PMID: 18614638; PMCID: PMC2546892.

164. Wu T, Guan J, Handel A, Tschärke DC, Sidney J, Sette A, Wakim LM, Sng XYX, Thomas PG, Croft NP, Purcell AW, La Gruta NL. Quantification of epitope abundance reveals the effect of direct and cross-presentation on influenza CTL responses. *Nat Commun*. 2019;10(1):2846. Epub 20190628. doi: 10.1038/s41467-019-10661-8. PubMed PMID: 31253788; PMCID: PMC6599079.

165. Liu J, Yu J, McMahan K, Jacob-Dolan C, He X, Giffin V, Wu C, Sciacca M, Powers O, Nampanya F, Miller J, Lifton M, Hope D, Hall K, Hachmann NP, Chung B, Anioke T, Li W, Muench J, Gamblin A, Boursiquot M, Cook A, Lewis MG, Andersen H, Barouch DH. CD8 T cells contribute to vaccine protection against SARS-CoV-2 in macaques. *Sci Immunol*.

2022;7(77):eabq7647. Epub 20221111. doi: 10.1126/sciimmunol.abq7647. PubMed PMID: 35943359; PMCID: PMC9407944.

166. Cokaric Brdovcak M, Materljan J, Sustic M, Ravlic S, Ruzic T, Lisnic B, Miklic K, Brizic I, Pribanic Matesic M, Juranic Lisnic V, Halassy B, Roncevic D, Knezevic Z, Stefan L, Bertoglio F, Schubert M, Cicin-Sain L, Markotic A, Jonjic S, Krmpotic A. ChAdOx1-S adenoviral vector vaccine applied intranasally elicits superior mucosal immunity compared to the intramuscular route of vaccination. *Eur J Immunol.* 2022;52(6):936-45. Epub 20220331. doi: 10.1002/eji.202249823. PubMed PMID: 35304741; PMCID: PMC9087383.

167. Price GE, Lo CY, Misplon JA, Epstein SL. Reduction of Influenza A Virus Transmission in Mice by a Universal Intranasal Vaccine Candidate is Long-Lasting and Does Not Require Antibodies. *J Virol.* 2022;96(12):e0032022. Epub 20220531. doi: 10.1128/jvi.00320-22. PubMed PMID: 35638848; PMCID: PMC9215256.

168. Ssemaganda A, Nguyen HM, Nuhu F, Jahan N, Card CM, Kiazzyk S, Severini G, Keynan Y, Su RC, Ji H, Abrenica B, McLaren PJ, Ball TB, Bullard J, Van Caesele P, Stein D, McKinnon LR. Expansion of cytotoxic tissue-resident CD8(+) T cells and CCR6(+)CD161(+) CD4(+) T cells in the nasal mucosa following mRNA COVID-19 vaccination. *Nat Commun.* 2022;13(1):3357. Epub 20220610. doi: 10.1038/s41467-022-30913-4. PubMed PMID: 35688805; PMCID: PMC9186487.

169. Kunzli M, O'Flanagan SD, LaRue M, Talukder P, Dileepan T, Stolley JM, Soerens AG, Quarnstrom CF, Wijeyesinghe S, Ye Y, McPartlan JS, Mitchell JS, Mandl CW, Vile R, Jenkins MK, Ahmed R, Vezys V, Chahal JS, Masopust D. Route of self-amplifying mRNA vaccination modulates the establishment of pulmonary resident memory CD8 and CD4 T cells. *Sci Immunol*. 2022;7(78):eadd3075. Epub 20221202. doi: 10.1126/sciimmunol.add3075. PubMed PMID: 36459542; PMCID: PMC9832918.

170. Hoft DF, Babusis E, Worku S, Spencer CT, Lottenbach K, Truscott SM, Abate G, Sakala IG, Edwards KM, Creech CB, Gerber MA, Bernstein DI, Newman F, Graham I, Anderson EL, Belshe RB. Live and inactivated influenza vaccines induce similar humoral responses, but only live vaccines induce diverse T-cell responses in young children. *J Infect Dis*. 2011;204(6):845-53. Epub 20110815. doi: 10.1093/infdis/jir436. PubMed PMID: 21846636; PMCID: PMC3156924.

171. Wang Z, Kedzierski L, Nuessing S, Chua BYL, Quinones-Parra SM, Huber VC, Jackson DC, Thomas PG, Kedzierska K. Establishment of memory CD8+ T cells with live attenuated influenza virus across different vaccination doses. *J Gen Virol*. 2016;97(12):3205-14. Epub 20161102. doi: 10.1099/jgv.0.000651. PubMed PMID: 27902386.

172. Zens KD, Chen JK, Farber DL. Vaccine-generated lung tissue-resident memory T cells provide heterosubtypic protection to influenza infection. *JCI Insight*. 2016;1(10). doi: 10.1172/jci.insight.85832. PubMed PMID: 27468427; PMCID: PMC4959801.

173. Zheng MZM, Fritzlar S, Wang Z, Tan TK, Kedzierska K, Townsend A, Reading PC, Wakim LM. Cutting Edge: High-Dose Live Attenuated Influenza Vaccines Elicit Pulmonary Tissue-Resident Memory CD8+ T Cells in the Face of Pre-Existing Humoral Immunity. *J Immunol.* 2022;209(10):1832-6. doi: 10.4049/jimmunol.2200577. PubMed PMID: 36426954.
174. Ambrose CS, Levin MJ, Belshe RB. The relative efficacy of trivalent live attenuated and inactivated influenza vaccines in children and adults. *Influenza Other Respir Viruses.* 2011;5(2):67-75. Epub 20101119. doi: 10.1111/j.1750-2659.2010.00183.x. PubMed PMID: 21306569; PMCID: PMC3151550.
175. Lobby JL, Danzy S, Holmes KE, Lowen AC, Kohlmeier JE. Both Humoral and Cellular Immunity Limit the Ability of Live Attenuated Influenza Vaccines to Promote T Cell Responses. *J Immunol.* 2024;212(1):107-16. doi: 10.4049/jimmunol.2300343. PubMed PMID: 37982700; PMCID: PMC10842048.

**CHAPTER II: Tissue resident memory CD8 T cells provide durable protection against respiratory virus transmission through IFN- $\gamma$**

Sarah E. Michalets<sup>1</sup>, Ida Uddbäck<sup>1</sup>, Ananya Saha<sup>2</sup>, M. Elliott Williams<sup>1</sup>, Cameron Mattingly<sup>1</sup>,  
Kirsten M. Kost<sup>1</sup>, Laurel Lawrence<sup>1</sup>, Sakeenah L. Hicks<sup>1</sup>, Hasan Ahmed<sup>2</sup>, Anice C. Lowen<sup>1</sup>,  
Christopher D. Scharer<sup>1</sup>, Katia Koelle<sup>2</sup>, Rustom Antia<sup>2</sup>, Jacob E. Kohlmeier<sup>1,3</sup>

<sup>1</sup> Emory University School of Medicine, Department of Microbiology & Immunology, Atlanta  
GA

<sup>2</sup> Emory University, Department of Biology, Atlanta GA

<sup>3</sup> Correspondence: Jacob Kohlmeier, 1510 Clifton Rd., RRC 3133, Atlanta GA 30322. Email:

[jkohlmeier@emory.edu](mailto:jkohlmeier@emory.edu)

Modified for thesis from publication in *Nature*

**Abstract**

An ideal vaccine both attenuates virus growth and disease in infected individuals and reduces the spread of infections in the population, thereby generating herd immunity. Although this strategy has proved successful by generating humoral immunity to measles, yellow fever and polio, many respiratory viruses evolve to evade pre-existing antibodies<sup>1</sup>. One approach for improving the breadth of antiviral immunity against escape variants is through the generation of memory T cells in the respiratory tract, which are positioned to respond rapidly to respiratory virus infections<sup>2-6</sup>. However, it is unknown whether memory T cells alone can effectively surveil the respiratory tract to the extent that they eliminate or greatly reduce viral transmission following exposure of an individual to infection. Here we use a mouse model of natural parainfluenza virus transmission to quantify the extent to which memory CD8<sup>+</sup> T cells resident in the respiratory tract can provide herd immunity by reducing the susceptibility of acquiring infection, even in the absence of virus-specific antibodies. We demonstrate that protection by resident memory CD8<sup>+</sup> T cells requires the antiviral cytokine interferon- $\gamma$  (IFN $\gamma$ ) and leads to altered transcriptional programming of epithelial cells within the respiratory tract. These results suggest that tissue-resident CD8<sup>+</sup> T cells in the respiratory tract can have important roles in protecting the host against viral disease and limiting viral spread throughout the population.

## Introduction

Current vaccines against respiratory viruses such as influenza and SARS-CoV-2 typically focus on the generation of antibody responses to viral proteins. However, it is well known from these and other viruses that viral evolution can give rise to variants that escape pre-existing antibodies, resulting in continued circulation in the population by infecting both naive and previously immune hosts<sup>7, 8</sup>. T cell-based vaccines have been proposed to counter the problem of viral immune-escape<sup>9-11</sup>. In contrast to antibody epitopes, viral epitopes recognized by memory T cells are often conserved across respiratory virus strains and show limited historical evidence of acquiring escape mutations due to T cell-mediated immune pressure<sup>12-14</sup>. Animal models and human studies have suggested that memory T cells can protect against pathology following infection with respiratory viruses<sup>15, 16</sup>. In particular, CD8<sup>+</sup> tissue-resident memory T cells (T<sub>RM</sub> cells) localized in the respiratory tract are critical for optimal T cell-mediated protection against respiratory viruses owing to their positioning at the site of viral entry and replication<sup>17</sup>. Following intranasal infection or vaccination, T<sub>RM</sub> cells are established throughout the respiratory tract, including in the nasal cavity, trachea, airways and lung parenchyma<sup>18, 19</sup>. In addition to limiting viral replication and immunopathology, T<sub>RM</sub> cells can prevent the spread of an established infection from the upper respiratory tract to the lung, averting severe disease that can result from viral pneumonia<sup>19</sup>. However, although the phenotype, developmental programs and protective capacities of respiratory tract T<sub>RM</sub> cells have been delineated over the past decade, their ability to protect against natural virus infection—that is, a virus spread by transmission from an infected host—remains unknown, largely owing to limitations in our current model systems, particularly for respiratory infections. These limitations include: (1) laboratory infections are typically performed by direct inoculation with high doses of virus, which does not mimic natural

transmission, as natural transmission is initiated by a small number of virions through direct contact, droplets or aerosols; (2) the lack of a model system that combines detailed immunological measurements (for example, in mice) and robust transmission in a laboratory setting<sup>20</sup> (for example, influenza in ferrets and guinea pigs); and (3) infection status and viral load measurements typically require destructive sampling which, precludes longitudinal measurements of viral load over time. We overcome these limitations using well-characterized Sendai virus infections of laboratory mice. Sendai virus is a natural mouse parainfluenza virus that is transmitted through both aerosols and direct contact in a laboratory setting<sup>21</sup>. Incorporation of a gene for luciferase in the virus enables longitudinal measurements of infection status and viral load. We show that intranasal immunization with vectors containing the immunodominant Sendai virus CD8<sup>+</sup> T cell epitope results in the robust generation of a durable Sendai-specific respiratory tract T<sub>RM</sub> population that markedly reduces the susceptibility of mice to acquiring infection following exposure. These findings suggest that CD8<sup>+</sup> T<sub>RM</sub> may not only attenuate virus replication and disease but could also have an important role in generating herd immunity and reducing the spread of respiratory viruses in populations.

## Materials and Methods

### *Mice and viruses*

Six- to eight-week-old female C57BL/6 (wild-type), *Ifngr*<sup>-/-</sup>, *Ifng*<sup>-/-</sup> or *Prf*<sup>-/-</sup> mice were obtained from Jackson Laboratory and housed under specific pathogen free conditions at Emory University. All mice were rested for one week upon arrival. Mice were housed on a 12 h:12 h light:dark cycle with lights turned on from 07:00 to 19:00. The room temperature set point was 22 °C and relative humidity was maintained at 40–50%. All experiments were completed in accordance with the Institutional Animal Care and Use Committee guidelines of Emory University, PROTO201700581. Sample sizes for animal experiments were determined based on previously published work in the field with similar experimental models to provide sufficient statistical power for evaluating the relevant biological effects. Age matched mice were randomly assigned to experimental groups for all experiments. For intranasal priming, 30 plaque-forming units (PFU) Influenza A/Puerto Rico/8/34 (PR8-WT), 50 PFU Influenza A/Puerto Rico/8/34 expressing Sendai nucleoprotein FAPGNYPAL epitope (PR8-SenNP), 30,000 50% egg infectious dose (EID50) A/HKx31 (x31-WT), 30,000 PFU A/HKx31 expressing Sendai nucleoprotein FAPGNYPAL peptide (x31-SenNP), 50,000 PFU live attenuated A/Puerto Rico/8/34 expressing Sendai nucleoprotein FAPGNYPAL peptide (LAIV-SenNP), and  $2 \times 10^7$  PFU adenovirus serotype 5 expressing Sendai nucleoprotein (Ad-SenNP) were administered in a 30  $\mu$ l volume under isoflurane anaesthesia<sup>22, 23</sup> (Patterson Veterinary). For intraperitoneal priming, mice were administered 300,000 PFU in 300  $\mu$ l. Sendai virus encoding luciferase (Sendai-Luc) was generated and grown as previously described<sup>24</sup>. For direct Sendai-Luc infection, 1500 PFU in 30  $\mu$ l was administered intranasally under isoflurane anesthesia. FasL blockade was performed by an initial loading dose of 500  $\mu$ g intraperitoneally and 400  $\mu$ g intranasally on the day prior to co-housing,

followed by intraperitoneal injection of 250 µg of InVivoMab anti-mouse FasL (BioXCell) per mouse every 3 days<sup>25</sup>.

### ***In vivo imaging***

Chest hair was removed from mice two days prior to the start of each experiment through shaving and application of depilation cream. All in vivo images were obtained using an In Vivo Imaging System (IVIS) Lumina LT Series III (Perkin Elmer) with an XFOV-24 lens. Ten minutes prior to image acquisition, mice were injected with 3 mg of XenoLight D-luciferase (Perkin Elmer) intraperitoneally and anaesthetized with isoflurane. A series of images was captured for each cage using a binning of 8, F/stop of 1, and exposure times of 5, 30 and 120 s within the Living Image 4.7.3 Software (Perkin Elmer). Background bioluminescence was determined by imaging two uninfected mice daily throughout the course of each experiment. Image analysis was performed using the Living Image 4.7.2 Software (Perkin Elmer). Bioluminescent signal was quantified by manually drawing regions of interest (ROI) around the respiratory tract using known anatomical markers. Data were exported to Microsoft Excel, and the logarithm of total flux (photons per second) was graphed over time for each mouse and area under the curve (AUC) was calculated using GraphPad Prism or R software. If total flux levels decreased by greater than tenfold or reached background level only to return to previous or higher levels the subsequent day, luciferin injection was considered ineffective, and this timepoint was excluded from analysis.

### ***Single-cell isolation, staining, and flow cytometry***

All animals were intravenously labelled via tail vein injection with a fluorescent antibody, either 2 mg CD45.2-PE clone 104 or 1.5 mg CD3e-PECF594 clone 145-2C11, in 200 µl phosphate-

buffered saline (PBS). Five minutes following injection, mice were euthanized by intraperitoneal injection of Avertin (2,2,2-tribromoethanol) and brachial exsanguination. Spleen, lungs, BAL and nasal cavity were then collected. Nasal cavity was isolated by first removing skin, the lower jaw, tongue, incisors, zygomatic bones, eyes, hard palette and remaining soft tissue from the skull. A transverse cut was then made distal to the first molars to minimize capture of olfactory epithelium, and the nasal cavity was placed in ice cold HBSS. To process the nasal cavity, it was cut into small pieces and enzymatically digested in 5 ml of warm HBSS containing  $1 \times 10^6$  U l<sup>-1</sup> DNase (Sigma), 5 g l<sup>-1</sup> Collagenase D (Roche) and 15 U ml<sup>-1</sup> Dispase (Thermo Fisher) at 37 °C for 30 min with vortexing every 10 min. Spleens were processed by mechanical disruption through a 70- $\mu$ m filter. Lungs were isolated into ice cold HBSS and processed in gentleMACS C tubes using Miltenyi gentleMACS Octo dissociators with heaters (program m\_LDK\_1) in 2.5 ml warm HBSS containing  $1 \times 10^6$  U ml<sup>-1</sup> DNase (Sigma) and 5 g ml<sup>-1</sup> Collagenase (Roche). After digestion, lymphocytes were isolated using a 40%–80% Percoll gradient. BAL was isolated using 5 ml of ice cold R10 (RPMI, 10% fetal bovine serum and 1% penicillin-streptomycin). Single-cell suspensions were strained through 70- $\mu$ m filters and RBC lysed with ACK lysis buffer prior to staining. Cell counts were determined manually using a hemocytometer or LUNA-II automatic cell counter (Logos Biosystems). For flow cytometry, samples were first incubated with Fc block using murine anti-CD16/32 2.4G2 for 10 min on ice. Suspensions were then surface stained with Sendai NP (K<sup>b</sup><sub>324–332</sub>) tetramer conjugated to APC or PE at a 1:100 dilution for 1 h at room temperature in the dark, followed by 30 min of extracellular staining with fluorescently conjugated antibodies at a 1:100 dilution: CD8 $\alpha$ , CD44, CD45.2, CD49a, CD69, CD103, CD19, CD11c, CD11b, Ly6G, SigLecF, Ly6C, CCR2, NK1.1, CD4, EpCAM, CD31 and CD62L. Cell viability was determined using a 1:200 dilution of Zombie NIR (Biolegend) or 7-AAD. Samples were

acquired on a Fortessa X20 or FACSymphony A3 (BD Biosciences) flow cytometer or sorted on a FACSARIAII (BD Biosciences). Flow cytometry data analysis was conducted using FlowJo v.10 software. All antibodies were purchased from Biolegend, and relevant tetramers were kindly provided by the NIH tetramer core facility in Atlanta, USA or S. Buus.

### ***Cytokine analysis***

Supernatants from nasal cavity tissue were assayed using the LEGENDplex Mouse Cytokine Release Syndrome Panel Multi-Analyte Flow Assay Kit (BioLegend) according to the manufacturer's protocol. Data were acquired on an Fortessa X20 (BD Biosciences) flow cytometer. Analysis was performed using the Qognit LEGENDplex Data Analysis Software Suite Version 2023-02-15 (BioLegend) and data were graphed in GraphPad Prism v9.

### ***RNA sequencing***

For each replicate, 2,000 virus-specific CD8<sup>+</sup> T cells or epithelial cells were sorted into RLT lysis buffer (Qiagen) containing 1% 2-mercaptoethanol and total RNA purified using the Quick-RNA Microprep kit (Zymo Research). All resulting RNA was used as an input for complementary DNA synthesis using the SMART-Seq v4 kit (Takara Bio) and 12 cycles of PCR amplification. Next, 200 pg cDNA was converted to a sequencing library using the NexteraXT DNA Library Prep Kit and NexteraXT indexing primers (Illumina) with 12 additional cycles of PCR. Final libraries were pooled at equimolar ratios and sequenced on a HiSeq2500 using 50-bp paired-end sequencing or a NextSeq500 using 75-bp paired-end sequencing. Raw fastq files were mapped to the mm10 build of the mouse genome using STAR<sup>26</sup> with the GENCODE v17 reference transcriptome. The overlap of reads with exons was computed and summarized using the GenomicRanges package<sup>27</sup> and data

normalized to fragments per kilobase per million (FPKM). Genes that were expressed at a minimum of three reads per million (RPM) in all samples were considered expressed. DEGs were determined using the `glm` function in DESeq2<sup>28</sup> using the mouse from which each cell type originated as a covariate. Genes with a false discovery rate of less than 0.05 were considered significant. For gene set enrichment analysis (GSEA)<sup>29</sup>, all detected genes were ranked by multiplying the sign of the fold change by the  $-\log_{10}$  of the  $P$  value between two comparisons. The resulting list was used in a GSEA pre-ranked analysis. All data display was performed in R v3.6.3.

### *Data analysis and statistics*

Analysis was performed using GraphPad Prism v9 or R. We calculated the AUC of the  $\log_{10}(\text{flux})$  using the `trapz` function in R and the background AUC was subtracted. The mean background bioluminescence level (arithmetic mean of  $\log_{10}(\text{flux})$ ) was calculated by analyzing longitudinal bioluminescence data from 2 uninfected mice (2 measurements/mouse, total 4 replicate data points per day). The infection limit used in the main analysis was set as the mean +  $2.5 \times$  s.d. of the background  $\log_{10}(\text{flux})$ . Before calculating AUC, any  $\log_{10}(\text{flux})$  value below the mean background  $\log_{10}(\text{flux})$  was replaced by the mean background  $\log_{10}(\text{flux})$ . AUC between groups were compared by Mann–Whitney test using the `wilcox_test` function in R.

For probabilities of infection and transmission, infected mice were defined as mice with  $\log_{10}(\text{flux})$  greater than the infection limit. The probability of infection / transmission equals the fraction of contact mice in each group that became infected. Confidence intervals were estimated assuming a binomial probability distribution using the `binconf` R function. Probability of infection and transmission were compared between groups by proportion test using the `prop_test` R function.

For correlation of AUC and probability of infection with resident memory CD8<sup>+</sup> T cell numbers, the mean  $\log_{10}$ (no. of T<sub>RM</sub> cells) at different locations were correlated with the probability of infection using Spearman's correlation. A line was fitted between AUC and mean  $\log_{10}$ (no. of T<sub>RM</sub> cells) using the glm R function with the gaussian family function.

## Results

### **T<sub>RM</sub> cells limit susceptibility to infection**

To study the effect of cellular immunity on transmission, we used a genetically modified influenza A virus encoding the immunodominant H-2K<sup>d</sup> CD8<sup>+</sup> T cell epitope (FAPGNYPAL) from Sendai virus nucleoprotein (PR8-SenNP) (**Extended Data Fig. 1a**). By immunizing mice intranasally, we induced both Sendai-specific effector memory T cells (T<sub>EM</sub> cells) in the circulation and T<sub>RM</sub> cells in the respiratory tract without inducing Sendai-specific memory CD4<sup>+</sup> T cells or Sendai-specific antibodies. When mice were immunized intraperitoneally, similar numbers of Sendai-specific T<sub>EM</sub> cells were generated in the spleen but significantly fewer Sendai-specific CD8<sup>+</sup> T<sub>RM</sub> cells were generated in the bronchoalveolar lavage (BAL), lung and nasal cavity, as defined by their expression of CD69 and CD103 and the absence of intravital staining (**Extended Data Fig. 1b–e**). To control for potential activation of innate immune cells and any effects of localized inflammation in the respiratory tract following intranasal infection, we primed an additional cohort intranasally with wild-type PR8 virus lacking the SenNP epitope (PR8-WT). As bioluminescence correlated strongly with viral titers, we use bioluminescent flux of Sendai-Luc as a surrogate for viral titer (**Extended Data Fig. 2a, b**).

We asked whether pre-existing CD8<sup>+</sup> T<sub>RM</sub> cells could effectively surveil the respiratory tract to affect both the susceptibility of mice to infection as well as attenuate the subsequent virus burden. To address this question, we immunized contact mice with PR8-SenNP intranasally, PR8-SenNP intraperitoneally, or PR8-WT intranasally (to generate mice with both Sendai-specific T<sub>RM</sub> and T<sub>EM</sub> cells, only circulating Sendai-specific T<sub>EM</sub> cells, or no Sendai-specific memory CD8<sup>+</sup> T cells, respectively) and assessed Sendai-Luc transmission from infected index mice to contact mice 35 days after immunization (**Fig. 1a**). Mice immunized with PR8-SenNP intranasally showed

significant reductions in total viral burden and in the probability of infection, with only 4 out of 15 (27%) of the contact mice being infected compared with 12 out of 13 (92%) of PR8-WT intranasal or 14 out of 16 (88%) of PR8-SenNP intraperitoneal immunized mice (**Fig. 1b–d**). These data demonstrate that T<sub>RM</sub> cells can reduce the susceptibility of mice to infection and the subsequent virus burden in the mice that do become infected.

To assess which antiviral mechanisms were important for T<sub>RM</sub> cells to prevent viral propagation following transmission, we immunized wild-type, *Ifng*<sup>-/-</sup>, *Ifngr*<sup>-/-</sup> or *Prf*<sup>-/-</sup> mice with a live attenuated PR8-SenNP (LAIV-SenNP) to control for potential differences in immunization due to the increased pathogenesis of PR8-WT virus in knockout mice (**Fig. 1e**). Similar numbers of Sendai-specific T<sub>RM</sub> cells, natural killer cells and inflammatory monocytes were observed in the respiratory tract of wild-type and knockout mice on day 35 post-immunization with LAIV-SenNP (**Extended Data Fig. 3**). We also tested the importance of Fas–Fas ligand (FasL) interactions in T<sub>RM</sub>-mediated protection by administering anti-FasL blocking antibody to wild-type mice immunized intranasally with LAIV-SenNP. Wild-type, *Prf*<sup>-/-</sup> and anti-FasL-treated wild-type mice showed similar levels of protection, with breakthrough infections detected in 8 out of 16 (50%) of wild-type, 6 out of 16 (38%) of *Prf*<sup>-/-</sup> and 8 out of 14 (57%) anti-FasL-treated wild-type mice (**Fig. 1g–i**). By contrast, immunized *Ifngr*<sup>-/-</sup> mice showed significantly higher viral burdens (by AUC; **Fig. 1h**), and immunized *Ifng*<sup>-/-</sup> (12 out of 13, 92%) and *Ifngr*<sup>-/-</sup> (8 out of 8, 100%) mice showed significantly increased probability of infection (**Fig. 1i**), demonstrating that IFN $\gamma$  signalling is a key mechanism for T<sub>RM</sub>-mediated protection against propagation of infection following viral transmission.

## IFN $\gamma$ alters epithelial cell programming

Previous studies have shown that T<sub>RM</sub> cells are capable of rapid sensing and alarm functions, resulting in local inflammation and the recruitment of innate immune cells into the tissue<sup>30</sup>. We hypothesized that respiratory tract T<sub>RM</sub> cells could enable rapid control of viral replication by increased recruitment of innate immune cells into the tissue. However, regardless of the immunization route or the presence of T<sub>RM</sub> cells, there was no difference in the number of natural killer cells or inflammatory monocytes recruited into the tissues of respiratory tract on day 2 post-transmission (**Extended Data Fig. 4a–c**). We also considered that T<sub>RM</sub>-mediated effector functions, such as IFN $\gamma$ , could alter the programming of epithelial cells, the primary target of many respiratory viruses. To discern between inflammatory cytokines and chemokines induced by T<sub>RM</sub> cells following antigen recognition versus those induced by innate recognition of an invading pathogen, we used a reductionist approach and directly administered SenNP peptide intranasally to wild-type and *Ifng*<sup>-/-</sup> mice that had been immunized intranasally with LAIV-SenNP one month earlier (**Fig. 2a**). Epithelial cells were sorted from the nasal cavity prior to (D30) or 3 days after (D30 + 3) peptide administration for RNA sequencing. Principal component analysis and hierarchical clustering of selected differentially expressed genes showed that nasal cavity epithelial cells from wild-type D30 + 3 mice had a distinct transcriptional signature compared with both wild-type D30 and *Ifng*<sup>-/-</sup> D30 + 3 mice and showed significant upregulation of genes associated with antiviral responses and antigen presentation (**Fig. 2b, c**). Pathway analysis showed that processes associated with limiting viral replication, interferon-stimulated genes, and antigen processing and presentation were enriched in wild-type D30 + 3 mice compared with both wild-type D30 and *Ifng*<sup>-/-</sup> D30 + 3 mice (**Fig. 2d**). Changes in gene expression associated with antigen presentation were confirmed by flow cytometry, as nasal cavity epithelial cells from wild-type

D30 + 3 mice showed a significant increase in MHC-I and MHC-II protein expression (**Fig. 2e**). As expected, cytokine analysis of nasal cavity tissue showed significant increases in IFN $\gamma$  and IFN $\gamma$ -associated chemokines in wild-type D30 + 3 mice (**Fig. 2f**). However, levels of IL-6, CCL3 and CCL4 were similar between wild-type and *Ifng*<sup>-/-</sup> D30 + 3 mice, demonstrating that T<sub>RM</sub> cells in *Ifng*<sup>-/-</sup> mice could drive localized inflammation following antigen encounter but did not upregulate genes associated with antiviral immunity in epithelial cells. Together, these data demonstrate that respiratory tract T<sub>RM</sub> cells can act on local epithelial cells via IFN $\gamma$  to rapidly induce an antiviral program.

### **CD8<sup>+</sup> T<sub>RM</sub> cells can provide durable protection**

As it has been previously shown that respiratory tract T<sub>RM</sub> cells can decline over time<sup>5</sup>, we investigated the durability of T<sub>RM</sub>-mediated protection against infection under several priming scenarios that differ in their ability to maintain T<sub>RM</sub> cells<sup>22</sup> (**Fig. 3a**). Six months post-immunization, contact mice immunized with influenza x31-SenNP intranasally showed no protection against infection compared with control mice immunized with x31-WT, although total viral burdens following infection were significantly reduced (**Fig. 3b, c**). Mice immunized with PR8-SenNP intranasally still showed significantly lower total viral burden when infected compared with intranasal immunization with x31-WT or x31-SenNP, but there was no longer any difference in the protection from acquiring infection, in contrast to PR8-SenNP intranasally immunized mice one month post-immunization (**Fig. 1b-d**). By contrast, intranasal immunization with a replication-deficient adenovirus vector encoding the Sendai virus nucleoprotein (Ad-SenNP) showed significant protection from infection and less total viral burden compared with all other groups at six months (**Fig. 3b-d**). The increased protection against infection in Ad-SenNP-

immunized mice corresponded to increased numbers of CD69<sup>+</sup>CD103<sup>+</sup> Sendai-specific T<sub>RM</sub> cells in the lung, BAL and nasal cavity, despite lower numbers of Sendai-specific T<sub>EM</sub> cells in the spleen (**Fig. 3e**).

To better quantify the effect of T<sub>RM</sub> cells on infection, we compiled data from different immunization regimens and different times post-immunization to determine the correlation between the number of T<sub>RM</sub> cells in different areas of respiratory tract, total viral burden (by AUC), and the probability of infection (**Extended Data Fig. 5a–d**). There was a significant negative correlation between total viral burden and the number of T<sub>RM</sub> cells in the BAL, lung and nasal cavity, with the strongest correlation in the nasal cavity (**Fig. 3f**). Similarly, there was a significant negative correlation between the number of T<sub>RM</sub> cells in the BAL, lung and nasal cavity and the probability of infection, with the strongest correlation in this case in the lung (**Fig. 3g**). However, there was no correlation between the total viral burden of the directly infected index mice with the total viral burden of the contact mice regardless of immunization status (**Extended Data Fig. 6**).

For many pathogens, multiple vaccine doses are utilized in a ‘prime–boost’ immunization strategy to achieve maximal immune responses. However, pre-existing immunity may limit the ability of vaccines to generate robust T cell responses by rapidly clearing vaccine antigens. To investigate whether pre-existing immunity limited T<sub>RM</sub>-mediated protection against infection, mice were first immunized with influenza A/Cal/09 (H1N1) or mock-immunized prior to intranasal LAIV-SenNP (also H1N1) or Ad-SenNP immunization (**Extended Data Fig. 7a**). Mice with pre-existing H1N1 immunity were not protected against Sendai virus infection after LAIV-SenNP immunization but did show decreased viral burden following infection compared with mice immunized with LAIV-WT. By contrast, Ad-SenNP immunization of A/Cal/09 immune mice resulted in significant protection from infection (**Extended Data Fig. 7b–d**). To evaluate whether

a heterologous prime–boost regimen could enhance the longevity of CD8<sup>+</sup> T<sub>RM</sub> cells in the respiratory tract and improve the durability of protection against infection, mice were primed with x31-SenNP followed by boosting with PR8-SenNP or Ad-SenNP (**Fig. 3h**). Three months after the second immunization, contact mice boosted with PR8-SenNP did not show increased protection against infection compared with mice that received priming only (**Fig. 3i–k**). However, secondary immunization with Ad-SenNP showed significantly decreased probability of infection (**Fig. 3i–k**). These results aligned with the increased number of CD69<sup>+</sup>CD103<sup>+</sup> Sendai-specific CD8<sup>+</sup> T<sub>RM</sub> cells in the respiratory tract of Ad-SenNP-boosted mice compared with PR8-SenNP-boosted mice (**Extended Data Fig. 8**). Together, these data show that the number of virus-specific T<sub>RM</sub> cells in the respiratory tract dictate the ability of cell-mediated immunity to protect against respiratory virus infection.

## Discussion

In this study, we demonstrate that pre-existing CD8<sup>+</sup> T<sub>RM</sub> cells in the respiratory tract can substantially limit viral transmission. It has been well documented that CD8<sup>+</sup> T<sub>RM</sub> cells can reduce viral loads and limit immunopathology in models of direct infection<sup>16,31-33</sup>, and we show that CD8<sup>+</sup> T<sub>RM</sub> cells are sufficient to significantly reduce both the susceptibility of immunized hosts to becoming infected and their ability to transmit virus if they do become infected. It is important to note that protective immunity provided by respiratory tract CD8<sup>+</sup> T<sub>RM</sub> cells is probably not sterilizing, as these cells must first encounter their specific antigen presented by a virus-infected cell to perform their effector functions. Many studies have made the case for development of T cell vaccines against respiratory pathogens, with an emphasis on the potential for mucosal resident memory T cells to provide rapid and robust immunity owing to their localization at the site of viral entry<sup>10, 34, 35</sup>. Our data demonstrate that several different immunization regimens, including live attenuated and replication-deficient vectors, can generate mucosal T<sub>RM</sub> cells in sufficient numbers to effectively surveil the respiratory tract to limit the susceptibility of becoming infected as well as transmission. Notably, these findings were observed in a stringent transmission model of direct, continuous contact, whereas most opportunities for transmission are brief interactions. Moreover, Sendai virus infection does not visibly alter the activity of infected mice, and thus does not affect their interaction with cage mates. Although antibody-mediated neutralization capable of preventing infection is an ideal outcome of vaccination against respiratory viruses, engaging the cellular arm of the immune response to also generate virus-specific T<sub>RM</sub> cells can provide a secondary method of protection for the host by severely limiting viral replication, and for the population by preventing virus transmission. This is especially important for highly mutable viruses, whereby variants that partially or fully escape pre-existing antibody responses can persist

in circulation. However, T cell-based vaccine platforms that encode a single immunodominant antigen are not practical for humans, owing to human leukocyte antigen (HLA) diversity in the population. Instead, an optimal approach would be to encode entire viral proteins—rather than individual epitopes—as vaccine antigens. This strategy would enable the delivery of multiple epitopes with the potential to induce virus-specific T cell responses without the need to tailor vaccines to specific HLA types. In addition, including more than one viral protein in the vaccine could increase the likelihood of generating virus-specific T cell responses directed against an immunodominant epitope. For example, immunodominant epitopes for different HLA types have been identified across several influenza proteins such as nucleoprotein, matrix and polymerase basic protein<sup>36-38</sup>, and a vaccine approach combining these antigens could provide broad coverage of T cell epitopes despite HLA diversity in the population.

The respiratory epithelium, particularly in the upper respiratory tract, is the primary target for initial seeding of respiratory infections such as influenza or SARS-CoV-2. In addition, studies in ferrets have shown that transmitted influenza viruses come primarily from the upper respiratory tract, specifically the nasal turbinates<sup>39</sup>. This raises interesting questions regarding the relative importance of T<sub>RM</sub> cells in different locations throughout the respiratory tract for limiting viral transmission. Although this study does not address the contributions of upper respiratory tract versus lower respiratory tract T<sub>RM</sub> cells, it is likely that upper respiratory tract T<sub>RM</sub> cells have an outsized role in this process, as initial transmission events are more likely to occur at this site. In this scenario, it is possible that lower respiratory tract T<sub>RM</sub> cells serve primarily to protect against severe disease by responding to virus that might spread to the lung after propagating in the upper respiratory tract. Statistical analysis of these transmission data also shows that the number of T<sub>RM</sub> cells in the respiratory tract negatively correlate with susceptibility to infection and viral load in

the infected mice. The extent to which  $T_{RM}$  cells attenuate transmission is likely to vary among different viruses, based on properties such as transmission efficiency, replication rates and viral mechanisms for evading the immune response<sup>40</sup>, and these factors must be considered in the development of cell-mediated vaccines against respiratory viruses.

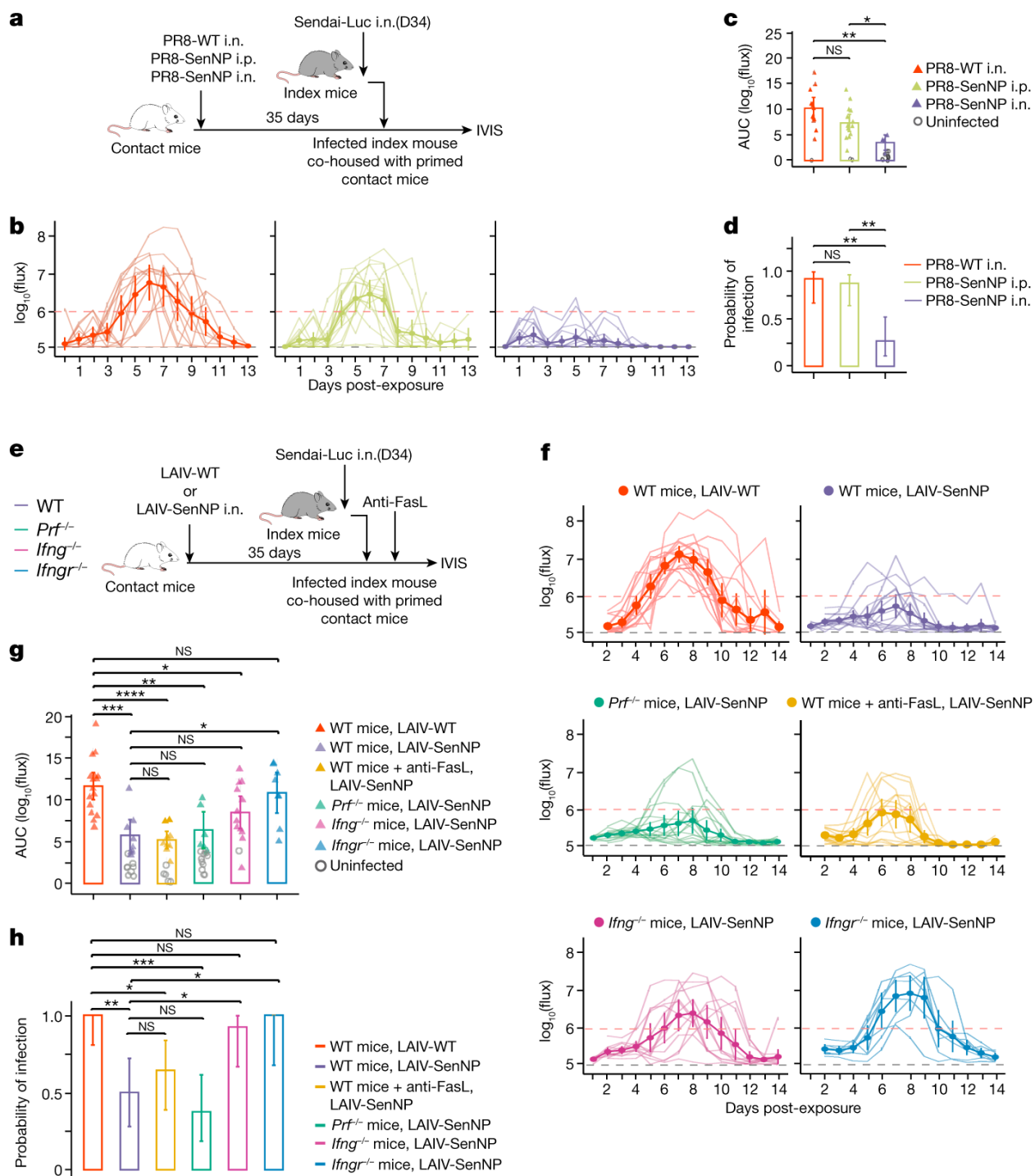
Although  $CD8^+$   $T_{RM}$  cells have a broad array of effector functions, our findings show a critical role for  $IFN\gamma$  in limiting virus transmission.  $IFN\gamma$  can act directly on epithelial and immune cells to induce an antiviral state, and previous studies have shown that  $IFN\gamma$  produced by respiratory tract  $T_{RM}$  cells can limit viral replication<sup>17, 41</sup>. In both transmission models, deletion of  $IFN\gamma$  or the  $IFN\gamma$  receptor abrogated the protection from virus-specific  $T_{RM}$  cells. Notably, deletion of perforin and blockade of FasL, primary mediators of cytolytic activity, had minimal effects on  $T_{RM}$ -mediated protection. Although other mediators may partially compensate for the loss of any single cytolytic pathway, these data suggest that promoting a local antiviral state via cytokine production, rather than direct lysis of infected epithelial cells, is the primary mechanism by which  $CD8^+$   $T_{RM}$  cells limit transmission. This also suggests that  $T_{RM}$  cells may not require direct contact with an infected epithelial cell, and could potentially mediate their protective effects through release of  $IFN\gamma$  into the local environment after encountering antigen presented by tissue macrophages or dendritic cells.

Overall, this study demonstrates that  $T_{RM}$  cells can not only reduce pathology in infected individuals but also significantly reduce viral transmission. We show that this reduction in transmission by  $T_{RM}$  cells accrues in two ways. First,  $T_{RM}$  cells can reduce susceptibility to infection, particularly when their numbers are high. Second, by reducing the virus burden in individuals that do get infected,  $T_{RM}$  cells reduce the magnitude and duration of infectivity. These effects are mediated by  $T_{RM}$  cells even in the absence of virus-specific antibody. Immunization

strategies that maintained high  $T_{RM}$  cells numbers in the respiratory tract provided durable protection for at least six months, and optimal protection was  $IFN\gamma$ -dependent. These data support a critical and underappreciated role for  $T_{RM}$  cells in limiting respiratory virus transmission. Therefore, they support the continued development of cell-mediated vaccines that can complement current antibody-directed strategies to provide broad protection against evolving viral variants.

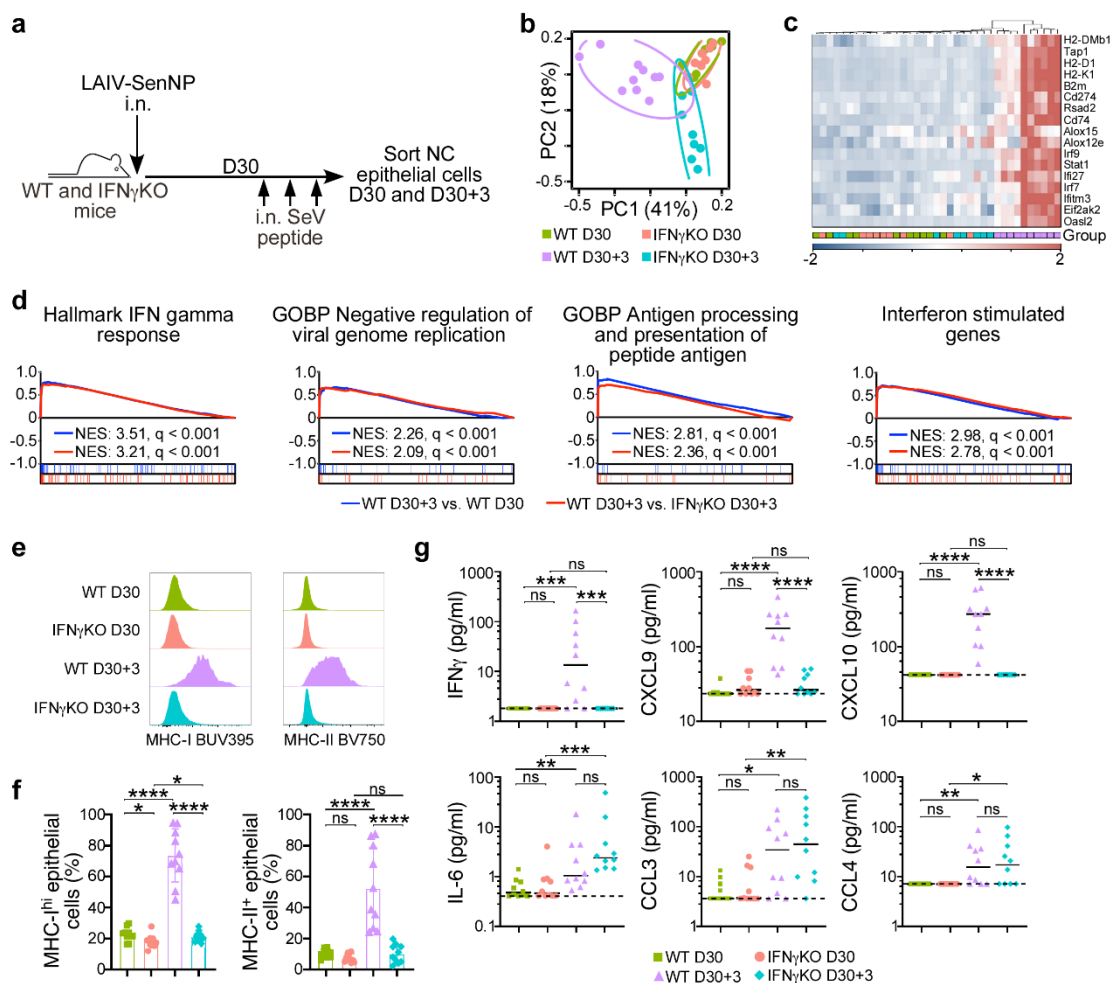
## Main Figures

Figure 1



**Figure 1. Respiratory tract CD8<sup>+</sup> T<sub>RM</sub> cells protect against viral propagation following transmission through IFN $\gamma$ .** **a**, Schematic of experimental setup in which immunized contact mice were co-housed with a Sendai-Luc infected index mouse. **b**, Bioluminescence curves of contact mice immunized with PR8-WT intranasally ( $n = 13$ ), PR8-SenNP intraperitoneally ( $n = 16$ ) or PR8-SenNP intranasally ( $n = 15$ ). Colours as in **c**. **c**, AUC of bioluminescence in immunized contact mice that become infected following co-housing with an infected index mouse. **d**, Probability of infection for immunized contact mice, calculated as the proportion of contact mice that became infected. **e**, Schematic of experiment to investigate protection from transmission in immunized WT, *Prf*<sup>-/-</sup>, *Ifng*<sup>-/-</sup> and *Ifngr*<sup>-/-</sup> contact mice, and WT mice treated with anti-FasL antibody. **f**, Bioluminescence curves of immunized WT ( $n = 16$  for LAIV-WT and LAIV-SenNP immunization), *Prf*<sup>-/-</sup> ( $n = 16$ ), *Ifng*<sup>-/-</sup> ( $n = 13$ ), *Ifngr*<sup>-/-</sup> ( $n = 8$ ) and anti-FasL-treated WT ( $n = 14$ ) contact mice after co-housing with an infected index mouse. **g**, AUC of bioluminescence in contact mice that become infected following co-housing with an infected index mouse. **h**, Probability of infection for immunized contact mice. Error bars represent 95% binomial confidence intervals (**d,h**). All data are combined from two independent replicates. For bioluminescence curves (**b,f**), solid dark lines represent means, solid pale lines represent individual mice, the dashed grey line represents background bioluminescence, and the dashed red line represents the limit of infection. Solid lines (**c,d,g,h**) and error bars (**b,c,f,g**) represent mean with 95% confidence interval. Statistical significance was determined using two-sided Mann–Whitney test.

Figure 2



**Figure 2. IFN $\gamma$  signalling induces antiviral gene expression and increases antigen presentation in nasal cavity epithelial cells.** **a**, Schematic of experiment to evaluate the effect of T<sub>RM</sub> cell-derived IFN $\gamma$  on nasal cavity epithelial cells. IFN $\gamma$ KO, IFN $\gamma$  knockout. **b**, PCA plot of sorted nasal cavity epithelial cells from LAIV-SenNP immunized WT and *Ifng*<sup>-/-</sup> mice at resting memory (D30; WT  $n = 10$  and *Ifng*<sup>-/-</sup>  $n = 9$ ) and 3 days after peptide administration (D30 + 3; WT  $n = 10$  and *Ifng*<sup>-/-</sup>  $n = 8$ ). **c**, Hierarchical clustering of RNA transcript expression for the listed differentially expressed genes. Colors as in **b**. **d**, Gene set enrichment analysis plots of listed immune pathways. **e**, Representative histograms of MHC-I and MHC-II expression on nasal cavity

epithelial cells. **f**, Frequency of MHC-I<sup>hi</sup> and MHC-II<sup>+</sup> nasal cavity epithelial cells ( $n = 10$  per group). Bars represent mean and s.d. **g**, Cytokine and chemokine concentrations in the nasal cavity of immunized WT ( $n = 10$  per timepoint) and *Ifng*<sup>-/-</sup> ( $n = 10$  per timepoint) mice at resting memory and 3 days following peptide administration. Bars represent median. The data shown are combined from two independent experiments. Statistical significance was determined using two-sided Mann–Whitney test.

Figure 3

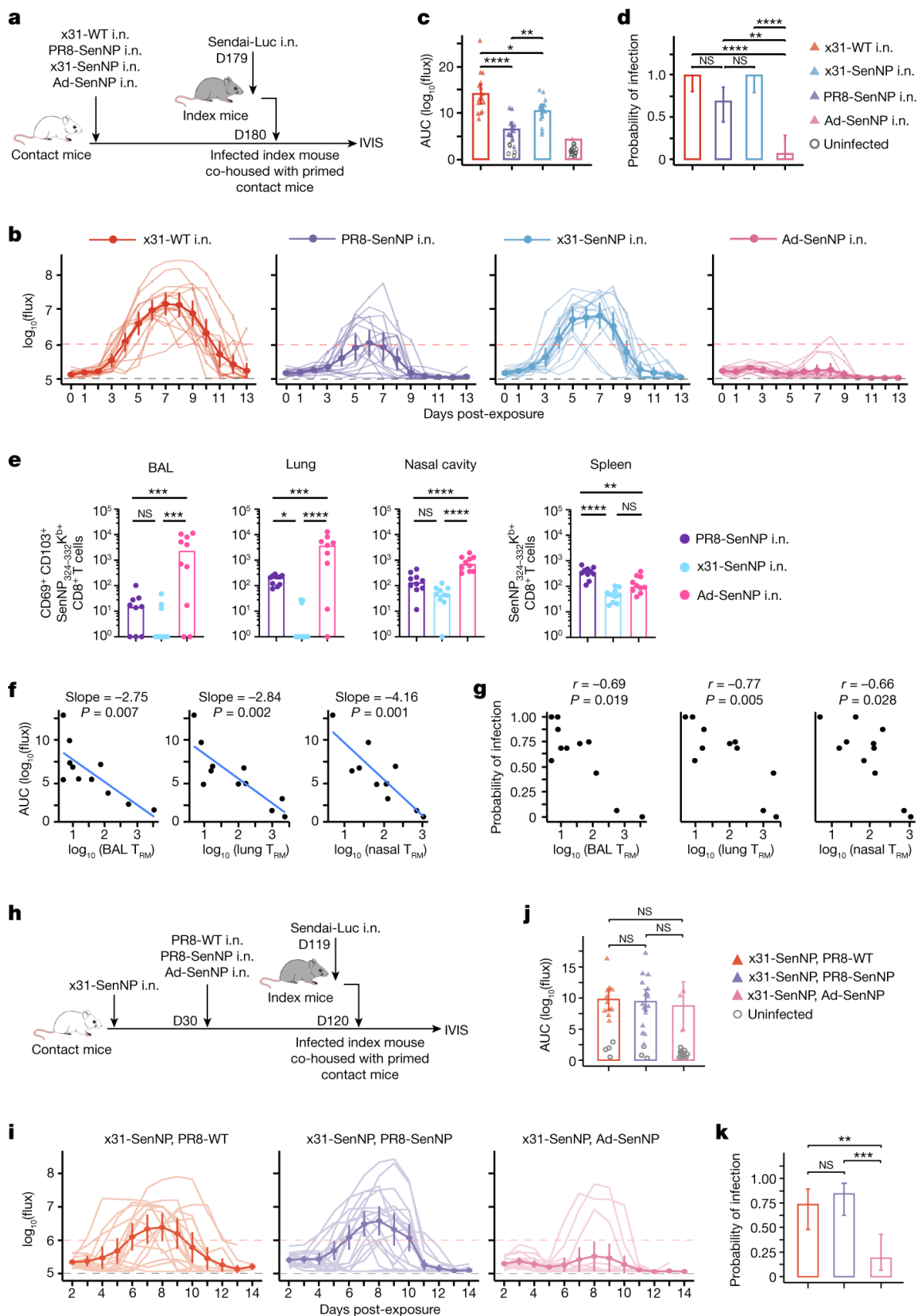
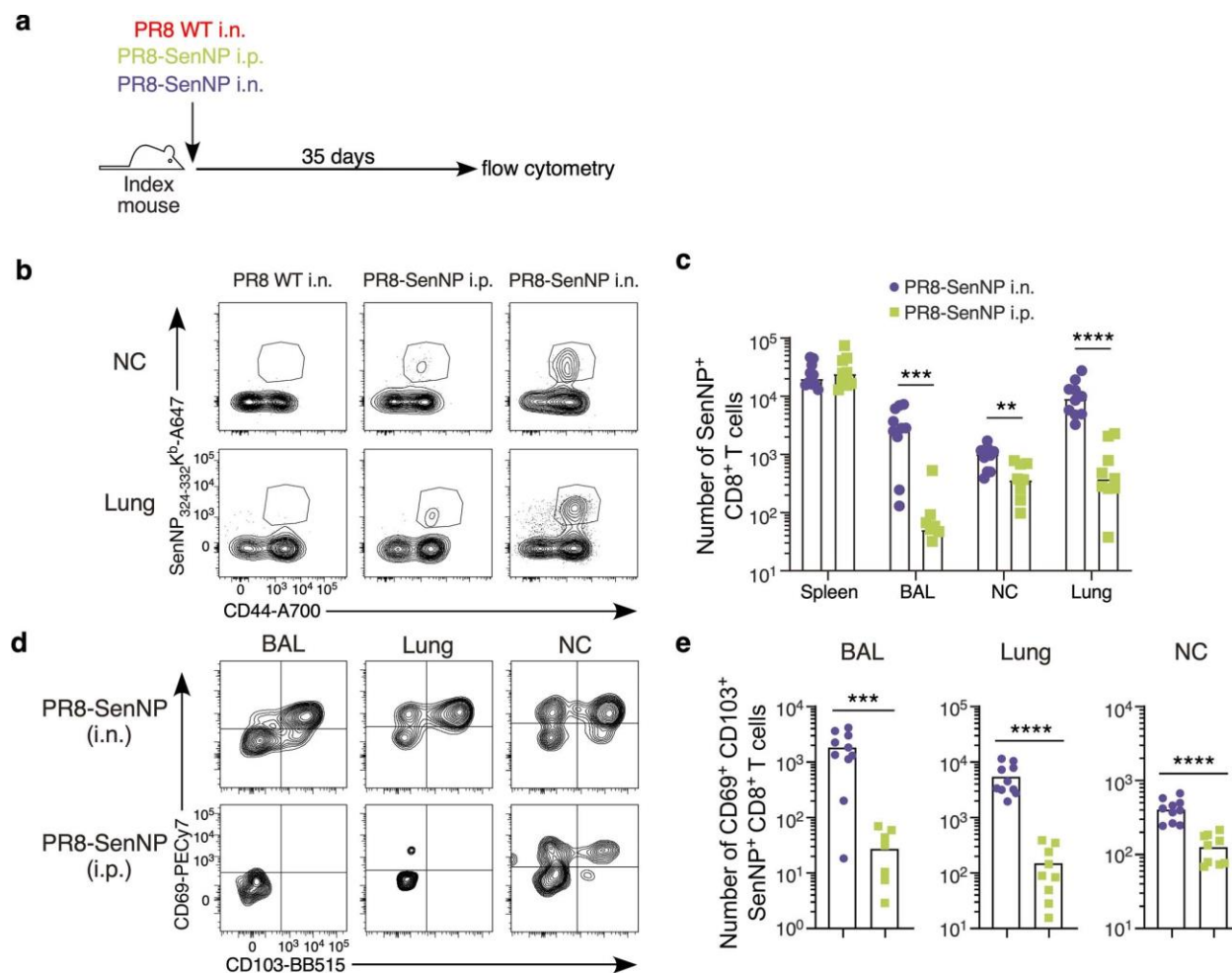


**Figure 3. The number of respiratory tract CD8<sup>+</sup> T<sub>RM</sub> cells is strongly linked to protection from transmission.** **a**, Schematic of experiment to investigate the durability of T<sub>RM</sub>-mediated protection and ability to limit viral transmission. **b**, Bioluminescence curves of contact mice immunized with x31-WT (*n* = 16), PR8-SenNP (*n* = 16), x31-SenNP (*n* = 15) and Ad-SenNP (*n* = 16) after co-housing with an infected index mouse. **c**, AUC of bioluminescence in contact mice that become infected following co-housing with an infected index mouse. **d**, Probability of infection for immunized contact mice, calculated as proportion of contact mice that become infected. **e**, Number of CD69<sup>+</sup>CD103<sup>+</sup> Sendai NP<sub>324-332</sub> K<sup>b+</sup> CD8<sup>+</sup> T<sub>RM</sub> cells in the BAL (*n* = 9 for PR8-SenNP, *n* = 10 for x31-SenNP and Ad-SenNP), lung (*n* = 9 for Ad-SenNP, *n* = 10 for PR8-SenNP and x31-SenNP) and nasal cavity (*n* = 10 per group); and Sendai NP<sub>324-332</sub> K<sup>b+</sup> CD8<sup>+</sup> T<sub>EM</sub> cells in the spleen (*n* = 10 per group) on D180 post-immunization. **f**, Correlation between AUC of bioluminescence and the number of CD69<sup>+</sup>CD103<sup>+</sup> Sendai NP<sub>324-332</sub> K<sup>b+</sup> T<sub>RM</sub> cells in the BAL, lung and nasal cavity. **g**, Correlation between the probability of infection and number of CD69<sup>+</sup>CD103<sup>+</sup> Sendai NP<sub>324-332</sub> as a proportion of K<sup>b+</sup> T<sub>RM</sub> cells in the BAL, lung and nasal cavity. **h**, Schematic of experiment to investigate the effect of multiple immunizations on the durability of T<sub>RM</sub>-mediated protection against Sendai virus transmission. **i**, Bioluminescence curves of immunized contact mice after co-housing with an infected index mouse (*n* = 15 for PR8-WT boosted contacts, *n* = 19 for PR8-SenNP boosted contacts and *n* = 16 for Ad-SenNP boosted contacts). **j**, AUC of bioluminescence in primed and boosted contact mice that become infected following co-housing with an infected index mouse. **k**, Probability of infection for immunized contact mice. Error bars represent 95% binomial proportion confidence intervals (**d,k**). All data are combined from two independent experiments. For bioluminescence curves (**b,i**), solid dark lines represent means, solid pale lines represent individual mice, the dashed grey line represents

background bioluminescence, and the dashed red line represents the limit of infection. Solid lines (**c–e,j,k**) and error bars (**b,c,i,j**) represent mean with 95% confidence interval. Statistical significance was determined using two-sided Mann–Whitney test.

## Supplementary Information

## Extended Data Figure 1

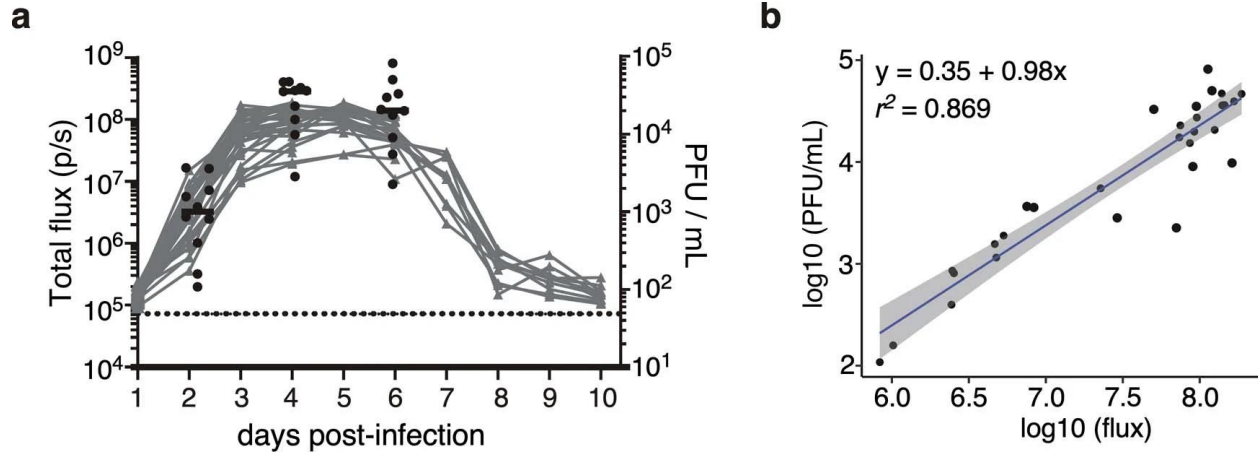


**Extended Data Figure 1. Distribution and characterization of tissue-resident Sendai-specific CD8<sup>+</sup> T cells limit intranasal and intraperitoneal infection with recombinant influenza virus.**

(a) Schematic of experiment for investigating immunization route on protection from direct infection. (b) Representative plots of tetramer staining at day 35 in immunized mice. (c) Absolute numbers of Sendai NP<sub>324-332</sub>/K<sup>b</sup> CD8 T cells in spleen, BAL, lung, and nasal cavity of immunized mice (n = 9 for PR8 SenNP i.p. and PR8 SenNP i.n.). (d) Representative plots of staining for TRM markers CD69 and CD103 on antigen-specific cells. (e) Absolute numbers of CD69<sup>+</sup>CD103<sup>+</sup>

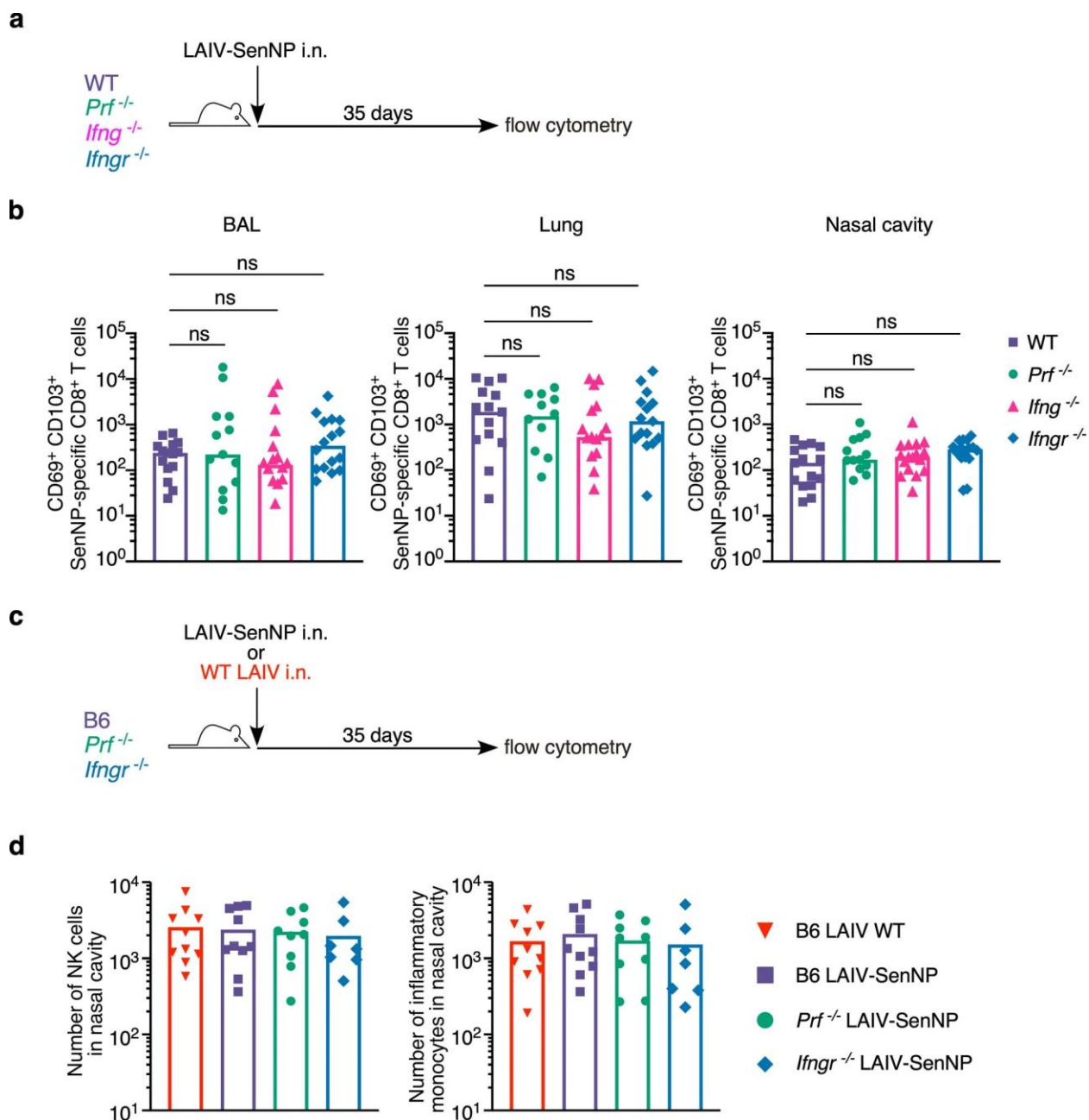
Sendai NP<sub>324-332</sub>/K<sup>b+</sup> CD8<sup>+</sup> T cells in BAL (n = 9 for PR8-SenNP i.n. and n = 8 for PR8-SenNP i.p.), lung and nasal cavity (n = 10 for PR8-SenNP i.n. and n = 9 for PR8-SenNP i.p.). Data are representative of two individual experiments. Lines represent mean values (c, e, g). Statistical significance was determined using two-sided Mann Whitney test. \* p < 0.05, \*\* p < 0.01, \*\*\* p < 0.001, \*\*\*\* p < 0.0001, ns: non-significant.

### Extended Data Figure 2



**Extended Data Figure 2. Sendai-luciferase bioluminescence strongly correlates with viral titer.** (a) Bioluminescence in Sendai-Luc infected mice combined with viral titer from the total respiratory tract (nasal cavity, trachea, and lungs) on days 2, 4 and 6 post-infection. Black dots represent viral titer, grey curves represent bioluminescence of individual mice, and dotted black line represents background bioluminescence. (b) Correlation of bioluminescence with viral titers. Data shown are from two independent pooled experiments with 10 mice per timepoint.

### Extended Data Figure 3

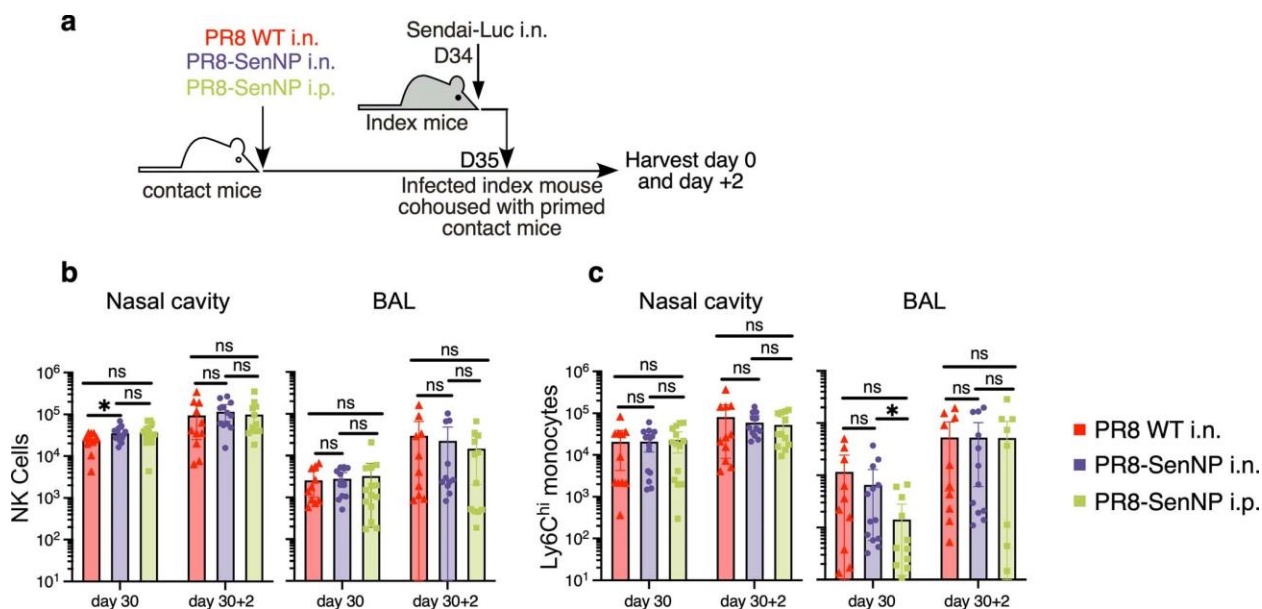


### Extended Data Figure 3. Number of SenNP-specific CD8<sup>+</sup> TRM in knockout mouse strains

**following immunization.** (a) Experimental schematic for immunizing WT and knockout mouse strains. (b) Number of CD69<sup>+</sup> CD103<sup>+</sup> Sendai NP<sub>324-332</sub>/K<sup>b</sup> CD8 T<sub>RM</sub> in the BAL, lung, and nasal cavity 35 days after immunization with LAIV-SenNP for WT (n = 15), *Prf*<sup>-/-</sup> (n = 12 for BAL,

n = 13 for lungs and nasal cavity), *Ifng*<sup>-/-</sup> (n = 18), and *Ifngr*<sup>-/-</sup> (n = 16 for lungs and nasal cavity, n = 15 for BAL). Data shown are from 3 independent pooled experiments. (c) Experimental schematic for immunizing WT and knockout mouse strains. (d) Number of natural killer (NK) cells (left graph) and inflammatory monocytes (right graph) in the nasal cavity 35 days after immunization with LAIV WT (n = 10) or LAIV-SenNP (n = 10 for WT, n = 9 for *Prf*<sup>-/-</sup>, n = 7 for *Ifngr*<sup>-/-</sup>). Data shown are from 2 pooled independent experiments. Lines represent means (b, d). Statistical significance was determined using two-sided Mann Whitney test. \* p < 0.05, \*\* p < 0.01, \*\*\* p < 0.001, \*\*\*\* p < 0.0001, ns: non-significant.

### Extended Data Figure 4



### Extended Data Figure 4. Immunization does not alter influx of NK cells and monocytes

#### following Sendai virus transmission. (a) Experimental schematic where immunized contact mice

were cohoused with a Sendai-Luc infected index mouse and tissues analyzed for innate immune

populations at the time of cohousing (D30) and two days after cohousing (D30 + 2). (b) Number

of NK cells in nasal cavity (D30: n = 11 for PR8 WT i.n., n = 15 for PR8-SenNP i.n., n = 14 for PR8-SenNP i.p.) (D30 + 2: n = 11 for PR8 WT i.n., n = 12 for PR8-SenNP i.n., n = 12 for PR8-

SenNP i.p.) and BAL (D30: n = 10 for PR8 WT i.n., n = 14 for PR8-SenNP i.n., n = 14 for PR8-

SenNP i.p.) (D30 + 2: n = 11 for PR8 WT i.n., n = 11 for PR8-SenNP i.n., n = 12 for PR8-SenNP

i.p.). (c) Number of inflammatory monocytes in nasal cavity and BAL (same n as (b), except n = 12

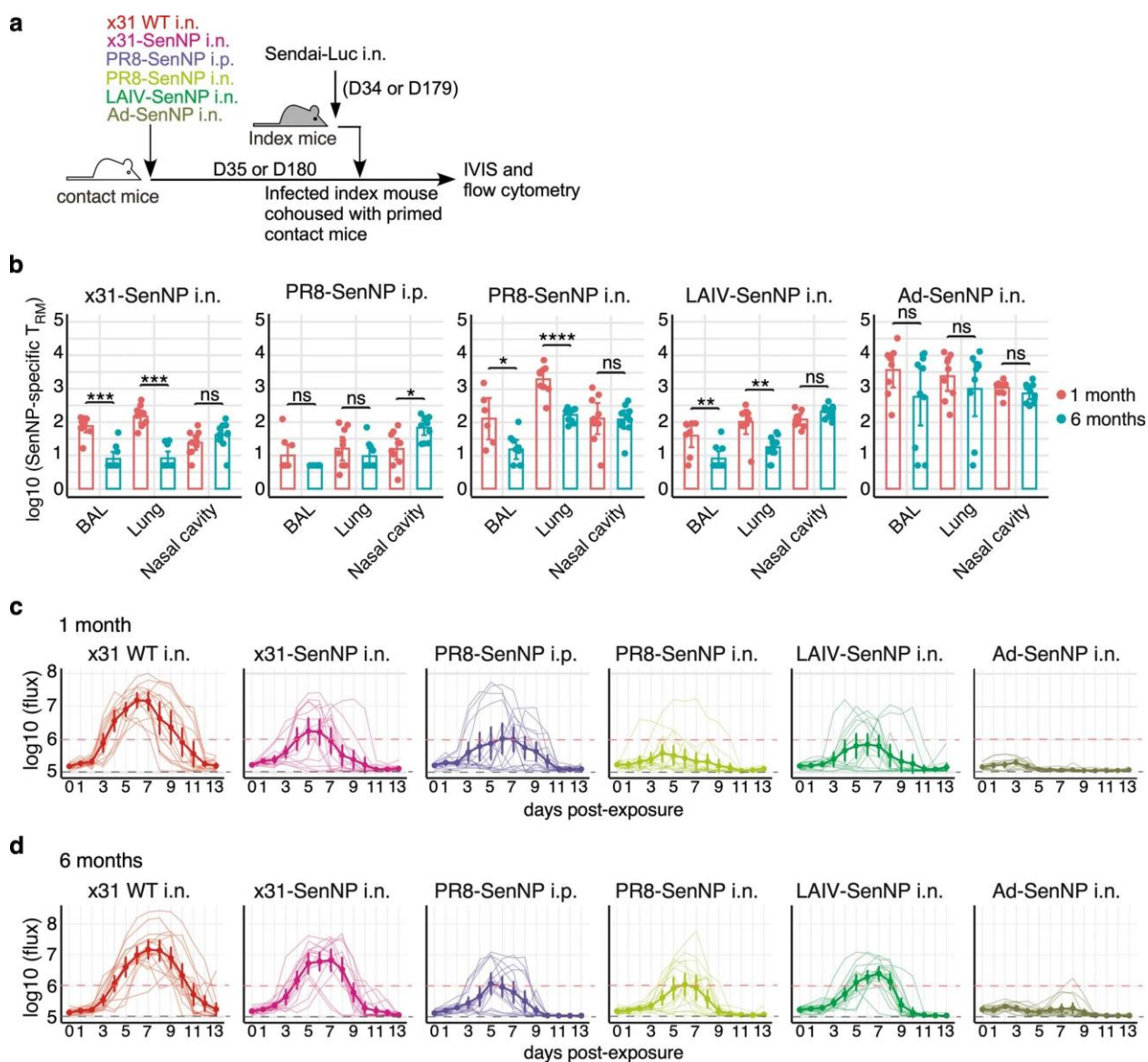
for D30 + 2 PR8-SenNP i.n. in BAL). Data shown are from 3 independent experiments. Lines

represent means and error bars represent 95% confidence interval (b, c). Statistical significance

was determined using two-sided Mann Whitney test. \* p < 0.05, \*\* p < 0.01, \*\*\* p < 0.001, \*\*\*\*

p < 0.0001, ns: non-significant.

## Extended Data Figure 5



### Extended Data Figure 5. Sendai-specific TRM numbers and assessment of transmission

under different immunization strategies at 1- and 6-months post immunization. (a)

Experimental schematic where contact mice, immunized as indicated, were cohoused with a

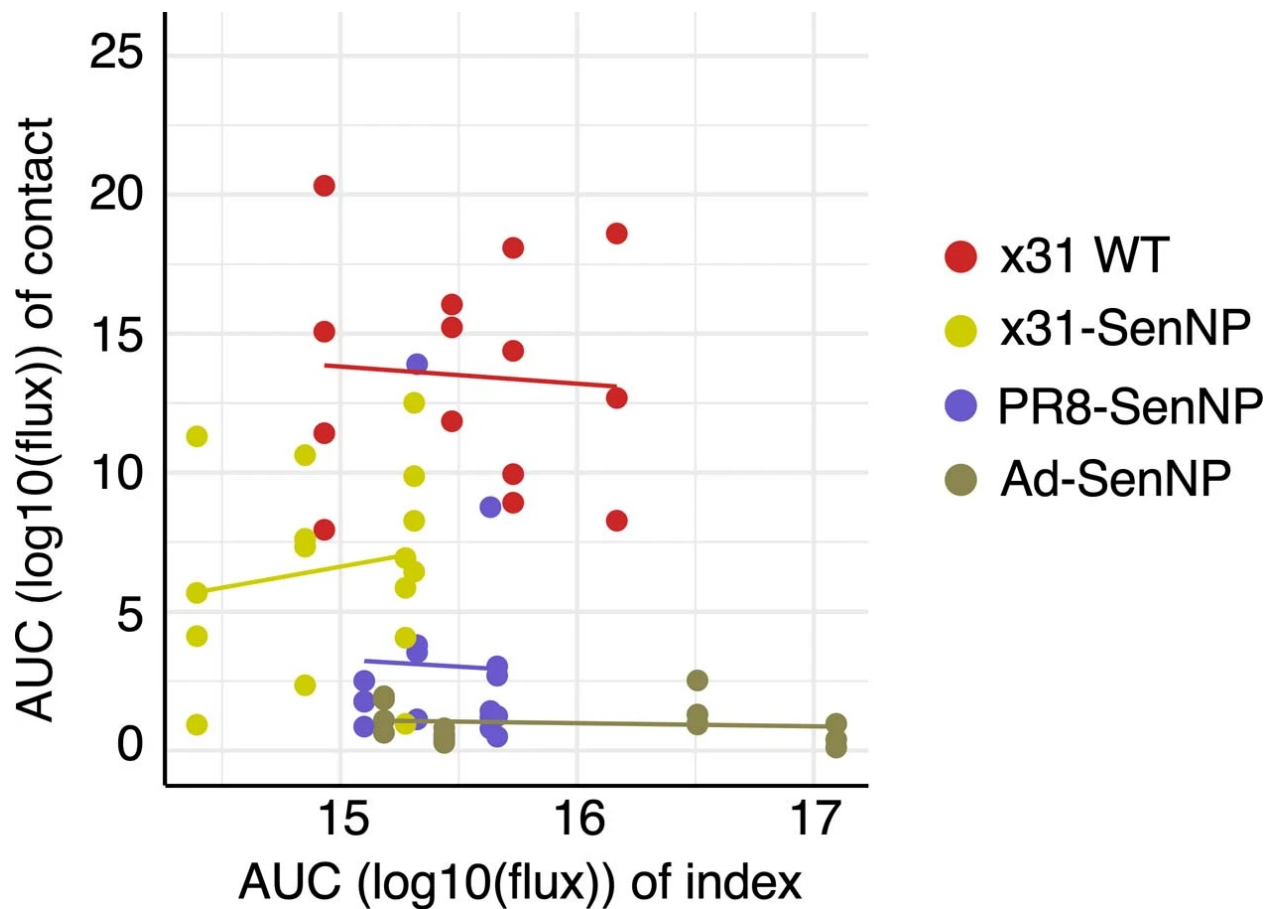
Sendai-Luc infected index mouse at 35- or 180-days post-immunization. (b) Number of

CD69<sup>+</sup>CD103<sup>+</sup> Sendai NP<sub>324-332</sub>/K<sup>b</sup> CD8 T<sub>RM</sub> in the BAL, lung, and nasal cavity at 1 month or

six months post-immunization with x31-SenNP i.n. (n = 10 per timepoint except n = 9 for 1 month

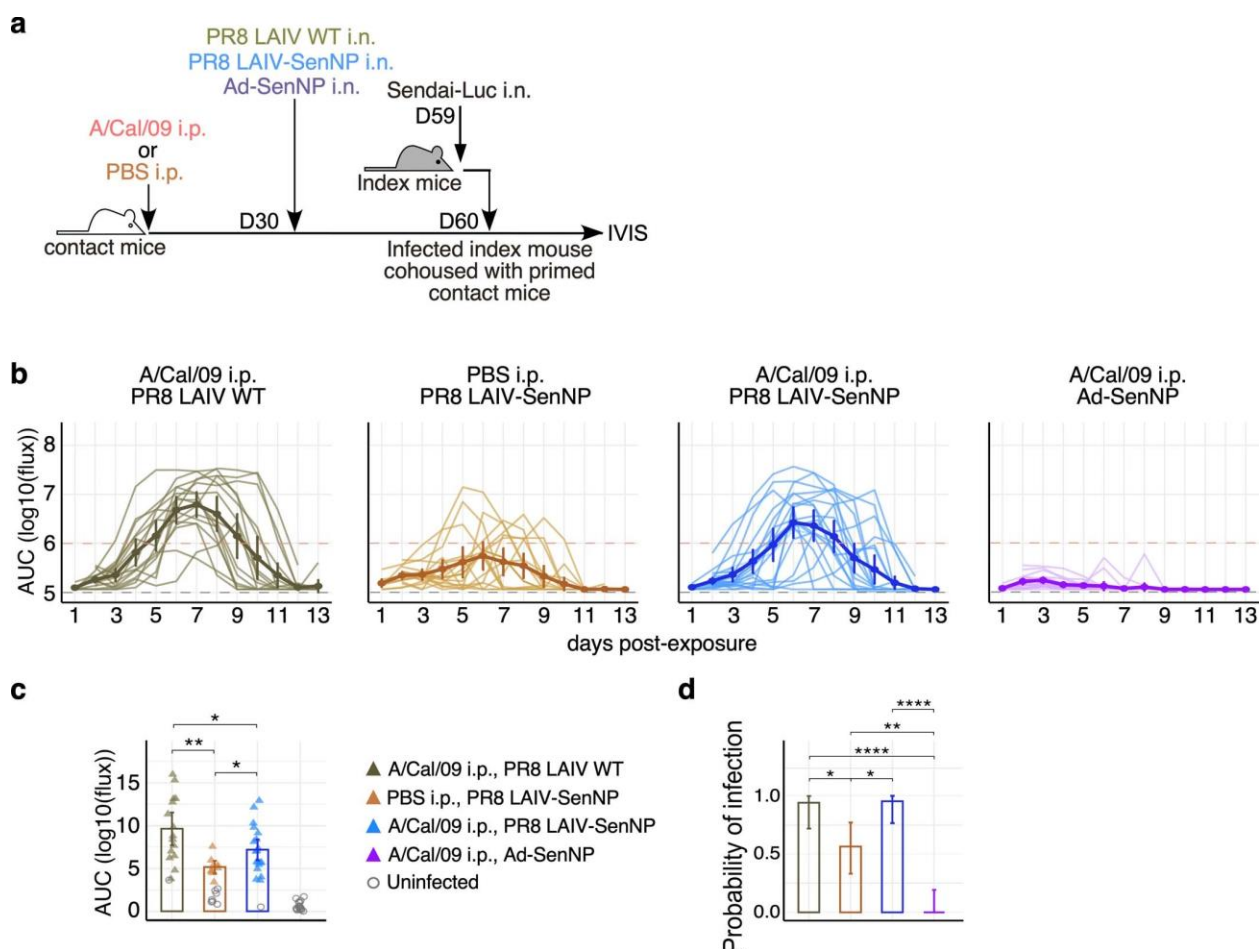
BAL), PR8-SenNP i.p. (n = 10 per timepoint except n = 9 for 1 month BAL), PR8-SenNP i.n. (1 month n = 9 for lung and nasal cavity and n = 6 for BAL, 6 month n = 10 for lung and nasal cavity and n = 9 for BAL), LAIV-SenNP i.n. (1 month n = 8, 6 month n = 10), and Ad-SenNP i.n. (1 month n = 9 for lung and nasal cavity and n = 8 for BAL, 6 month n = 10 for nasal cavity and BAL, n = 9 for lung). **(c and d)** Bioluminescence curves of immunized contact mice following exposure to an infected index mouse at 1 month (c) or 6 months (d) post-immunization with x31 WT (1 month n = 14, 6 month n = 16), x31-SenNP (1 month n = 16, 6 month n = 15), PR8-SenNP i.p. (1 month n = 16, 6 month n = 16), PR8-SenNP i.n. (1 month n = 16, 6 month n = 16), LAIV-SenNP i.n. (1 month n = 15, 6 month n = 16), and Ad-SenNP i.n. (1 month n = 15, 6 month n = 16). Solid dark lines represent means, solid pale lines represent individual mice, dashed grey line represents background bioluminescence, and dashed red line represents the limit of infection (c, d). Solid lines (b) and error bars <sup>33</sup> represent mean with 95% confidence interval. Statistical significance was determined using two-sided Mann Whitney test. Data are combined from two independent experiments. \* p < 0.05, \*\* p < 0.01, \*\*\* p < 0.001, \*\*\*\* p < 0.0001, ns: non-significant.

Extended Data Figure 6



**Extended Data Figure 6. High viral burden in index mice does not correlate with increased viral burden in contact mice.** Contact mice were infected intranasally with WT x31 (n = 14), x31-SenNP (n = 16), PR8-SenNP (n = 16), or Ad-SenNP (n = 15) and cohoused with a Sendai-Luc infected index mouse at day 35 post-immunization. n = 4 index mice per immunization group are plotted. Total viral burden (AUC) of the co-housed index and contact mice were plotted for each cage. Data were fitted to a generalized linear model with gaussian family for each immunization group to investigate the relationship between AUCs of the index mice and contact mice. Data are combined from two independent experiments.

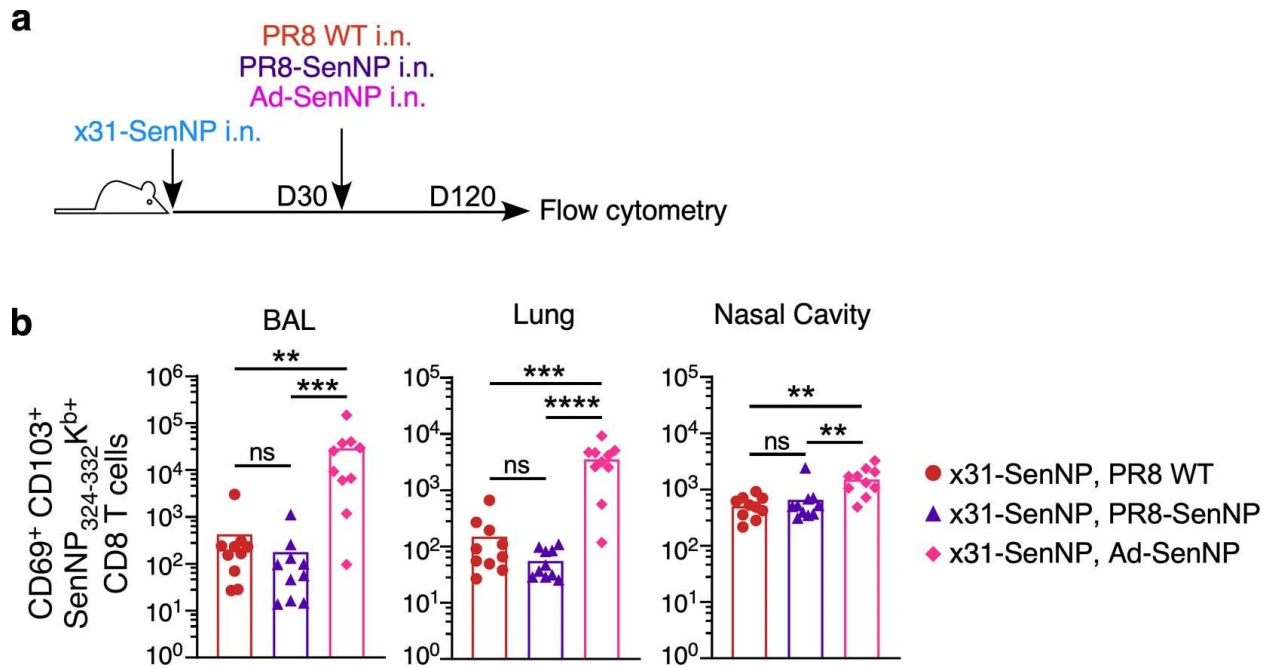
## Extended Data Figure 7



**Extended Data Figure 7. Pre-existing immunity to related influenza strains limits the efficacy of protective T cell immunity induced by LAIV-SenNP immunization but can be overcome by Ad-SenNP immunization.** (a) Experimental schematic for testing the impact of pre-existing influenza immunity on the ability of LAIV-SenNP to protect against transmission. (b) Bioluminescence curves of A/Cal/09 i.p. & PR8 LAIV WT ( $n = 16$ ), PBS i.p. & PR8 LAIV-SenNP ( $n = 16$ ), A/Cal/09 i.p. & PR8 LAIV-SenNP ( $n = 20$ ), and A/Cal/09 i.p. & Ad-SenNP ( $n = 16$ ) immunized contact mice following exposure to an infected index mouse 30 days after the second immunization. Solid dark lines represent means, solid pale lines represent individual mice, dashed grey line represents background bioluminescence, and dashed red line represents the limit of

infection. **(c)** AUC of bioluminescence in immunized contact mice that become infected following co-housing with an infected index mouse. **(d)** Probability of infection for immunized contact mice calculated as the proportion of contact mice that became infected. Bars represent 95% binomial confidence intervals (d). Lines represent means <sup>33</sup> and error bars represent 95% confidence intervals (b, c). Data are combined from two independent experiments. Statistical significance was determined using two-sided Mann Whitney test. \*  $p < 0.05$ , \*\*  $p < 0.01$ , \*\*\*  $p < 0.001$ , \*\*\*\*  $p < 0.0001$ , ns: non-significant.

## Extended Data Figure 8



**Extended Data Figure 8. Heterologous influenza prime-boost does not improve the durability of respiratory tract TRM.** (a) Experimental schematic to assess the durability of respiratory tract TRM following heterologous PR8-SenNP or Ad-SenNP boosting. (b) Number of CD69<sup>+</sup>CD103<sup>+</sup> Sendai NP<sub>324-332</sub>K<sup>b+</sup> CD8 TRM in the BAL, lung, and nasal cavity at day 120. Data are combined from two independent experiments with n = 10 mice for PR8 WT i.n., PR8-SenNP i.n., and Ad-SenNP i.n. secondary immunization groups. Lines represent means. Statistical significance was determined using two-sided Mann Whitney test. \* p < 0.05, \*\* p < 0.01, \*\*\* p < 0.001, \*\*\*\* p < 0.0001, ns: non-significant.

## **Acknowledgements**

We acknowledge the NIH tetramer core facility at Emory University for providing Sendai NP<sub>324-332</sub>, influenza NP<sub>366-374</sub> and influenza PA<sub>224-233</sub> tetramers (NIAID contract 75N93020D00005). We thank the Emory+Children's Flow Cytometry Core for cell sorting and the Emory Integrated Genomics Core for assistance with preparation of RNA-sequencing libraries. This work was supported by NIH grants R35 HL150803 and U01 HL139483 (J.E.K.). I.U. was supported by Lundbeck Foundation and Carlsberg Foundation. C.M. was supported by F31 HL164049. S.E.M. was supported by F31 HL168914.

## **Author Contributions**

S.E.M., I.U. and J.E.K. designed the study. I.U. performed experiments in Fig. 1a-1d and Extended Data Fig. 4. K.N.K. performed experiments in Extended Data Fig. 3c-d. C.M. performed experiment in Extended Data Fig. 2a-b. S.E.M. performed all other experiments. A.S. analyzed transmission data and data for Extended Data Fig. 6. S.L.H. and M.E.W. sequenced and analyzed RNA-seq data.

## References

1. Viana R, Moyo S, Amoako DG, Tegally H, Scheepers C, Althaus CL, Anyaneji UJ, Bester PA, Boni MF, Chand M, Choga WT, Colquhoun R, Davids M, Deforche K, Doolabh D, du Plessis L, Engelbrecht S, Everatt J, Giandhari J, Giovanetti M, Hardie D, Hill V, Hsiao NY, Iranzadeh A, Ismail A, Joseph C, Joseph R, Koopile L, Kosakovsky Pond SL, Kraemer MUG, Kuate-Lere L, Laguda-Akingba O, Lesetedi-Mafoko O, Lessells RJ, Lockman S, Lucaci AG, Maharaj A, Mahlangu B, Maponga T, Mahlakwane K, Makatini Z, Marais G, Maruapula D, Masupu K, Matshaba M, Mayaphi S, Mbhele N, Mbulawa MB, Mendes A, Mlisana K, Mnguni A, Mohale T, Moir M, Moruisi K, Mosepele M, Motsatsi G, Motswaledi MS, Mphoyakgosi T, Msomi N, Mwangi PN, Naidoo Y, Ntuli N, Nyaga M, Olubayo L, Pillay S, Radibe B, Ramphal Y, Ramphal U, San JE, Scott L, Shapiro R, Singh L, Smith-Lawrence P, Stevens W, Strydom A, Subramoney K, Tebeila N, Tshiabuila D, Tsui J, van Wyk S, Weaver S, Wibmer CK, Wilkinson E, Wolter N, Zarebski AE, Zuze B, Goedhals D, Preiser W, Treurnicht F, Venter M, Williamson C, Pybus OG, Bhiman J, Glass A, Martin DP, Rambaut A, Gaseitsiwe S, von Gottberg A, de Oliveira T. Rapid epidemic expansion of the SARS-CoV-2 Omicron variant in southern Africa. *Nature*. 2022;603(7902):679-86. Epub 20220107. doi: 10.1038/s41586-022-04411-y. PubMed PMID: 35042229; PMCID: PMC8942855.
2. Zheng MZM, Wakim LM. Tissue resident memory T cells in the respiratory tract. *Mucosal Immunol*. 2022;15(3):379-88. Epub 20211020. doi: 10.1038/s41385-021-00461-z. PubMed PMID: 34671115; PMCID: PMC8526531.

3. Nelson SA, Sant AJ. Potentiating Lung Mucosal Immunity Through Intranasal Vaccination. *Front Immunol.* 2021;12:808527. Epub 20211214. doi: 10.3389/fimmu.2021.808527. PubMed PMID: 34970279; PMCID: PMC8712562.
4. Mettelman RC, Allen EK, Thomas PG. Mucosal immune responses to infection and vaccination in the respiratory tract. *Immunity.* 2022;55(5):749-80. doi: 10.1016/j.immuni.2022.04.013. PubMed PMID: 35545027; PMCID: PMC9087965.
5. Hayward SL, Scharer CD, Cartwright EK, Takamura S, Li ZT, Boss JM, Kohlmeier JE. Environmental cues regulate epigenetic reprogramming of airway-resident memory CD8(+) T cells. *Nat Immunol.* 2020;21(3):309-20. Epub 20200117. doi: 10.1038/s41590-019-0584-x. PubMed PMID: 31953534; PMCID: PMC7044042.
6. Grau-Exposito J, Sanchez-Gaona N, Massana N, Suppi M, Astorga-Gamaza A, Perea D, Rosado J, Falco A, Kirkegaard C, Torrella A, Planas B, Navarro J, Suanzes P, Alvarez-Sierra D, Ayora A, Sansano I, Esperalba J, Andres C, Anton A, Ramon YCS, Almirante B, Pujol-Borrell R, Falco V, Burgos J, Buzon MJ, Genesca M. Peripheral and lung resident memory T cell responses against SARS-CoV-2. *Nat Commun.* 2021;12(1):3010. Epub 20210521. doi: 10.1038/s41467-021-23333-3. PubMed PMID: 34021148; PMCID: PMC8140108.
7. Dejnirattisai W, Huo J, Zhou D, Zahradnik J, Supasa P, Liu C, Duyvesteyn HME, Ginn HM, Mentzer AJ, Tuekprakhon A, Nutalai R, Wang B, Dijokaite A, Khan S, Avinoam O, Bahar M, Skelly D, Adele S, Johnson SA, Amini A, Ritter TG, Mason C, Dold C, Pan D, Assadi S,

Bellass A, Omo-Dare N, Koeckerling D, Flaxman A, Jenkin D, Aley PK, Voysey M, Costa Clemens SA, Naveca FG, Nascimento V, Nascimento F, Fernandes da Costa C, Resende PC, Pauvolid-Correa A, Siqueira MM, Baillie V, Serafin N, Kwatra G, Da Silva K, Madhi SA, Nunes MC, Malik T, Openshaw PJM, Baillie JK, Semple MG, Townsend AR, Huang KA, Tan TK, Carroll MW, Klenerman P, Barnes E, Dunachie SJ, Constantinides B, Webster H, Crook D, Pollard AJ, Lambe T, Consortium O, Consortium IC, Paterson NG, Williams MA, Hall DR, Fry EE, Mongkolsapaya J, Ren J, Schreiber G, Stuart DI, Sreaton GR. SARS-CoV-2 Omicron-B.1.1.529 leads to widespread escape from neutralizing antibody responses. *Cell*. 2022;185(3):467-84 e15. Epub 20220104. doi: 10.1016/j.cell.2021.12.046. PubMed PMID: 35081335; PMCID: PMC8723827.

8. Smith DJ, Lapedes AS, de Jong JC, Bestebroer TM, Rimmelzwaan GF, Osterhaus AD, Fouchier RA. Mapping the antigenic and genetic evolution of influenza virus. *Science*. 2004;305(5682):371-6. Epub 20040624. doi: 10.1126/science.1097211. PubMed PMID: 15218094.

9. Valkenburg SA, Leung NHL, Bull MB, Yan LM, Li APY, Poon LLM, Cowling BJ. The Hurdles From Bench to Bedside in the Realization and Implementation of a Universal Influenza Vaccine. *Front Immunol*. 2018;9:1479. Epub 20180702. doi: 10.3389/fimmu.2018.01479. PubMed PMID: 30013557; PMCID: PMC6036122.

10. Auladell M, Jia X, Hensen L, Chua B, Fox A, Nguyen THO, Doherty PC, Kedzierska K. Recalling the Future: Immunological Memory Toward Unpredictable Influenza Viruses. *Front*

Immunol. 2019;10:1400. Epub 20190702. doi: 10.3389/fimmu.2019.01400. PubMed PMID: 31312199; PMCID: PMC6614380.

11. Hassert M, Harty JT. Tissue resident memory T cells- A new benchmark for the induction of vaccine-induced mucosal immunity. *Front Immunol.* 2022;13:1039194. Epub 20221004. doi: 10.3389/fimmu.2022.1039194. PubMed PMID: 36275668; PMCID: PMC9581298.

12. Rimmelzwaan GF, Kreijtz JH, Bodewes R, Fouchier RA, Osterhaus AD. Influenza virus CTL epitopes, remarkably conserved and remarkably variable. *Vaccine.* 2009;27(45):6363-5. doi: 10.1016/j.vaccine.2009.01.016. PubMed PMID: 19840674.

13. Li ZT, Zarnitsyna VI, Lowen AC, Weissman D, Koelle K, Kohlmeier JE, Antia R. Why Are CD8 T Cell Epitopes of Human Influenza A Virus Conserved? *J Virol.* 2019;93(6). Epub 20190305. doi: 10.1128/JVI.01534-18. PubMed PMID: 30626684; PMCID: PMC6401462.

14. Bhatt S, Holmes EC, Pybus OG. The genomic rate of molecular adaptation of the human influenza A virus. *Mol Biol Evol.* 2011;28(9):2443-51. Epub 20110316. doi: 10.1093/molbev/msr044. PubMed PMID: 21415025; PMCID: PMC3163432.

15. Zens KD, Chen JK, Farber DL. Vaccine-generated lung tissue-resident memory T cells provide heterosubtypic protection to influenza infection. *JCI Insight.* 2016;1(10). doi: 10.1172/jci.insight.85832. PubMed PMID: 27468427; PMCID: PMC4959801.

16. Wu T, Hu Y, Lee YT, Bouchard KR, Benechet A, Khanna K, Cauley LS. Lung-resident memory CD8 T cells (TRM) are indispensable for optimal cross-protection against pulmonary virus infection. *J Leukoc Biol.* 2014;95(2):215-24. Epub 20130904. doi: 10.1189/jlb.0313180. PubMed PMID: 24006506; PMCID: PMC3896663.
17. McMaster SR, Wilson JJ, Wang H, Kohlmeier JE. Airway-Resident Memory CD8 T Cells Provide Antigen-Specific Protection against Respiratory Virus Challenge through Rapid IFN-gamma Production. *J Immunol.* 2015;195(1):203-9. Epub 20150529. doi: 10.4049/jimmunol.1402975. PubMed PMID: 26026054; PMCID: PMC4475417.
18. Tang J, Zeng C, Cox TM, Li C, Son YM, Cheon IS, Wu Y, Behl S, Taylor JJ, Chakaraborty R, Johnson AJ, Shiavo DN, Utz JP, Reisenauer JS, Midthun DE, Mullan JJ, Edell ES, Alameh MG, Borish L, Teague WG, Kaplan MH, Weissman D, Kern R, Hu H, Vassallo R, Liu SL, Sun J. Respiratory mucosal immunity against SARS-CoV-2 after mRNA vaccination. *Sci Immunol.* 2022;7(76):eadd4853. Epub 20221021. doi: 10.1126/sciimmunol.add4853. PubMed PMID: 35857583; PMCID: PMC9348751.
19. Pizzolla A, Nguyen THO, Smith JM, Brooks AG, Kedzieska K, Heath WR, Reading PC, Wakim LM. Resident memory CD8(+) T cells in the upper respiratory tract prevent pulmonary influenza virus infection. *Sci Immunol.* 2017;2(12). doi: 10.1126/sciimmunol.aam6970. PubMed PMID: 28783656.

20. Lowen AC, Bouvier NM, Steel J. Transmission in the guinea pig model. *Curr Top Microbiol Immunol.* 2014;385:157-83. doi: 10.1007/82\_2014\_390. PubMed PMID: 25001209; PMCID: PMC7121145.
  
21. Burke CW, Bridges O, Brown S, Rahija R, Russell CJ. Mode of parainfluenza virus transmission determines the dynamics of primary infection and protection from reinfection. *PLoS Pathog.* 2013;9(11):e1003786. Epub 20131121. doi: 10.1371/journal.ppat.1003786. PubMed PMID: 24278024; PMCID: PMC3836739.
  
22. Uddback I, Cartwright EK, Scholler AS, Wein AN, Hayward SL, Lobby J, Takamura S, Thomsen AR, Kohlmeier JE, Christensen JP. Long-term maintenance of lung resident memory T cells is mediated by persistent antigen. *Mucosal Immunol.* 2021;14(1):92-9. Epub 20200609. doi: 10.1038/s41385-020-0309-3. PubMed PMID: 32518368; PMCID: PMC7726002.
  
23. Lobby JL, Uddback I, Scharer CD, Mi T, Boss JM, Thomsen AR, Christensen JP, Kohlmeier JE. Persistent Antigen Harbored by Alveolar Macrophages Enhances the Maintenance of Lung-Resident Memory CD8(+) T Cells. *J Immunol.* 2022;209(9):1778-87. Epub 20220926. doi: 10.4049/jimmunol.2200082. PubMed PMID: 36162870; PMCID: PMC9588742.
  
24. Burke CW, Mason JN, Surman SL, Jones BG, Dalloneau E, Hurwitz JL, Russell CJ. Illumination of parainfluenza virus infection and transmission in living animals reveals a tissue-

specific dichotomy. *PLoS Pathog.* 2011;7(7):e1002134. Epub 20110707. doi:

10.1371/journal.ppat.1002134. PubMed PMID: 21750677; PMCID: PMC3131265.

25. Upadhyay R, Boiarsky JA, Pantsulaia G, Svensson-Arvelund J, Lin MJ, Wroblewska A, Bhalla S, Scholler N, Bot A, Rossi JM, Sadek N, Parekh S, Lagana A, Baccarini A, Merad M, Brown BD, Brody JD. A Critical Role for Fas-Mediated Off-Target Tumor Killing in T-cell Immunotherapy. *Cancer Discov.* 2021;11(3):599-613. Epub 20201217. doi: 10.1158/2159-8290.CD-20-0756. PubMed PMID: 33334730; PMCID: PMC7933082.

26. Dobin A, Davis CA, Schlesinger F, Drenkow J, Zaleski C, Jha S, Batut P, Chaisson M, Gingeras TR. STAR: ultrafast universal RNA-seq aligner. *Bioinformatics.* 2013;29(1):15-21. Epub 20121025. doi: 10.1093/bioinformatics/bts635. PubMed PMID: 23104886; PMCID: PMC3530905.

27. Lawrence M, Huber W, Pages H, Aboyoun P, Carlson M, Gentleman R, Morgan MT, Carey VJ. Software for computing and annotating genomic ranges. *PLoS Comput Biol.* 2013;9(8):e1003118. Epub 20130808. doi: 10.1371/journal.pcbi.1003118. PubMed PMID: 23950696; PMCID: PMC3738458.

28. Love MI, Huber W, Anders S. Moderated estimation of fold change and dispersion for RNA-seq data with DESeq2. *Genome Biol.* 2014;15(12):550. doi: 10.1186/s13059-014-0550-8. PubMed PMID: 25516281; PMCID: PMC4302049.

29. Subramanian A, Tamayo P, Mootha VK, Mukherjee S, Ebert BL, Gillette MA, Paulovich A, Pomeroy SL, Golub TR, Lander ES, Mesirov JP. Gene set enrichment analysis: a knowledge-based approach for interpreting genome-wide expression profiles. *Proc Natl Acad Sci U S A*. 2005;102(43):15545-50. Epub 20050930. doi: 10.1073/pnas.0506580102. PubMed PMID: 16199517; PMCID: PMC1239896.
30. Schenkel JM, Fraser KA, Vezys V, Masopust D. Sensing and alarm function of resident memory CD8(+) T cells. *Nat Immunol*. 2013;14(5):509-13. Epub 20130331. doi: 10.1038/ni.2568. PubMed PMID: 23542740; PMCID: PMC3631432.
31. Slutter B, Pewe LL, Kaech SM, Harty JT. Lung airway-surveilling CXCR3(hi) memory CD8(+) T cells are critical for protection against influenza A virus. *Immunity*. 2013;39(5):939-48. doi: 10.1016/j.immuni.2013.09.013. PubMed PMID: 24238342; PMCID: PMC3872058.
32. Gilchuk P, Hill TM, Guy C, McMaster SR, Boyd KL, Rabacal WA, Lu P, Shyr Y, Kohlmeier JE, Sebzda E, Green DR, Joyce S. A Distinct Lung-Interstitium-Resident Memory CD8(+) T Cell Subset Confers Enhanced Protection to Lower Respiratory Tract Infection. *Cell Rep*. 2016;16(7):1800-9. Epub 20160804. doi: 10.1016/j.celrep.2016.07.037. PubMed PMID: 27498869; PMCID: PMC5021515.
33. McMahan K, Yu J, Mercado NB, Loos C, Tostanoski LH, Chandrashekar A, Liu J, Peter L, Atyeo C, Zhu A, Bondzie EA, Dagotto G, Gebre MS, Jacob-Dolan C, Li Z, Nampanya F, Patel S, Pessaint L, Van Ry A, Blade K, Yalley-Ogunro J, Cabus M, Brown R, Cook A, Teow E,

Andersen H, Lewis MG, Lauffenburger DA, Alter G, Barouch DH. Correlates of protection against SARS-CoV-2 in rhesus macaques. *Nature*. 2021;590(7847):630-4. Epub 20201204. doi: 10.1038/s41586-020-03041-6. PubMed PMID: 33276369; PMCID: PMC7906955.

34. Bertoletti A, Le Bert N, Tan AT. SARS-CoV-2-specific T cells in the changing landscape of the COVID-19 pandemic. *Immunity*. 2022;55(10):1764-78. Epub 20220818. doi: 10.1016/j.immuni.2022.08.008. PubMed PMID: 36049482; PMCID: PMC9385766.

35. Clemens EB, van de Sandt C, Wong SS, Wakim LM, Valkenburg SA. Harnessing the Power of T Cells: The Promising Hope for a Universal Influenza Vaccine. *Vaccines (Basel)*. 2018;6(2). Epub 20180326. doi: 10.3390/vaccines6020018. PubMed PMID: 29587436; PMCID: PMC6027237.

36. Gotch F, McMichael A, Smith G, Moss B. Identification of viral molecules recognized by influenza-specific human cytotoxic T lymphocytes. *J Exp Med*. 1987;165(2):408-16. doi: 10.1084/jem.165.2.408. PubMed PMID: 3029268; PMCID: PMC2188513.

37. Boon AC, de Mutsert G, Graus YM, Fouchier RA, Sintnicolaas K, Osterhaus AD, Rimmelzwaan GF. The magnitude and specificity of influenza A virus-specific cytotoxic T-lymphocyte responses in humans is related to HLA-A and -B phenotype. *J Virol*. 2002;76(2):582-90. doi: 10.1128/jvi.76.2.582-590.2002. PubMed PMID: 11752149; PMCID: PMC136822.

38. Koutsakos M, Illing PT, Nguyen THO, Mifsud NA, Crawford JC, Rizzetto S, Eltahla AA, Clemens EB, Sant S, Chua BY, Wong CY, Allen EK, Teng D, Dash P, Boyd DF, Grzelak L, Zeng W, Hurt AC, Barr I, Rockman S, Jackson DC, Kotsimbos TC, Cheng AC, Richards M, Westall GP, Loudovaris T, Mannering SI, Elliott M, Tangye SG, Wakim LM, Rossjohn J, Vijaykrishna D, Luciani F, Thomas PG, Gras S, Purcell AW, Kedzierska K. Human CD8(+) T cell cross-reactivity across influenza A, B and C viruses. *Nat Immunol.* 2019;20(5):613-25. Epub 20190218. doi: 10.1038/s41590-019-0320-6. PubMed PMID: 30778243.
39. Richard M, van den Brand JMA, Bestebroer TM, Lexmond P, de Meulder D, Fouchier RAM, Lowen AC, Herfst S. Influenza A viruses are transmitted via the air from the nasal respiratory epithelium of ferrets. *Nat Commun.* 2020;11(1):766. Epub 20200207. doi: 10.1038/s41467-020-14626-0. PubMed PMID: 32034144; PMCID: PMC7005743.
40. Yang W, Shaman J. Viral replication dynamics could critically modulate vaccine effectiveness and should be accounted for when assessing new SARS-CoV-2 variants. *Influenza Other Respir Viruses.* 2022;16(2):366-7. Epub 20220110. doi: 10.1111/irv.12961. PubMed PMID: 35014184; PMCID: PMC8818828.
41. Jacobs S, Zeippen C, Wavreil F, Gillet L, Michiels T. IFN-lambda Decreases Murid Herpesvirus-4 Infection of the Olfactory Epithelium but Fails to Prevent Virus Reactivation in the Vaginal Mucosa. *Viruses.* 2019;11(8). Epub 20190816. doi: 10.3390/v11080757. PubMed PMID: 31426334; PMCID: PMC6722623.

**CHAPTER III: Vaccine-induced upper respiratory tract resident memory CD8 T cells are sufficient to inhibit productive infection after viral transmission**

Sarah E. Michalets<sup>1</sup>, M. Elliott Williams<sup>1</sup>, Ananya Saha<sup>2</sup>, Ariana Jimenez<sup>1</sup>, Yixel Soto-Vazquez<sup>1</sup>, Anice C. Lowen<sup>1</sup>, Christopher D. Scharer<sup>1</sup>, Rustom Antia<sup>2</sup>, Jacob E. Kohlmeier<sup>1,3</sup>.

<sup>1</sup>Emory University School of Medicine, Department of Microbiology & Immunology, Atlanta GA

<sup>2</sup>Emory University, Department of Biology, Atlanta GA

<sup>3</sup>Correspondence: Jacob Kohlmeier, 1510 Clifton Rd., RRC 3133, Atlanta GA 30322. Email: jkohlmeier@emory.edu.

**Abstract**

Intranasal vaccination elicits CD8 tissue resident memory T cells (TRM) throughout the respiratory tract that are capable of providing cross protection against heterosubtypic viral strains and reducing immunopathology. Recently, we demonstrated that CD8 TRM can prevent respiratory virus transmission using Sendai virus, a murine parainfluenza virus. Here, we show that CD8 TRM-mediated protection occurs independently of circulating leukocytes, B cells, or CD4 T cells. Additionally, we investigate the contributions of CD8 TRM in different anatomical compartments of the respiratory tract for protection against transmission and illustrate that CD8 TRM in the upper respiratory tract (URT), but not the lower respiratory tract (LRT), become activated and proliferate in response to transmitted virus. Furthermore, we demonstrate that CD8 TRM in the URT alone provide sufficient immune surveillance to prevent propagation of infection after viral transmission. These findings offer insights into the development of T cell-based respiratory virus vaccines and shed light on the critical role for URT CD8 TRM in the prevention of viral transmission.

## Introduction

While the ideal endpoint of vaccination is the induction of neutralizing antibodies and sterilizing immunity, respiratory virus infections such as SARS-CoV-2 and influenza have demonstrated the inadequacy of antibody-mediated immunity to provide broad protection against emerging and drifted viral variants<sup>1-4</sup>. In contrast, vaccine-induced T cell responses target conserved internal viral epitopes enabling cross protection among viral strains<sup>5,6</sup>. As such, T-cell based vaccines represent a promising complement to conventional respiratory virus vaccines and circumvent the need for frequently updated strain-specific vaccines.

Tissue resident memory T cells (TRM) are an essential cellular population of a mucosal vaccine-induced T cell response. Following a vaccination or viral infection, antigen-specific TRM remain localized in nonlymphoid tissues where they persist, poised to rapidly initiate effector mechanisms and proliferate upon recognition of their cognate antigen. Unique transcriptional programs alter TRM's trafficking capabilities and promote expression of canonical identification markers CD103 and/or CD69, enabling TRM to establish tissue residency and delineating them from their central memory and effector memory T cell counterparts<sup>7,8</sup>. CD8 TRM have been shown to mediate protection against heterosubtypic influenza virus and SARS-CoV-2 infections by significantly decreasing viral loads, limiting immunopathology, and preventing viral spread to the lungs<sup>9-12</sup>. While informative, these prior studies utilized high viral titer infection models that delivered antigen throughout the entire respiratory tract and did not recapitulate natural viral transmission dynamics where one infected individual transmit virus to another. To address this gap in knowledge, we previously developed a natural transmission model using Sendai virus, a murine parainfluenza virus that transmits by both contact and airborne routes of transmission<sup>13</sup>.

The respiratory tract is divided into the upper respiratory tract (URT) consisting of the nasal cavity, pharynx, and larynx, and the lower respiratory tract (LRT), comprised by the trachea, airways, and lung<sup>14</sup>. The properties of TRM in the lung have been well defined and studied in the context of respiratory virus infections. However, an unappreciated role for cellular immunity in the nasal cavity of the URT is emerging, as the SARS-CoV-2 pandemic highlighted the lack of knowledge regarding vaccine-induced immune responses at this site. The question remains as to whether immune surveillance is required throughout the entire respiratory tract to prevent viral transmission, or if one anatomical compartment plays an outsized role in this process.

Here, we used our Sendai virus model of respiratory virus transmission to evaluate the contributions of TRM in the URT and LRT in preventing infection from transmission. We show that TRM in the URT become activated through their TCRs, proliferate, and exert antiviral transcriptional programs in response to transmitted virus. Additionally, we demonstrate that TRM in the URT alone are sufficient to protect against respiratory virus transmission. These findings provide new evidence for the importance of vaccine-induced memory T cell responses in the URT and will inform future vaccine design aimed at preventing respiratory virus spread in the population.

## Materials and Methods

### *Mice*

Female C57/BL/6J, B6.129S2-*Ighm*<sup>tm1Cgn</sup>/J (mMT<sup>-/-</sup>), and C57BL/6-Tg(Nr4a1-EGFP/cre)820Khog/J (Nur77<sup>GFP</sup>) mice were purchased from Jackson Laboratory and bred in-house. Mice were housed at Emory University under specific pathogen-free conditions and used in experiments between 8 and 12 weeks of age. All experiments were conducted in accordance with the Institutional Animal Care and Use Committee guidelines of Emory University (PROTO201700581).

### *Viruses*

All intranasal (i.n.) infections were administered under anesthesia with isoflurane (Patterson Veterinary). Mice received 50,000 plaque forming units (PFU) of live attenuated Influenza A/Puerto Rico/8/34 (LAIV WT), 20,000 PFU of live attenuated Influenza A/Puerto Rico/8/34 expressing Sendai virus nucleoprotein FAPGNYPAL epitope (LAIV-SenNP), 50 PFU of Influenza A/Puerto Rico/8/34 expressing Sendai virus nucleoprotein FAPGNYPAL epitope (PR8-SenNP),  $2 \times 10^7$  PFU of replication-deficient adenovirus serotype 5 expressing the Influenza nucleoprotein ASNENMETM epitope (Ad-FluNP), or  $2 \times 10^7$  PFU of replication-deficient adenovirus serotype 5 expressing the Sendai virus nucleoprotein FAPGNYPAL epitope (Ad-SenNP) i.n. in a 30 $\mu$ L volume, as previously described<sup>15</sup>. Upper respiratory tract only infections were performed using a 5 $\mu$ L i.n. immunization of  $2 \times 10^7$  PFU of Ad-SenNP under isoflurane anesthesia. Index mice used in transmission experiments were infected i.n. with 1,500 PFU of Sendai virus encoding a luciferase reporter (Sendai-Luc) in a 30 $\mu$ L inoculum under isoflurane anesthesia<sup>16</sup>.

### ***Chemical Treatments and CD4 Depletion***

For FTY720 treatments, mice were injected daily intraperitoneally (i.p.) with 150mg (Cayman Chemical) suspended in PBS, starting 3 days before initiation of co-housing<sup>17</sup>. For CD4+ T cell depletion, mice were given an initial loading dose of anti-CD4 mAb clone GK1.5 (BioXCell) 200 mg i.n. and 200 mg i.p., followed by 200 mg i.p. every 3 days. A control group was administered an isotype control (BioXCell) in the same dose and schedule. 1 mg of 5-ethynyl-2'-deoxyuridine (EdU; Cayman Chemical) was administered 1 day prior to sacrifice i.p. in 200 $\mu$ L PBS<sup>18</sup>.

### ***In Vivo Imaging***

In vivo imaging was performed using an In Vivo Imaging System (IVIS) Lumina LT Series III (Perkin Elmer) as previously described<sup>15</sup>. Mice were injected i.p. with 3 mg of IVISbrite D-Luciferin (Revvity) reconstituted in D-PBS, 10 minutes prior to image acquisition. Images were captured using an XFOV-24 lens and acquisition settings were a binning of 8, F/stop of 1, with exposure times of 5, 30, and 120 seconds. Background bioluminescence was calculated by imaging two uninfected mice each day of the experiment. At least one day prior to co-housing for transmission experiments, chest hair was removed from mice by shaving and applying a depilation cream. Images were analyzed in the Living Image 4.7.2 software (Perkin Elmer), where region of interest gates were manually drawn around the respiratory tract region and used to quantitate bioluminescent flux. Data were exported to Microsoft Excel. Bioluminescent curves and statistics were performed using GraphPad Prism or R software.

### *Plaque Assays*

Samples for nasal shedding analyses were collected by dipping the nose of isoflurane anesthetized mice into a 12-well plate with 1% BSA in PBS. Samples were then frozen at  $-80^{\circ}\text{C}$  until performing the assay. 12-well plates were seeded with  $4 \times 10^5$  Vero cells and grown to near 100% confluency. Cells were incubated with samples for 1 hour at  $34^{\circ}\text{C}$  and 5%  $\text{CO}_2$ , and then treated with a 1x MEM, HEPES buffer, 0.5% gelatin, 0.5% agarose, 0.4% BSA, 1x GlutaMAX, 0.02 mg/mL penicillin-streptomycin, 0.3% sodium bicarbonate and 5 U/mL TPCK trypsin overlay. After 4 days, the overlay was removed, cells were fixed with 10% formaldehyde and stained with 1% crystal violet. All samples were titrated in duplicate. Plaques were counted manually, and PFU was calculated by multiplying the average number of plaques by the dilution factor. The limit of detection (LOD) was established as 5 plaques for the lowest dilution, equating to 25 PFU.

### *Tissue Collection, Cellular Isolation, and Flow Cytometry*

5 minutes prior to euthanasia, mice were injected i.v. with 1.5mg of anti-CD3e-PECF594 clone 145-2C11 (Biolegend) or 2 mg CD45.2-BV650 clone 104 in 200 $\mu\text{L}$  of PBS to distinguish circulating cells from tissue-resident cells. Mice were euthanized with a lethal i.p. injection of 2,2,2-tribromoethanol (Avertin) followed by brachial exsanguination. Lungs, bronchoalveolar lavage (BAL), nasal cavity, and spleen were harvested from each animal. Lungs and nasal cavities were enzymatically digested with Collagenase D (5 g/l; Roche) and DNase ( $1 \times 10^6$  U/l; Sigma) for 30 minutes at  $37^{\circ}\text{C}$ . Lymphocytes were further isolated from lungs using 40%/80% Percoll density centrifugation. Cells were filtered through a 70-mm membrane and RBCs were lysed using ACK buffer prior to staining. For flow cytometry and FACS, cells were  $\text{F}_c$  blocked using murine anti-CD16/32 2.4.G2 for 10 minutes. Samples were then stained with 1:100 Sendai-NP ( $\text{K}^b_{324-332}$ )

tetramer- PE or APC (provided by NIH Tetramer Core Facility) for 1 hour. Extracellular staining with 1:100 dilutions of fluorescently conjugated antibodies including anti-CD8a-BV711 clone 53-6.7, CD4-UV496 clone GK1.5, CD4-A700 clone RM4-4, CD103-BV421 clone 2E7, CD69-A488/PE-Cy7 clone H1.2F3, CD62L-BV605 clone MEL-14, CD44-BV510 clone IM7, CD19-APC eFluor780 clone 1D3, CD3-APC clone 17A2, CD45-A700/PerCPCy5.5 clone 30-F11 was performed for 30 minutes. Zombie NIR or 7-aminoactinomycin D (7-AAD) was used to determine cellular viability. For EdU experiments, samples were further stained using the Click-iT Plus EdU Flow Cytometry Kit – Alexa Fluor 647 (Invitrogen) according to the kit’s standard protocol. Cell counts were calculated manually using a hemocytometer for nasal cavity and BAL samples or a LUNA-II automatic cell counter (Logos Biosystems) for spleen and lung tissues. All samples were acquired on a Fortessa X20 flow cytometer or sorted on a FACS Aria II (BD Biosciences). SenNP+ TRM were gated on singlets, lymphocytes, i.v. label- live cells, CD4-CD8a+, CD44<sup>hi</sup> Tetramer+, CD69+ CD103+. Flow cytometry data were analyzed using FlowJo v.10 software.

### ***Single Cell RNA Sequencing***

Single cell RNA sequencing gene expression libraries were generated following the Chromium Single Cell 5' Reagent Kits User Guide, v2 Chemistry Dual Index (10x Genomics). Illumina fastq files were processed and mapped to the GRCh38-2024-A reference transcriptome using 10x Genomics Cell Ranger 8.0.0<sup>19</sup> and each biological replicate aggregated on a per-batch basis for downstream analysis using the “aggr” command in Cell Ranger with the default parameters. Aggregated data were analyzed using Seurat v5.0.0<sup>20</sup>. Subsequent command references are from this software and default parameters were used for all commands unless otherwise specified. Low quality cells with the following criteria were filtered out: percent of mitochondrial reads in

each cell greater than 5 percent and less than 500 (Replicate 1) and 300 (Replicate 2) uniquely expressed genes per cell. The remaining counts from each batch were separately normalized and scaled, and the batch-corrected, integrated UMAP was created using Harmony<sup>21</sup> and clustered using the top four principal components of the dimensional reduction with a resolution of 0.24 that resulted in six clusters. RNA velocity analysis was performed by first estimating the quantity of unspliced and spliced reads on a per-sample basis with *velocyto* v0.17.15<sup>22</sup>. Then, using *scvelo* v0.2.5<sup>23</sup>, RNA velocity was computed with a steady-state model. The vector field of the RNA velocity was averaged into streamlines and overlaid on the 2D UMAP for visualization of broader flows and additional metadata information about the cells was underlaid.

### *Statistical Analysis*

Statistical analyses were performed using GraphPad Prism v9 or R software. For in vivo imaging analyses, the threshold of infection was calculated as the mean background bioluminescence flux +2.5 x standard deviation of the background flux. Any flux values below the mean background flux were replaced by the mean background flux. Area under the curve (AUC) for each animal was calculated using the *trapz* function in R and the background AUC was subtracted. AUC values were compared using a Mann-Whitney test with the *wilcox\_test* function in R. The probability of infection was calculated as the proportion of mice in each group that became infected and had bioluminescent flux values greater than the threshold of infection. Confidence intervals were generated using a binomial probability distribution with the *binconf* function in R. Probability of infection values were compared using a proportion test with the *prop\_test* function in R. Unless otherwise indicated, data points represent individual mice for at least 2 independent replicates. Statistical significance for cell number analyses were determined using a two-sided Mann-Whitney

test in GraphPad Prism. *P* values for all statistics are indicated as \**P*<0.05, \*\**P*<0.01, \*\*\**P*<0.001, \*\*\*\**P*<0.0001, N.S. not significant.

## Results

### CD8 TRM are sufficient to inhibit productive infection following transmission

Following intranasal immunization with engineered adenoviral vectors and live-attenuated influenza A viruses that express the immunodominant H-2K<sup>d</sup> CD8 T cell epitope (FAPGNYPAL) for the Sendai virus nucleoprotein (SenNP), mice generate Sendai virus-specific central, effector, and respiratory tract resident memory T cells (TRM)<sup>15</sup>. By combining these immunization strategies with a firefly luciferase encoding Sendai virus (Sendai-Luc), we previously demonstrated that Sendai-specific CD8 TRM were capable of surveying the respiratory tract to prevent the establishment of infection following transmission using *in vivo* bioluminescent imaging<sup>15</sup>.

First, we tested whether these *in vivo* bioluminescent imaging results were recapitulated by nasal shedding of infectious virus. Contact mice were immunized intranasally with a live attenuated PR8 influenza A virus encoding the FAPGNYPAL epitope for SenNP (LAIV-SenNP) or a replication-deficient adenoviral serotype 5 vector expressing the Sendai virus nucleoprotein (Ad-SenNP). After 35 days, mice were co-housed with a Sendai-Luc infected index mouse. Transmission from the infected index mouse to the immunized contact mice was tracked longitudinally by both *in vivo* imaging and nose dips for viral shedding analysis (**Fig. 1a**). A control group was inoculated with a live attenuated influenza A virus control lacking the SenNP antigen (LAIV-WT) to account for the role of inflammation or trained innate immunity during immunization, while not generating any Sendai virus-specific immune responses. Infection was evident in LAIV-WT and LAIV-SenNP immunized mice by 6 days post co-housing (D35+6), and the LAIV-SenNP group exhibited significantly reduced nasal shedding at D35+6 and D35+9. Notably, mice immunized with Ad-SenNP did not exhibit nasal shedding at any time point (**Fig.**

**1b).** Viral titer differences between LAIV-SenNP and Ad-SenNP immunized mice can be attributed to the number of Sendai-specific TRM elicited during vaccination, as we previously showed that LAIV-SenNP elicits fewer CD8 TRM in the respiratory tract<sup>15</sup>, resulting a higher probability of infection compared to Ad-SenNP. While these findings demonstrate that CD8 TRM can significantly limit both viral infection and nasal shedding from transmission, they do not exclude potential contributions from other immune cell populations.

To further define the ability of CD8 TRM to prevent respiratory transmission we evaluated whether the influx of circulating immune cells, mucosal B cell responses, or CD4 T cells play a role in this response. We utilized FTY720 dosing to inhibit S1P-dependent cellular trafficking and evaluate whether circulating memory CD8 T cell subsets and other S1P-dependent leukocytes aid in protection against transmission. Contact mice were immunized intranasally with Ad-SenNP or an adenoviral vector control (Ad-FluNP) and exposed to transmission of Sendai-Luc. In vivo imaging was performed to monitor transmission from the index mouse to immunized contact mice, and bioluminescent curves were graphed (**Fig. 1c, 1d**). As expected, all contact mice (8 out of 8) who received the Ad-FluNP control and lacked any Sendai-specific immunity became infected. Interestingly, regardless of whether S1P-dependent cellular trafficking was inhibited, all animals with SenNP-specific CD8 TRM were protected from infection (**Fig. 1d, 1e**). These results were reiterated when using LAIV-SenNP priming (**Extended Data Fig. 1a-c**). These data demonstrate that CD8 TRM present in the respiratory tract are sufficient to protect against viral transmission and that the recruitment of circulating effector lymphocyte populations is dispensable.

To determine whether potential B cell responses elicited during immunization aid in protection against transmission, we used *mMT*<sup>-/-</sup> mice which lack functional mature B cells. Unlike LAIV-SenNP which only encodes the 9 amino acid FAPGNYPAL sequence from SenNP and is

thus extremely unlikely to induce any Sendai-specific B cells, Ad-SenNP expresses the entire Sendai virus nucleoprotein and could potentially lead to SenNP-specific B cell responses after immunization. We immunized *mMT*<sup>-/-</sup> contact mice with Ad-SenNP and Ad-FluNP as a control and challenged them using the Sendai-Luc transmission model (**Fig. 1f**). 90% (9 out of 10) of Ad-FluNP immunized *mMT*<sup>-/-</sup> contact mice became infected, while all (12 out of 12) of the Ad-SenNP immunized *mMT*<sup>-/-</sup> contact mice were protected from infection, mimicking the results observed in WT mice (**Fig. 1g, 1h**). Priming *mMT*<sup>-/-</sup> mice with LAIV-SenNP resulted in a similar trend (**Extended Data Fig. 1d-f**). CD4 T cells have been shown to provide “help” and amplify memory CD8 T cell responses through cytokine secretion and co-stimulation<sup>24,25</sup>. To evaluate whether bystander CD4 T cells were necessary for CD8 TRM mediated protection, we vaccinated contact mice with LAIV-SenNP and administered either a polyclonal IgG isotype control or CD4 depleting antibody during Sendai-Luc transmission challenge (**Fig. 1i**). While 100% (16 out of 16) of mice immunized with LAIV-WT became infected, 37% (6 out of 16) and 50% (8 out of 16) of LAIV-SenNP vaccinated mice treated with the isotype control or CD4 depleting antibody became infected, respectively (**Fig. 1j, 1k**). The area under the bioluminescent curves for each animal that became infected, representative of the total viral burden during a breakthrough infection, did not differ between the isotype control and anti-CD4 group (**Fig. 1k**). Taken together, these findings definitively show that CD8 TRM in isolation can protect against respiratory virus transmission, independent of circulating immune cells, B cell responses, or CD4 T cell help.

### **Antigen-specific CD8 T cells in the upper respiratory tract respond to transmitted virus**

Although intranasal vaccination to induce mucosal immune responses is highly appealing, there are concerns over the feasibility and safety of generating virus-specific memory T cells in

the lungs of human vaccine recipients. Previous work has shown that antigen must be delivered locally to the lung to elicit TRM, which may necessitate inhalation of large doses and cause significant discomfort, as well as adverse side effects, in vaccine recipients<sup>26</sup>. Due to these concerns, we sought to investigate which respiratory tract compartments, either the URT and/or LRT, required T cell surveillance to prohibit infection following transmission.

To address this question, we first examined the localization of virus-specific T cell activation during transmission. We used Nur77<sup>GFP</sup> reporter mice as a readout for T cell activation, where TCR stimulation results in GFP expression<sup>27</sup>. Nur77<sup>GFP</sup> contact mice were immunized with LAIV-SenNP, co-housed with Sendai-Luc infected index mice, and sacrificed at 3 days (D35+3) and 6 days (D35+6) post co-housing to assess GFP expression in SenNP-specific CD8 T cells in different areas of the respiratory tract (**Fig. 2a, Extended Data Fig. 2**). Substantial populations of GFP+ Sendai virus-specific T cells were observed in the nasal cavity at D35+6. No T cell activation was seen in the airways (bronchoalveolar lavage, BAL) or lung at either time point (**Fig. 2b, 2c**). Due to the large number of mice at D35+6 (12 out of 19) that were not infected by in vivo imaging (represented by open circles), and concordantly did not acquire GFP expression, the frequency of GFP+ SenNP+ CD8 T cells at D35+6 in the nasal cavity was trending but did not reach statistical significance. When stratified according to infection status, we observe that infected animals have a significant enrichment of activated antigen-specific CD8 T cells in the URT, but not LRT (**Fig. 2d**). We next assessed whether Sendai virus-specific CD8 T cells were proliferating in the URT or LRT in response to transmitted virus by 5-Ethynyl-2'-deoxyuridine (EdU) labelling. WT mice were vaccinated with a non-attenuated influenza A virus encoding FAPGNYPAL (PR8-SenNP), co-housed for Sendai-Luc transmission after 35 days, and dosed with EdU 24 hours prior to sacrifice at D35+0, D35+3, or D35+6 (**Fig. 2e**). Consistent with our

previous results, EdU was detected in SenNP-specific CD8 T cells within the nasal cavity at D35+6, but not within the BAL or lungs at either time point (**Fig. 2f, 2g**). These findings establish the nasal cavity, or URT, as the predominant site of the T cell response to transmitted respiratory viruses and highlight the need to characterize the role of URT tissue resident memory T cells in preventing respiratory virus transmission.

### **Activated nasal cavity resident memory CD8 T cells undergo antiviral effector transcriptional changes**

To further understand the activation kinetics and effector programs of upper respiratory tract resident memory CD8 T cells during viral transmission, we FACS sorted intravital antibody negative, SenNP<sup>+</sup> CD8<sup>+</sup> T cells from the nasal tissue of PR8-SenNP i.n. immunized contact mice after co-housing with a Sendai-Luc infected index mouse and performed single cell RNA sequencing (**Fig. 3a**). Cells stratified into 6 clusters; clusters 4 and 5 predominantly consisted of cells from the D35+6 timepoint, while clusters 0 through 3 were a heterogeneous mix from all timepoints (**Fig. 3b, 3c**). Cluster 4 exhibited increased expression of many canonical CD8 T cell effector function genes including *Ifng*, *Gzmb*, and *Tnf* (**Fig. 3d**). *Nr4a1* (Nur77) expression was upregulated in cluster 4, aligning with our previous results that Nur77<sup>GFP</sup> expression denotes activated nasal cavity SenNP-specific CD8 T cells at D35+6 post co-housing. Nearly all of the cells in cluster 5 expressed *Mki67*, indicating that this cluster represents proliferating SenNP<sup>+</sup> CD8 T cells. Notably, cells in clusters 0 through 3 had low to non-detectable levels of expression for these activation genes, indicating that these cells likely represent SenNP-specific CD8 T cells that are present at steady state after priming, but have not encountered their cognate antigen following transmission. It is important to note that we sorted all SenNP<sup>+</sup> IV<sup>-</sup> CD8<sup>+</sup> T cells from

the nasal cavities of these mice, a population which includes tissue resident memory T cells, effector memory T cells, and activated effector T cells. Cells that expressed canonical TRM marker genes *Cd69* and *Itgae*, which encodes CD103, were dispersed throughout clusters 0 through 3, while very few *Itgae*<sup>+</sup> *Cd69*<sup>+</sup> cells were identified in the activated and proliferating cells of clusters 4 and 5 (**Fig. 3e**). We hypothesized that these activated cells in clusters 4 and 5 likely originated from TRM and performed RNA velocity analysis to visualize the cellular transitions occurring between clusters. Streamlines from TRM-rich regions directed towards the activated clusters, in accordance with the time points of sample collection and corroborating the notion that these activated effector cells arise from TRM (**Fig. 3f, 3g**). These results support the nasal cavity as the critical site for TRM activation during transmission, as cells in this location rapidly transition to and adopt antiviral effector transcriptional states.

### **Upper respiratory tract CD8 TRM prevent infection from transmission**

Taken together, the observations that CD8 TRM protect against respiratory virus transmission and that antigen-specific CD8 T cell activation is restricted to the URT led us to ask whether URT TRM alone were capable of preventing infection from transmission. 30 $\mu$ L intranasal inoculums used throughout the rest of this study delivered antigen to the entire respiratory tract and elicited CD8 TRM in both the URT and LRT (total respiratory tract, TRT). To induce a similar number of Sendai virus-specific CD8 TRM in the URT without inducing an antigen-specific response in the LRT, we utilized a low volume 5 $\mu$ L intranasal immunization with Ad-SenNP (**Fig. 4a-4c**). Immunized mice were then co-housed with Sendai-Luc infected index mice for transmission, and infection outcomes were measured by in vivo imaging. As expected, 100% of animals (24 out of 24) that received the Ad-FluNP control became infected and 0% of animals (16

out of 16) that received the 30 $\mu$ L TRT immunization became infected. Animals with only URT TRM were largely protected against transmission with only 20% (5 out of 24) becoming infected, and this was not statistically significant compared to TRT immunization (**Fig. 2d, 2e**). When viewing the in vivo bioluminescent images of the 5 mice in the 5 $\mu$ L URT TRM group that became infected, it can be seen that infection remained isolated in the trachea region and bypassed the nasal region in most mice (4 out of 5, 80%) (**Extended Data Fig. 3a**). Comparatively few infections in the AdFluNP control group initiated in the trachea (3 out of 24, 12%) while the majority initiated in the nasal region (13 out of 24, 54%) or nasal and trachea region concurrently (8 out of 24, 33%) (Sup. Fig 3b). Overall, these findings demonstrate that URT resident memory CD8 T cells are sufficient to protect against respiratory virus transmission.

## Discussion

Previous studies have shown that intranasal T cell-mediated vaccines can abrogate pathology and viral burdens of respiratory virus infections<sup>9, 28, 29</sup>. However, these studies often utilize high dose, intranasal challenge models that do not accurately mimic the dynamics of viral transmission and propagation in humans. Here, we use a natural respiratory virus transmission challenge model to demonstrate that CD8 TRM act as sentinels of the respiratory tract to prevent the establishment of infection, independent of B cell responses, CD4 T cell help, or circulating immune cells. Understanding which respiratory tract tissues require immune surveillance to prevent infection is crucial to develop intranasal vaccines that generate herd immunity and stop the chain of transmission among populations. To this end, we show that URT CD8 TRM are preferentially activated during respiratory virus transmission and can prevent infection. In accordance with an emerging body of literature on nasal-mediated immunity, our data support the development of nasal-localized T cell-based vaccines for respiratory viruses.

While the sole presence of URT CD8 TRM was largely effective in providing protection against transmission, a handful of breakthrough infections, located in the trachea region, occurred in these mice. It is important to note that we did not investigate the role of trachea TRM in this study, due to the technical difficulty of isolating sufficient numbers of antigen-specific TRM in this site. We propose that these trachea-localized infections can likely be attributed to the mode of transmission, as smaller sized aerosolized virions can travel deeper within the respiratory tract and bypass nasal mucosal membranes, while larger sized droplets typically deposit in the nasal epithelium<sup>30, 31</sup>. Our transmission model does not differentiate between contact-dependent or aerosolized modes of transmission, as index and contact mice freely interact with each other for the duration of the experiment. We hypothesize that these breakthrough infections in the trachea

of URT immunized mice are a result of fine aerosol transmission. SARS-CoV-2 and Influenza virus infections in humans initiate primarily from contact-dependent and large droplet transmission, although aerosol transmission has been recorded in some instances<sup>32-36</sup>. Thus, we theorize that URT CD8 TRM-mediated protection would be sufficient to generate herd immunity and impair viral spread for circulating respiratory viruses.

The mouse nasal cavity is stratified by posterior olfactory epithelium and anterior respiratory epithelium, with the latter containing the nasal associated lymphoid tissue, nasal turbinates, septum, and maxillary sinus<sup>14, 37</sup>. After influenza virus infection, CD103+ URT CD8 TRM reside in each of the aforementioned regions of the nasal tissue where they are poised to rapidly respond to challenge with their cognate antigen<sup>12</sup>. It is possible that URT CD8 TRM localized around the conducting air passages of the nose play a more fundamental role in limiting respiratory virus transmission than those located deeper within the tissue, aligning with the earliest events during pathogen entry. A spatial understanding of URT CD8 TRM activation upon initial recognition of transmitted virus would serve to inform vaccine design and correlates of protection for human vaccination. Human influenza challenge and transmission studies, where human participants are directly infected with influenza in controlled environments and the modes of transmission to exposed participants are analyzed, will prove highly useful in deciphering how different routes of viral transmission impact the localization of immune responses in the context of human infection<sup>38-40</sup>. One recent study in ferrets showed that transmissible influenza virus particles originate from the nasal turbinates as opposed to the lung<sup>41</sup>. Based on these findings, we believe it is reasonable to assume that URT CD8 TRM would also limit transmission from infected individuals in addition to preventing infection upon exposure, as we have illustrated here.

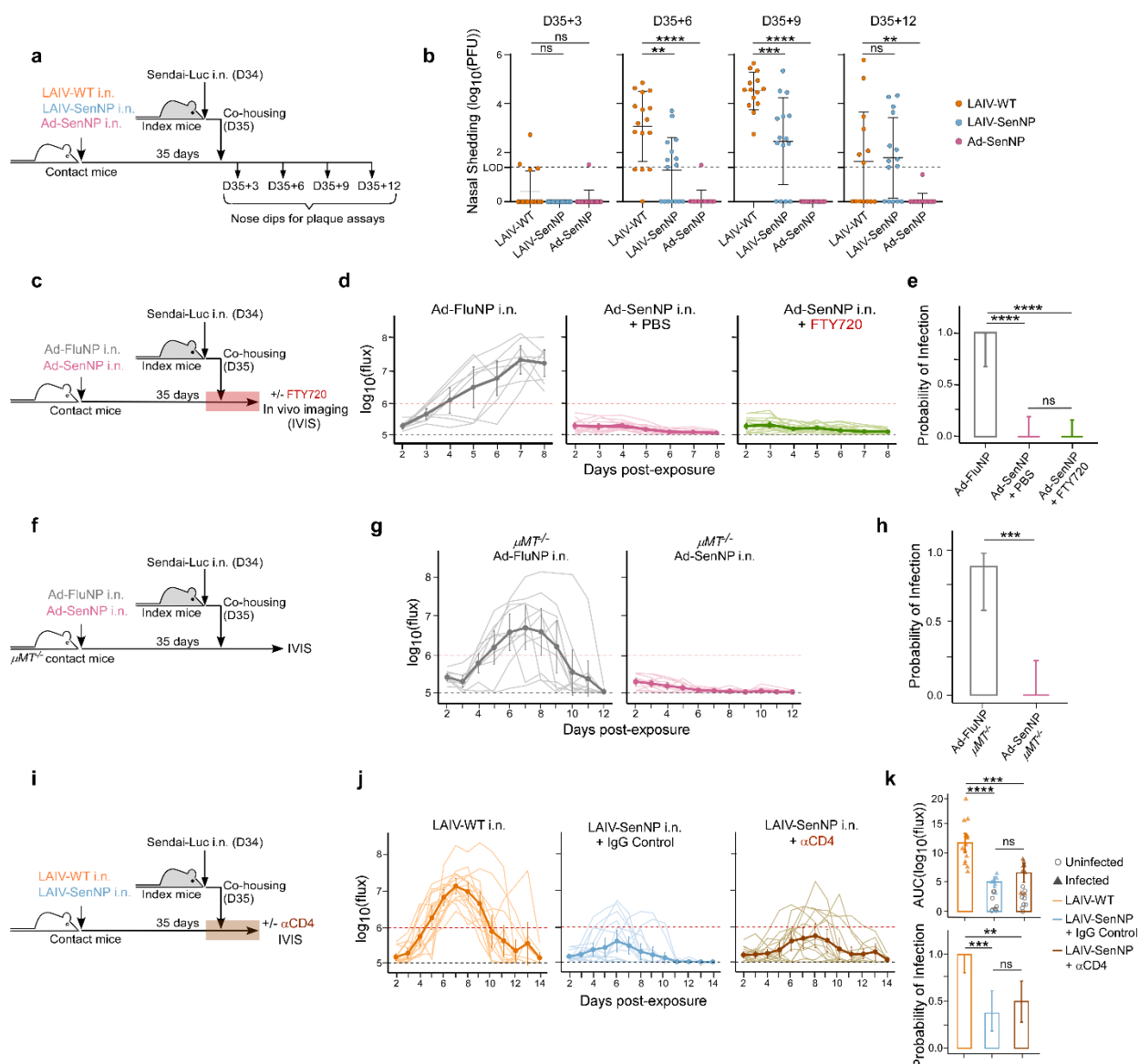
To develop an intranasal URT-targeted vaccine, understanding the mechanisms of TRM differentiation and maintenance in the URT would inform vaccine formulation and adjuvant selection. In the lungs following intranasal adenoviral vector vaccination, alveolar macrophages are the predominant cellular population transduced to enable generation and maintenance of LRT CD8 TRM<sup>42</sup>. Previous studies have shown that URT TRM are primed in the cervical lymph nodes<sup>43</sup>, but which antigen presenting cells are involved, particularly for adenoviral vector vaccines, is unknown. The FluMist, a commercially available LAIV vaccine delivered as a nasal spray, replicates more effectively at colder temperatures found in the URT due to attenuating mutations<sup>44, 45</sup>. Although LAIV vaccination has been shown to induce nasal IgA responses in human vaccine recipients<sup>46-48</sup>, whether LAIV successfully induces URT CD8 TRM in humans is unknown. Additionally, an optimal intranasal vaccine should result in durable protection and long-lasting T cell responses. Although LRT CD8 TRM decline over time, our previous work demonstrates that URT CD8 TRM are more long-lived and can provide enduring protection against transmission in a mouse model<sup>15</sup>. One recent study was the first to provide evidence of URT CD8 TRM from nasal swabs of human SARS-CoV-2 vaccine recipients<sup>49</sup>. Using such nasal swab sampling strategies, future studies should focus on understanding the longevity of URT CD8 TRM in humans to assess whether URT T cell-mediated vaccines would necessitate boosting regimens or provide long-lived protection.

In summary, we have uncovered a novel role for nasal, URT CD8 TRM in preventing infection in a natural transmission model. We show that URT CD8 TRM are the predominant virus-specific T cell population responding to respiratory virus transmission and that when present in sufficient quantities, can inhibit the establishment of infection. These findings have

significant implications for the development of intranasal vaccines to prevent the spread of respiratory viruses.

## Main Figures

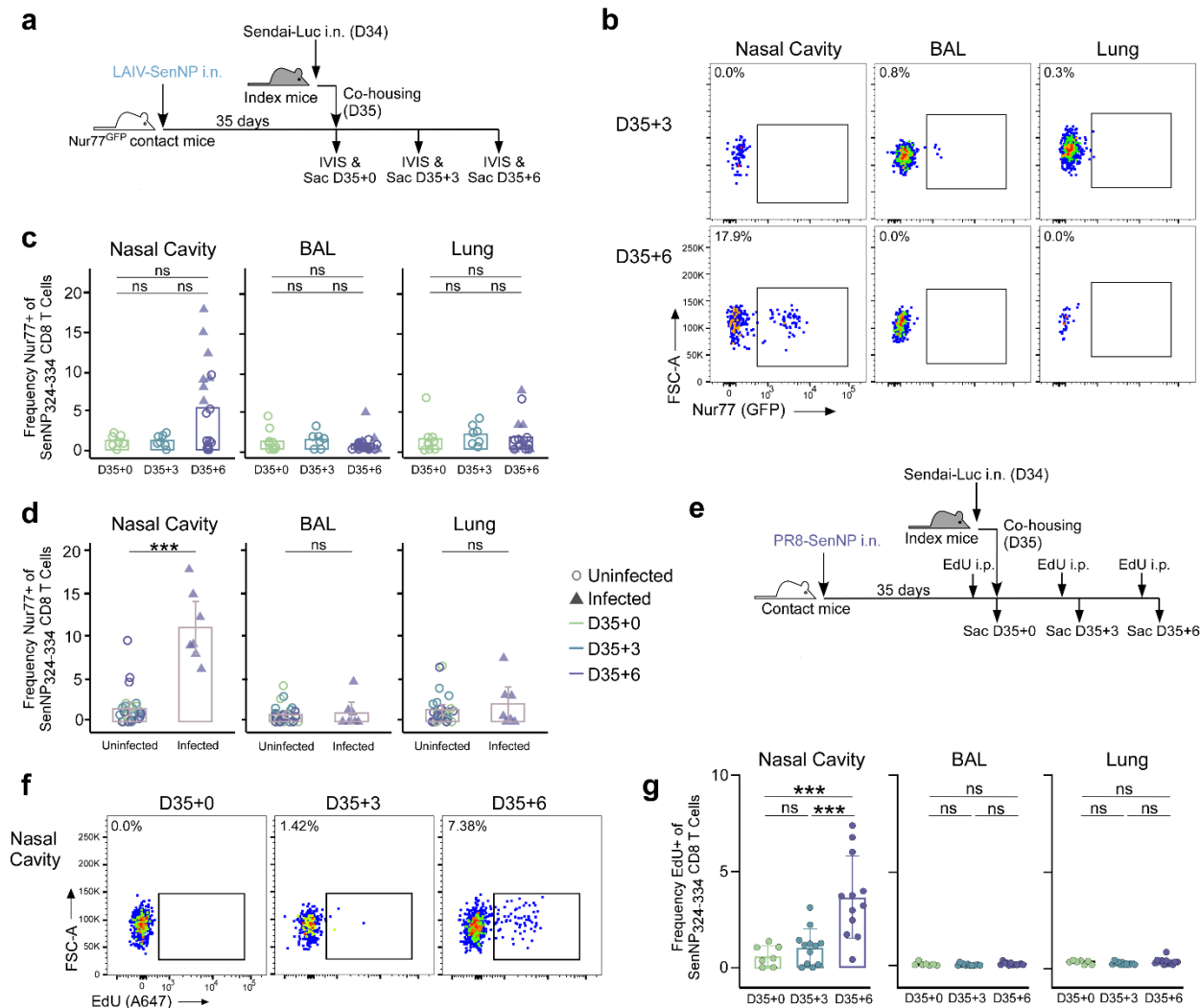
Figure 1



**Figure 1. CD8 tissue resident memory T cells prevent infection from transmission in the absence of circulating immune cells, B cells, or CD4 T cells.** **a)** Experimental schematic where contact mice immunized intranasally (i.n.) with LAIV-WT, LAIV-SenNP, or Ad-SenNP were co-housed with a Sendai-Luc infected index mouse and transmission was assessed by nasal shedding titers. **b)** Nasal shedding titers of immunized contact mice (n=14-16 per group) at 3, 6, 9, and 12

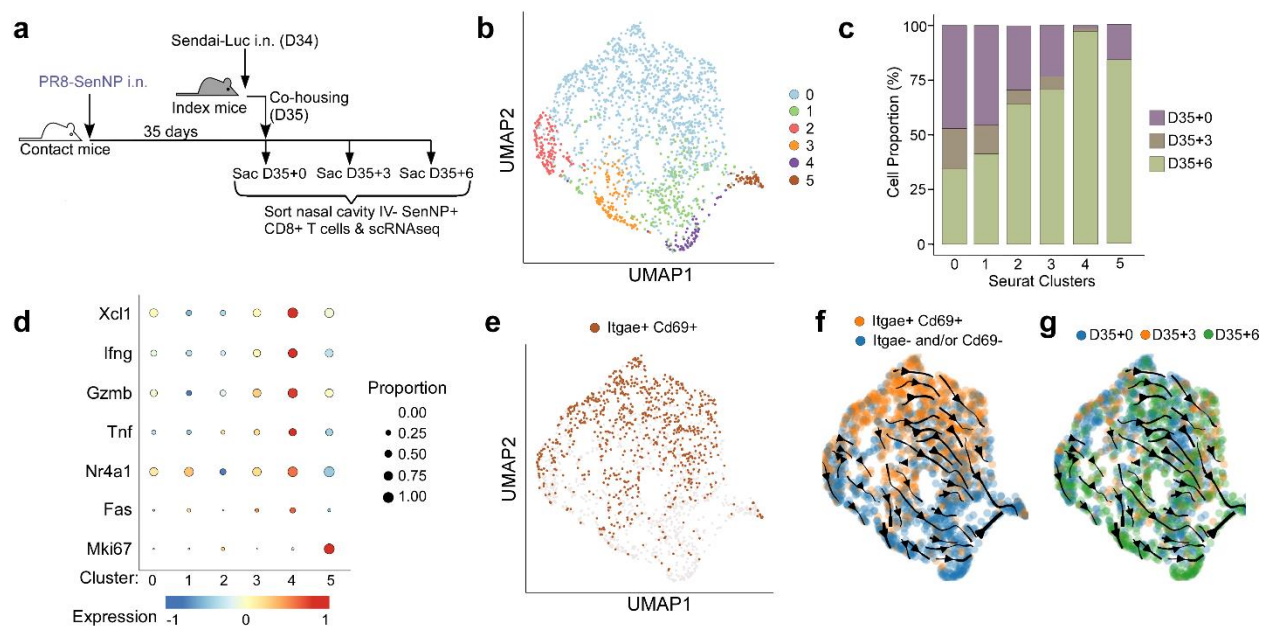
days post co-housing. **c)** Experimental schematic where AdFluNP i.n. or AdSenNP i.n. immunized contact mice were co-housed with Sendai-Luc infected index mouse and treated with FTY720 or PBS control intraperitoneally (i.p.). **d)** Bioluminescence curves of AdFluNP i.n. (n=8), AdSenNP i.n. with PBS (n=16), and AdSenNP i.n. with FTY720 (n=20) contact mice following co-housing with index mice. **e)** Probability of infection for immunized contact mice, calculated as proportion of contact mice that became infected. **f)** Experimental schematic where *mMT*<sup>-/-</sup> mice were immunized i.n. with AdFluNP or AdSenNP prior to co-housing with Sendai-Luc infected index mouse. **g)** Bioluminescence curves of *mMT*<sup>-/-</sup> mice immunized with AdFluNP (n=10) and AdSenNP (n=12). **h)** Probability of infection for *mMT*<sup>-/-</sup> contact mice immunized with AdFluNP and AdSenNP. **i)** Experimental schematic to assess role of CD4 T cells where LAIV-SenNP i.n. immunized contact mice were administered anti-CD4 depleting monoclonal antibody every 3 days, starting on day prior to co-housing with Sendai-Luc infected index mouse. **j)** Bioluminescence curves of contact mice (n=16/group) immunized with LAIV WT, LAIV-SenNP with isotype control antibody, and LAIV-SenNP with anti-CD4 antibody. **k)** Probability of infection of immunized contact mice and area under the curve (AUC) of bioluminescence in immunized contact mice that become infected following co-housing. Grey circles represent uninfected mice, and triangles represent infected mice. For **(d, g, j)**, solid dark lines represent means, solid pale lines represent individual mice, dashed grey lines represent limit of detection, and dashed red lines represent the threshold of infection. Error bars **(e,h,k)** represent 95% binomial confidence intervals or standard deviation **(b)**. All data are combined from at least two independent replicates. Statistical significance was determined using two-sided Mann-Whitney test with \**P*<0.05, \*\**P*<0.01, \*\*\**P*<0.001, \*\*\*\**P*<0.0001, NS for not significant.

Figure 2



**Figure 2. Antigen-specific CD8 T cells in the upper, but not lower, respiratory tract become activated and proliferate in response to transmitted virus. a)** Experimental schematic in which *Nur77<sup>GFP</sup>* contact mice immunized i.n. with LAIV-SenNP were co-housed with a Sendai-Luc infected index mouse and sacrificed at D35+0 (n=10), D35+3 (n=7), or D35+6 (n=19). **b)** Representative flow cytometry plots of Nur77 expression gated on IV- CD8+ SenNP+ T cells in immunized contact mice. **c)** Frequency Nur77+ of IV- CD8+ SenNP+ T cells in nasal cavity, BAL, and lung of immunized mice at D35+0, D35+3, and D35+6. Circles represent uninfected mice,

and triangles represent infected mice by IVIS. **d)** Frequency Nur77<sup>+</sup> of IV<sup>-</sup> CD8<sup>+</sup> SenNP<sup>+</sup> T cells separated by infection status. **e)** Experiment schematic to assess T cell proliferation, where PR8-SenNP i.n. immunized contact mice were injected with 1 mg EdU intraperitoneally 1 day prior to sacrifice at D35+0 (n=7), D35+3 (n=12), or D35+6 (n=12) post co-housing with index mouse. **f)** Representation flow cytometry plots of EdU expression gated on IV<sup>-</sup> CD8<sup>+</sup> SenNP<sup>+</sup> T cells in immunized contact mice. **g)** Frequency EdU<sup>+</sup> of IV<sup>-</sup> CD8<sup>+</sup> SenNP<sup>+</sup> T cells in nasal cavity, BAL, and lung of immunized contact mice D35+0, D35+3, and D35+6. Data are combined from three (**b-d**) or two (**f, g**) independent replicates. Statistical significance was determined using two-sided Mann-Whitney test.

**Figure 3**

**Figure 3. Upper respiratory tract resident memory CD8 T cells initiate antiviral effector transcriptional programs during respiratory virus transmission. a)** Experimental schematic where PR8-SenNP i.n. immunized contact mice were co-housed with a Sendai-Luc infected index mouse and SenNP+ CD8+ T cells from the nasal cavity were sorted for single cell RNA sequencing at D35+0, D35+3, and D35+6. **b)** UMAP projection of nasal cavity SenNP+ IV- CD8+ T cells from contact mice during Sendai-Luc transmission. **c)** Composition of UMAP Seurat clusters by day post co-housing. **d)** Bubble plot with expression of effector function genes for each cluster. **e)** Itgae+ Cd69+ cells overlaid on UMAP. **f)** RNA velocity analysis with streamlines in direction of cellular trajectory and Itgae+ Cd69+ expression status overlaid. **g)** RNA velocity with timepoint post co-housing overlaid. Data are combined fr

Figure 4

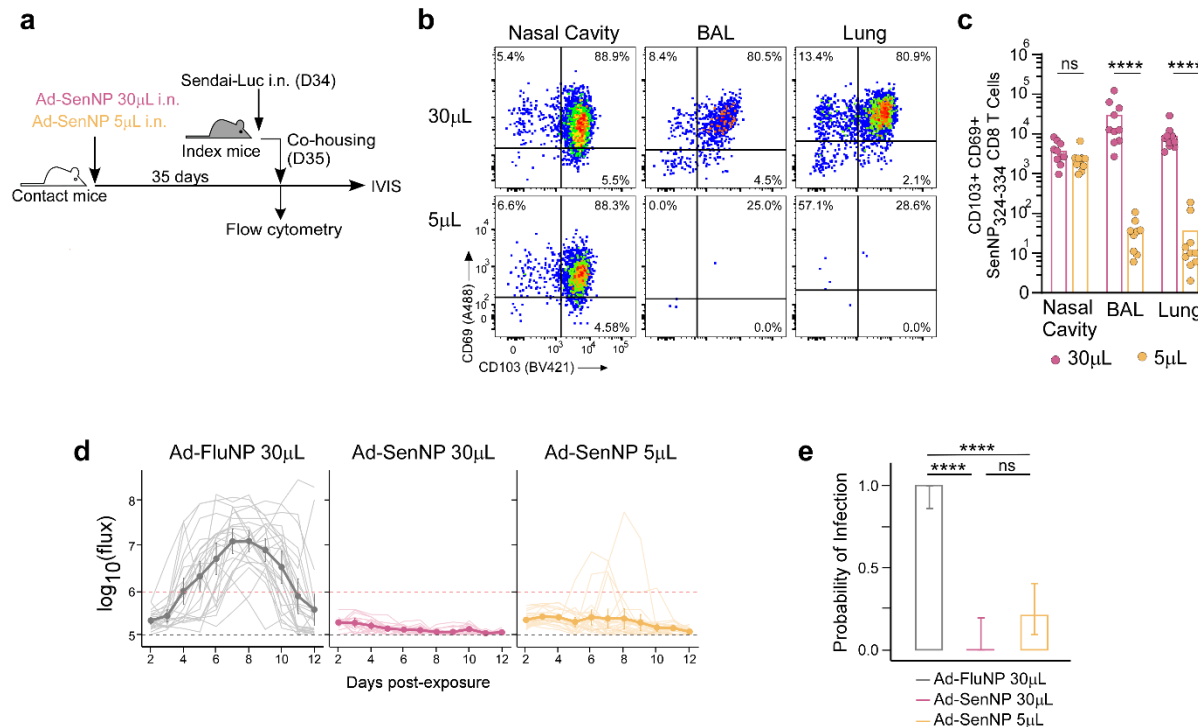
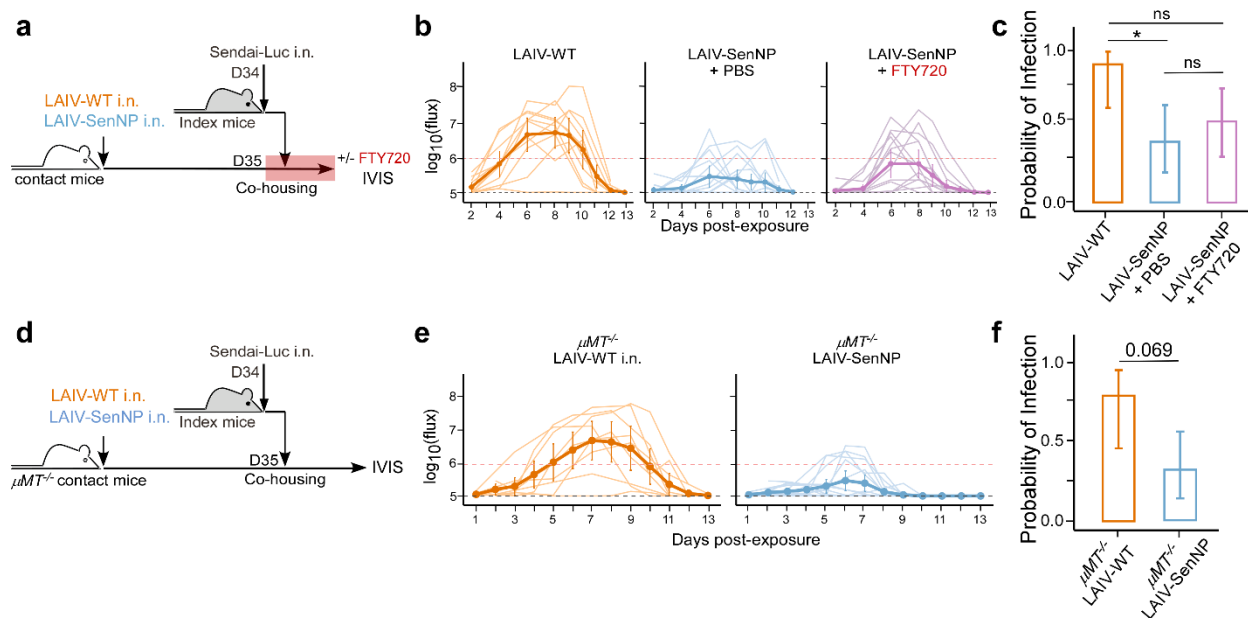


**Figure 4. CD8 tissue resident memory T cells in the upper respiratory alone are sufficient to prevent respiratory virus transmission.** **a)** Experimental schematic in which immunized contact mice were co-housed with a Sendai-Luc infected index mouse. **b)** Representative flow cytometry plots of CD103 and CD69 expression gated on IV- CD8+ SenNP+ T cells in AdSenNP 30µL and 5µL immunized mice. **c)** Number of CD103+ CD69+ TRM in the nasal cavity, BAL, and lung of AdSenNP 30µL (n=10) and 5µL (n=10) immunized mice. **d)** Bioluminescence curves of AdFluNP 30µL (n=24), AdSenNP 30µL (n=16), and AdSenNP 5µL (n=24) immunized contact mice when co-housed with Sendai-Luc infected index mouse. **e)** Probability of infection in whole respiratory tract region for immunized contact mice, calculated as proportion of contact mice that become infected. For **(d)**, solid dark lines represent means, solid pale lines represent individual mice, dashed grey lines represent limit of detection, and dashed red lines represent the threshold of infection. Error bars **(e)** represent 95% binomial confidence intervals. Data are combined from two

**(b-c)** or three **(d-e)** independent replicates. Statistical significance was determined using two-sided Mann-Whitney test.

## Supplementary Information

## Extended Data Figure 1



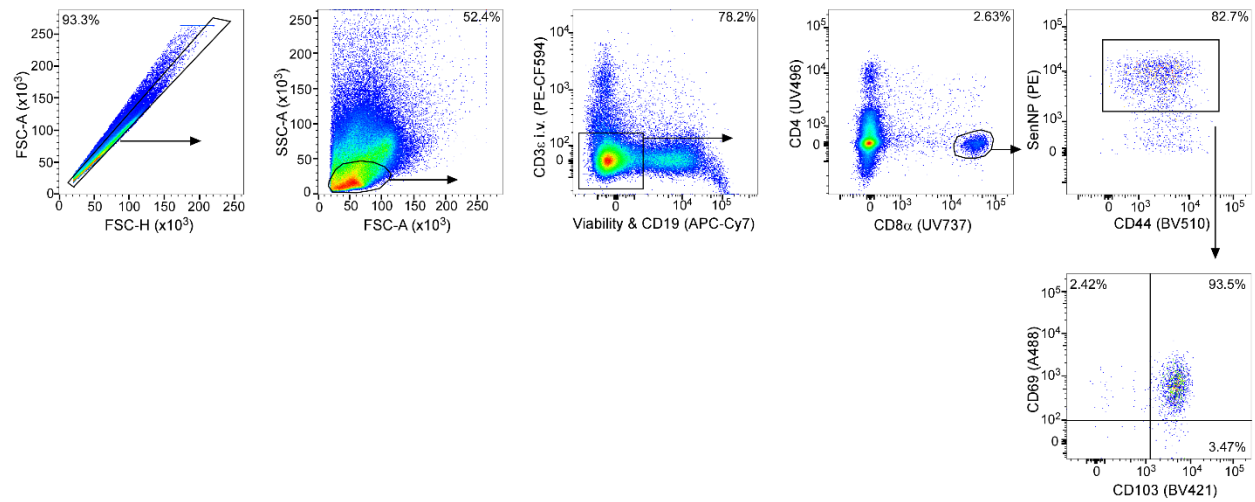
**Extended Data Figure 1. Circulating effector cells and B cells are dispensable for protection against transmission even when a lower quantity of respiratory tract TRM are present. a)**

Experimental schematic where LAIV-WT i.n. or LAIV-SenNP i.n. immunized contact mice were co-housed with Sendai-Luc infected index mouse and treated with FTY720 or PBS control intraperitoneally (i.p). **b**) Bioluminescence curves of LAIV-WT i.n. (n=11), LAIV-SenNP i.n. with PBS (n=15), and LAIV-SenNP i.n. with FTY720 (n=15) contact mice following co-housing with index mice. **c**) Probability of infection for immunized contact mice, calculated as proportion of contact mice that became infected. **d**) Experimental schematic where  $mMT^{-/-}$  mice were immunized i.n. with LAIV-WT or LAIV-SenNP prior to co-housing with Sendai-Luc infected index mouse. **e**) Bioluminescence curves of  $mMT^{-/-}$  mice immunized with LAIV-WT (n=9) and LAIV-SenNP (n=16). **f**) Probability of infection for  $mMT^{-/-}$  contact mice immunized with LAIV-WT and LAIV-SenNP. For **(b, e)**, solid dark lines represent means, solid pale lines represent individual mice,

dashed grey lines represent limit of detection, and dashed red lines represent the threshold of infection. Error bars (**c**, **f**) represent 95% binomial confidence intervals. Data are combined from two independent replicates. Statistical significance was determined using two-sided Mann-Whitney test.

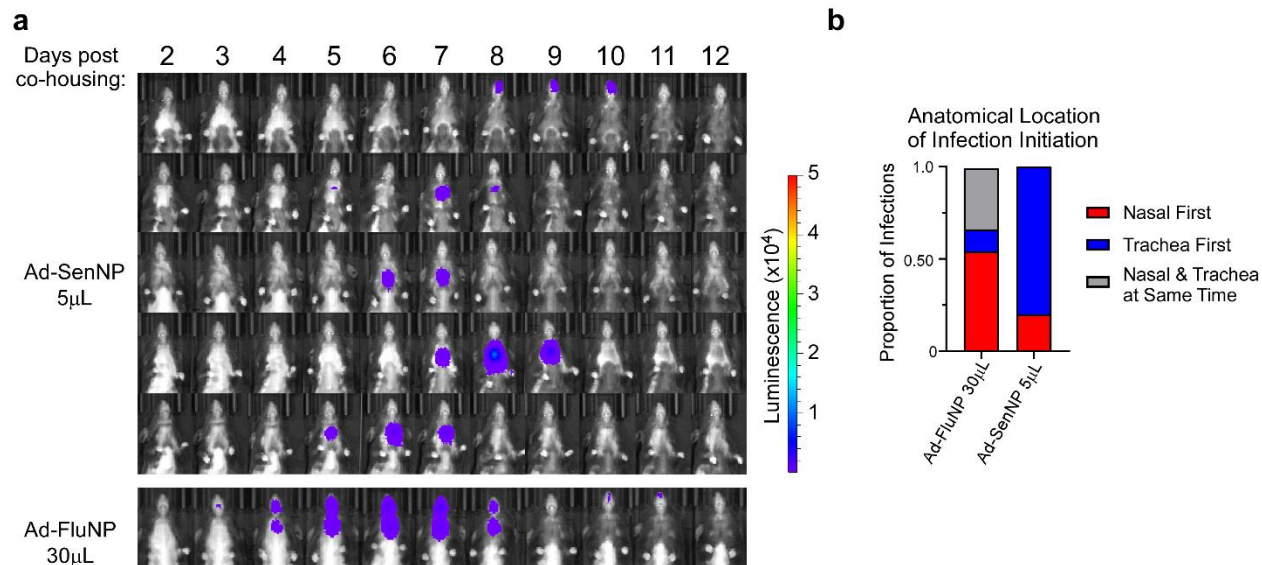
## Extended Data Figure 2

### Nasal Cavity



**Extended Data Figure 2. Flow cytometry gating strategy used to identify CD8+ SenNP-specific T cells and TRM relating to Figure 2, 3 and 4.**

### Extended Data Figure 3



**Extended Data Figure 3. Breakthrough infections in Ad-SenNP 5 $\mu$ L i.n. immunized mice localized in the trachea region.** **a)** Bioluminescent images of the 5 out of 24 Ad-SenNP 5 $\mu$ L immunized mice that became infected during Sendai-Luc transmission challenge. A representative infection in an Ad-FluNP 30 $\mu$ L immunized mouse is shown. **b)** Proportion of infections that initiated in the nasal region, trachea region, or nasal & trachea regions concurrently for Ad-FluNP 30 $\mu$ L i.n. and Ad-SenNP 5 $\mu$ L i.n. immunized contact mice.

**Acknowledgements**

We acknowledge the NIH tetramer core facility at Emory University for providing Sendai NP<sub>324-332</sub> tetramers (NIAID contract 75N93020D00005). We thank the Emory Children's Flow Cytometry Core for cell sorting, the Emory Integrated Genomics Core for assistance with bioanalyzer assays for single cell RNA sequencing library preparation, and the Emory Primate Center Genomics Core for sequencing of single cell RNA sequencing libraries. This work was supported by NIH grants R35 HL150803 and U01 HL139483 (J.E.K.). S.E.M. was supported by F31 HL168914.

**Author Contributions**

S.E.M. and J.E.K. designed the study. A.J. performed experiments in Extended Data Fig. 1a-1c. Y. S. V. performed experiments in Extended Data Fig. 1d-1f. S.E.M. performed all other experiments. A.S. performed transmission data analysis and statistics. M.E.W. performed single cell RNA sequencing analysis and RNA velocity analysis.

## References

1. Smith DJ, Lapedes AS, de Jong JC, Bestebroer TM, Rimmelzwaan GF, Osterhaus AD, Fouchier RA. Mapping the antigenic and genetic evolution of influenza virus. *Science*. 2004;305(5682):371-6. Epub 20040624. doi: 10.1126/science.1097211. PubMed PMID: 15218094.
2. Doud MB, Hensley SE, Bloom JD. Complete mapping of viral escape from neutralizing antibodies. *PLoS Pathog*. 2017;13(3):e1006271. Epub 20170313. doi: 10.1371/journal.ppat.1006271. PubMed PMID: 28288189; PMCID: PMC5363992.
3. Cox M, Peacock TP, Harvey WT, Hughes J, Wright DW, Consortium C-GU, Willett BJ, Thomson E, Gupta RK, Peacock SJ, Robertson DL, Carabelli AM. SARS-CoV-2 variant evasion of monoclonal antibodies based on in vitro studies. *Nat Rev Microbiol*. 2023;21(2):112-24. Epub 20221028. doi: 10.1038/s41579-022-00809-7. PubMed PMID: 36307535; PMCID: PMC9616429.
4. Greaney AJ, Starr TN, Barnes CO, Weisblum Y, Schmidt F, Caskey M, Gaebler C, Cho A, Agudelo M, Finkin S, Wang Z, Poston D, Muecksch F, Hatzioannou T, Bieniasz PD, Robbiani DF, Nussenzweig MC, Bjorkman PJ, Bloom JD. Mapping mutations to the SARS-CoV-2 RBD that escape binding by different classes of antibodies. *Nat Commun*. 2021;12(1):4196. Epub 20210707. doi: 10.1038/s41467-021-24435-8. PubMed PMID: 34234131; PMCID: PMC8263750.

5. Meyer S, Blaas I, Bollineni RC, Delic-Sarac M, Tran TT, Knetter C, Dai KZ, Madssen TS, Vaage JT, Gustavsen A, Yang W, Nissen-Meyer LSH, Douvlataniotis K, Laos M, Nielsen MM, Thiede B, Soraas A, Lund-Johansen F, Rustad EH, Olweus J. Prevalent and immunodominant CD8 T cell epitopes are conserved in SARS-CoV-2 variants. *Cell Rep.* 2023;42(1):111995. Epub 20230109. doi: 10.1016/j.celrep.2023.111995. PubMed PMID: 36656713; PMCID: PMC9826989.
  
6. Koutsakos M, Illing PT, Nguyen THO, Mifsud NA, Crawford JC, Rizzetto S, Eltahla AA, Clemens EB, Sant S, Chua BY, Wong CY, Allen EK, Teng D, Dash P, Boyd DF, Grzelak L, Zeng W, Hurt AC, Barr I, Rockman S, Jackson DC, Kotsimbos TC, Cheng AC, Richards M, Westall GP, Loudovaris T, Mannering SI, Elliott M, Tangye SG, Wakim LM, Rossjohn J, Vijaykrishna D, Luciani F, Thomas PG, Gras S, Purcell AW, Kedzierska K. Human CD8(+) T cell cross-reactivity across influenza A, B and C viruses. *Nat Immunol.* 2019;20(5):613-25. Epub 20190218. doi: 10.1038/s41590-019-0320-6. PubMed PMID: 30778243.
  
7. Zheng MZM, Wakim LM. Tissue resident memory T cells in the respiratory tract. *Mucosal Immunol.* 2022;15(3):379-88. Epub 20211020. doi: 10.1038/s41385-021-00461-z. PubMed PMID: 34671115; PMCID: PMC8526531.
  
8. Mueller SN, Gebhardt T, Carbone FR, Heath WR. Memory T cell subsets, migration patterns, and tissue residence. *Annu Rev Immunol.* 2013;31:137-61. Epub 20121203. doi: 10.1146/annurev-immunol-032712-095954. PubMed PMID: 23215646.

9. Wu T, Hu Y, Lee YT, Bouchard KR, Benechet A, Khanna K, Cauley LS. Lung-resident memory CD8 T cells (TRM) are indispensable for optimal cross-protection against pulmonary virus infection. *J Leukoc Biol.* 2014;95(2):215-24. Epub 20130904. doi: 10.1189/jlb.0313180. PubMed PMID: 24006506; PMCID: PMC3896663.
  
10. Zens KD, Chen JK, Farber DL. Vaccine-generated lung tissue-resident memory T cells provide heterosubtypic protection to influenza infection. *JCI Insight.* 2016;1(10). doi: 10.1172/jci.insight.85832. PubMed PMID: 27468427; PMCID: PMC4959801.
  
11. Grau-Exposito J, Sanchez-Gaona N, Massana N, Suppi M, Astorga-Gamaza A, Perea D, Rosado J, Falco A, Kirkegaard C, Torrella A, Planas B, Navarro J, Suanzes P, Alvarez-Sierra D, Ayora A, Sansano I, Esperalba J, Andres C, Anton A, Ramon YCS, Almirante B, Pujol-Borrell R, Falco V, Burgos J, Buzon MJ, Genesca M. Peripheral and lung resident memory T cell responses against SARS-CoV-2. *Nat Commun.* 2021;12(1):3010. Epub 20210521. doi: 10.1038/s41467-021-23333-3. PubMed PMID: 34021148; PMCID: PMC8140108.
  
12. Pizzolla A, Nguyen THO, Smith JM, Brooks AG, Kedzieska K, Heath WR, Reading PC, Wakim LM. Resident memory CD8(+) T cells in the upper respiratory tract prevent pulmonary influenza virus infection. *Sci Immunol.* 2017;2(12). doi: 10.1126/sciimmunol.aam6970. PubMed PMID: 28783656.
  
13. Burke CW, Bridges O, Brown S, Rahija R, Russell CJ. Mode of parainfluenza virus transmission determines the dynamics of primary infection and protection from reinfection.

PLoS Pathog. 2013;9(11):e1003786. Epub 20131121. doi: 10.1371/journal.ppat.1003786.  
PubMed PMID: 24278024; PMCID: PMC3836739.

14. Mettelman RC, Allen EK, Thomas PG. Mucosal immune responses to infection and vaccination in the respiratory tract. *Immunity*. 2022;55(5):749-80. doi: 10.1016/j.immuni.2022.04.013. PubMed PMID: 35545027; PMCID: PMC9087965.

15. Uddback I, Michalets SE, Saha A, Mattingly C, Kost KN, Williams ME, Lawrence LA, Hicks SL, Lowen AC, Ahmed H, Thomsen AR, Russell CJ, Scharer CD, Boss JM, Koelle K, Antia R, Christensen JP, Kohlmeier JE. Prevention of respiratory virus transmission by resident memory CD8(+) T cells. *Nature*. 2024;626(7998):392-400. Epub 20231212. doi: 10.1038/s41586-023-06937-1. PubMed PMID: 38086420; PMCID: PMC11040656.

16. Burke CW, Mason JN, Surman SL, Jones BG, Dalloneau E, Hurwitz JL, Russell CJ. Illumination of parainfluenza virus infection and transmission in living animals reveals a tissue-specific dichotomy. *PLoS Pathog*. 2011;7(7):e1002134. Epub 20110707. doi: 10.1371/journal.ppat.1002134. PubMed PMID: 21750677; PMCID: PMC3131265.

17. Dunbar PR, Cartwright EK, Wein AN, Tsukamoto T, Tiger Li ZR, Kumar N, Uddback IE, Hayward SL, Ueha S, Takamura S, Kohlmeier JE. Pulmonary monocytes interact with effector T cells in the lung tissue to drive T(RM) differentiation following viral infection. *Mucosal Immunol*. 2020;13(1):161-71. Epub 20191113. doi: 10.1038/s41385-019-0224-7. PubMed PMID: 31723250; PMCID: PMC6917844.

18. Lobby JL, Danzy S, Holmes KE, Lowen AC, Kohlmeier JE. Both Humoral and Cellular Immunity Limit the Ability of Live Attenuated Influenza Vaccines to Promote T Cell Responses. *J Immunol.* 2024;212(1):107-16. doi: 10.4049/jimmunol.2300343. PubMed PMID: 37982700; PMCID: PMC10842048.
19. Zheng GX, Terry JM, Belgrader P, Ryvkin P, Bent ZW, Wilson R, Ziraldo SB, Wheeler TD, McDermott GP, Zhu J, Gregory MT, Shuga J, Montesclaros L, Underwood JG, Masquelier DA, Nishimura SY, Schnall-Levin M, Wyatt PW, Hindson CM, Bharadwaj R, Wong A, Ness KD, Beppu LW, Deeg HJ, McFarland C, Loeb KR, Valente WJ, Ericson NG, Stevens EA, Radich JP, Mikkelsen TS, Hindson BJ, Bielas JH. Massively parallel digital transcriptional profiling of single cells. *Nat Commun.* 2017;8:14049. Epub 20170116. doi: 10.1038/ncomms14049. PubMed PMID: 28091601; PMCID: PMC5241818.
20. Hao Y, Stuart T, Kowalski MH, Choudhary S, Hoffman P, Hartman A, Srivastava A, Molla G, Madad S, Fernandez-Granda C, Satija R. Dictionary learning for integrative, multimodal and scalable single-cell analysis. *Nat Biotechnol.* 2024;42(2):293-304. Epub 20230525. doi: 10.1038/s41587-023-01767-y. PubMed PMID: 37231261; PMCID: PMC10928517.
21. Korsunsky I, Millard N, Fan J, Slowikowski K, Zhang F, Wei K, Baglaenko Y, Brenner M, Loh PR, Raychaudhuri S. Fast, sensitive and accurate integration of single-cell data with

Harmony. *Nat Methods*. 2019;16(12):1289-96. Epub 20191118. doi: 10.1038/s41592-019-0619-0. PubMed PMID: 31740819; PMCID: PMC6884693.

22. La Manno G, Soldatov R, Zeisel A, Braun E, Hochgerner H, Petukhov V, Lidschreiber K, Kastrioti ME, Lonnerberg P, Furlan A, Fan J, Borm LE, Liu Z, van Bruggen D, Guo J, He X, Barker R, Sundstrom E, Castelo-Branco G, Cramer P, Adameyko I, Linnarsson S, Kharchenko PV. RNA velocity of single cells. *Nature*. 2018;560(7719):494-8. Epub 20180808. doi: 10.1038/s41586-018-0414-6. PubMed PMID: 30089906; PMCID: PMC6130801.

23. Bergen V, Lange M, Peidli S, Wolf FA, Theis FJ. Generalizing RNA velocity to transient cell states through dynamical modeling. *Nat Biotechnol*. 2020;38(12):1408-14. Epub 20200803. doi: 10.1038/s41587-020-0591-3. PubMed PMID: 32747759.

24. Novy P, Quigley M, Huang X, Yang Y. CD4 T cells are required for CD8 T cell survival during both primary and memory recall responses. *J Immunol*. 2007;179(12):8243-51. doi: 10.4049/jimmunol.179.12.8243. PubMed PMID: 18056368.

25. Laidlaw BJ, Craft JE, Kaech SM. The multifaceted role of CD4(+) T cells in CD8(+) T cell memory. *Nat Rev Immunol*. 2016;16(2):102-11. Epub 20160119. doi: 10.1038/nri.2015.10. PubMed PMID: 26781939; PMCID: PMC4860014.

26. McMaster SR, Wein AN, Dunbar PR, Hayward SL, Cartwright EK, Denning TL, Kohlmeier JE. Pulmonary antigen encounter regulates the establishment of tissue-resident CD8

memory T cells in the lung airways and parenchyma. *Mucosal Immunol.* 2018;11(4):1071-8. Epub 20180216. doi: 10.1038/s41385-018-0003-x. PubMed PMID: 29453412; PMCID: PMC6030505.

27. Moran AE, Holzapfel KL, Xing Y, Cunningham NR, Maltzman JS, Punt J, Hogquist KA. T cell receptor signal strength in Treg and iNKT cell development demonstrated by a novel fluorescent reporter mouse. *J Exp Med.* 2011;208(6):1279-89. Epub 20110523. doi: 10.1084/jem.20110308. PubMed PMID: 21606508; PMCID: PMC3173240.

28. Luangrath MA, Schmidt ME, Hartwig SM, Varga SM. Tissue-Resident Memory T Cells in the Lungs Protect against Acute Respiratory Syncytial Virus Infection. *Immunohorizons.* 2021;5(2):59-69. Epub 20210203. doi: 10.4049/immunohorizons.2000067. PubMed PMID: 33536235; PMCID: PMC8299542.

29. Gilchuk P, Hill TM, Guy C, McMaster SR, Boyd KL, Rabacal WA, Lu P, Shyr Y, Kohlmeier JE, Sebzda E, Green DR, Joyce S. A Distinct Lung-Interstitial-Resident Memory CD8(+) T Cell Subset Confers Enhanced Protection to Lower Respiratory Tract Infection. *Cell Rep.* 2016;16(7):1800-9. Epub 20160804. doi: 10.1016/j.celrep.2016.07.037. PubMed PMID: 27498869; PMCID: PMC5021515.

30. Leung NHL. Transmissibility and transmission of respiratory viruses. *Nat Rev Microbiol.* 2021;19(8):528-45. Epub 20210322. doi: 10.1038/s41579-021-00535-6. PubMed PMID: 33753932; PMCID: PMC7982882.

31. Gralton J, Tovey E, McLaws ML, Rawlinson WD. The role of particle size in aerosolised pathogen transmission: a review. *J Infect.* 2011;62(1):1-13. Epub 20101119. doi: 10.1016/j.jinf.2010.11.010. PubMed PMID: 21094184; PMCID: PMC7112663.
32. Brankston G, Gitterman L, Hirji Z, Lemieux C, Gardam M. Transmission of influenza A in human beings. *Lancet Infect Dis.* 2007;7(4):257-65. doi: 10.1016/S1473-3099(07)70029-4. PubMed PMID: 17376383.
33. Zhou L, Ayeh SK, Chidambaram V, Karakousis PC. Modes of transmission of SARS-CoV-2 and evidence for preventive behavioral interventions. *BMC Infect Dis.* 2021;21(1):496. Epub 20210528. doi: 10.1186/s12879-021-06222-4. PubMed PMID: 34049515; PMCID: PMC8160404.
34. Bao L, Gao H, Deng W, Lv Q, Yu H, Liu M, Yu P, Liu J, Qu Y, Gong S, Lin K, Qi F, Xu Y, Li F, Xiao C, Xue J, Song Z, Xiang Z, Wang G, Wang S, Liu X, Zhao W, Han Y, Wei Q, Qin C. Transmission of Severe Acute Respiratory Syndrome Coronavirus 2 via Close Contact and Respiratory Droplets Among Human Angiotensin-Converting Enzyme 2 Mice. *J Infect Dis.* 2020;222(4):551-5. doi: 10.1093/infdis/jiaa281. PubMed PMID: 32444876; PMCID: PMC7313959.
35. Jayaweera M, Perera H, Gunawardana B, Manatunge J. Transmission of COVID-19 virus by droplets and aerosols: A critical review on the unresolved dichotomy. *Environ Res.*

2020;188:109819. Epub 20200613. doi: 10.1016/j.envres.2020.109819. PubMed PMID: 32569870; PMCID: PMC7293495.

36. Meyerowitz EA, Richterman A, Gandhi RT, Sax PE. Transmission of SARS-CoV-2: A Review of Viral, Host, and Environmental Factors. *Ann Intern Med.* 2021;174(1):69-79. Epub 20200917. doi: 10.7326/M20-5008. PubMed PMID: 32941052; PMCID: PMC7505025.

37. Wellford SA, Moseman AP, Dao K, Wright KE, Chen A, Plevin JE, Liao TC, Mehta N, Moseman EA. Mucosal plasma cells are required to protect the upper airway and brain from infection. *Immunity.* 2022;55(11):2118-34 e6. Epub 20220921. doi: 10.1016/j.immuni.2022.08.017. PubMed PMID: 36137543; PMCID: PMC9649878.

38. Killingley B, Enstone JE, Greatorex J, Gilbert AS, Lambkin-Williams R, Cauchemez S, Katz JM, Booy R, Hayward A, Oxford J, Bridges CB, Ferguson NM, Nguyen Van-Tam JS. Use of a human influenza challenge model to assess person-to-person transmission: proof-of-concept study. *J Infect Dis.* 2012;205(1):35-43. Epub 20111130. doi: 10.1093/infdis/jir701. PubMed PMID: 22131338.

39. McIlwain DR, Chen H, Rahil Z, Bidoki NH, Jiang S, Bjornson Z, Kolhatkar NS, Martinez CJ, Gaudilliere B, Hedou J, Mukherjee N, Schurch CM, Trejo A, Affrime M, Bock B, Kim K, Liebowitz D, Aghaeepour N, Tucker SN, Nolan GP. Human influenza virus challenge identifies cellular correlates of protection for oral vaccination. *Cell Host Microbe.*

2021;29(12):1828-37 e5. Epub 20211115. doi: 10.1016/j.chom.2021.10.009. PubMed PMID: 34784508; PMCID: PMC8665113.

40. Liebowitz D, Gottlieb K, Kolhatkar NS, Garg SJ, Asher JM, Nazareno J, Kim K, McIlwain DR, Tucker SN. Efficacy, immunogenicity, and safety of an oral influenza vaccine: a placebo-controlled and active-controlled phase 2 human challenge study. *Lancet Infect Dis.* 2020;20(4):435-44. Epub 20200121. doi: 10.1016/S1473-3099(19)30584-5. PubMed PMID: 31978354.

41. Richard M, van den Brand JMA, Bestebroer TM, Lexmond P, de Meulder D, Fouchier RAM, Lowen AC, Herfst S. Influenza A viruses are transmitted via the air from the nasal respiratory epithelium of ferrets. *Nat Commun.* 2020;11(1):766. Epub 20200207. doi: 10.1038/s41467-020-14626-0. PubMed PMID: 32034144; PMCID: PMC7005743.

42. Lobby JL, Uddback I, Scharer CD, Mi T, Boss JM, Thomsen AR, Christensen JP, Kohlmeier JE. Persistent Antigen Harbored by Alveolar Macrophages Enhances the Maintenance of Lung-Resident Memory CD8(+) T Cells. *J Immunol.* 2022;209(9):1778-87. Epub 20220926. doi: 10.4049/jimmunol.2200082. PubMed PMID: 36162870; PMCID: PMC9588742.

43. Pizzolla A, Wang Z, Groom JR, Kedzierska K, Brooks AG, Reading PC, Wakim LM. Nasal-associated lymphoid tissues (NALTs) support the recall but not priming of influenza virus-

specific cytotoxic T cells. *Proc Natl Acad Sci U S A*. 2017;114(20):5225-30. Epub 20170501. doi: 10.1073/pnas.1620194114. PubMed PMID: 28461487; PMCID: PMC5441821.

44. Fischer WA, 2nd, King LS, Lane AP, Pekosz A. Restricted replication of the live attenuated influenza A virus vaccine during infection of primary differentiated human nasal epithelial cells. *Vaccine*. 2015;33(36):4495-504. Epub 20150718. doi: 10.1016/j.vaccine.2015.07.023. PubMed PMID: 26196325; PMCID: PMC4547880.

45. Martinez-Sobrido L, Peersen O, Nogales A. Temperature Sensitive Mutations in Influenza A Viral Ribonucleoprotein Complex Responsible for the Attenuation of the Live Attenuated Influenza Vaccine. *Viruses*. 2018;10(10). Epub 20181015. doi: 10.3390/v10100560. PubMed PMID: 30326610; PMCID: PMC6213772.

46. Barria MI, Garrido JL, Stein C, Scher E, Ge Y, Engel SM, Kraus TA, Banach D, Moran TM. Localized mucosal response to intranasal live attenuated influenza vaccine in adults. *J Infect Dis*. 2013;207(1):115-24. Epub 20121019. doi: 10.1093/infdis/jis641. PubMed PMID: 23087433; PMCID: PMC3571238.

47. Thwaites RS, Uruchurtu ASS, Negri VA, Cole ME, Singh N, Poshai N, Jackson D, Hoschler K, Baker T, Scott IC, Ros XR, Cohen ES, Zambon M, Pollock KM, Hansel TT, Openshaw PJM. Early mucosal events promote distinct mucosal and systemic antibody responses to live attenuated influenza vaccine. *Nat Commun*. 2023;14(1):8053. Epub 20231205. doi: 10.1038/s41467-023-43842-7. PubMed PMID: 38052824; PMCID: PMC10697962.

48. Boyce TG, Gruber WC, Coleman-Dockery SD, Sannella EC, Reed GW, Wolff M, Wright PF. Mucosal immune response to trivalent live attenuated intranasal influenza vaccine in children. *Vaccine*. 1999;18(1-2):82-8. doi: 10.1016/s0264-410x(99)00183-8. PubMed PMID: 10501238.
49. Ramirez SI, Faraji F, Hills LB, Lopez PG, Goodwin B, Stacey HD, Sutton HJ, Hastie KM, Saphire EO, Kim HJ, Mashoof S, Yan CH, DeConde AS, Levi G, Crotty S. Immunological memory diversity in the human upper airway. *Nature*. 2024;632(8025):630-6. Epub 20240731. doi: 10.1038/s41586-024-07748-8. PubMed PMID: 39085605.

## CHAPTER IV: Discussion

The work presented in this thesis studies CD8 tissue resident memory T cells (TRM) in the context of respiratory virus transmission. TRM, a subset of memory T cells that establish residency in the tissue and do not recirculate, have been thoroughly investigated using direct intranasal respiratory virus challenge models, where TRM have been shown to reduce viral burdens and immunopathology<sup>1-3</sup>. However, these models do not recapitulate the true physiological events that occur during respiratory virus infection, where one infected individual transmits virus to another. During natural respiratory virus transmission, a low number of virions, spread from respiratory secretions or contact with a contaminated surface, will posit along the respiratory tract, replicate, and initiate an infection replete with physiological symptoms and pathology<sup>4</sup>. Investigating immunological mechanisms and cellular populations that impact respiratory virus transmission has been historically difficult due to the lack of appropriate animal models and experimental tools. The majority of publications on respiratory viruses that use mice as an experimental model use influenza or more recently SARS-CoV-2 which do not transmit in healthy immune system, adult mice<sup>5-8</sup>. While guinea pigs and ferrets do support transmission of many human respiratory viruses including influenza and SARS-CoV-2, experimental immunological tools, such as MHC tetramers and a wide specificity of fluorescently conjugated antibodies, are not readily available. Additionally, obtaining samples for viral titer analysis of respiratory tract tissues necessitates destructive sampling and euthanasia. To address this gap in knowledge and investigate the impact of CD8 T cells during transmission, we chose to focus on mouse models and utilized Sendai virus, a parainfluenza virus that transmits naturally by airborne and contact modes.

In Chapter II, we introduce the model used to investigate the role of vaccine-induced CD8 TRM in respiratory virus transmission. Influenza A vectors, an H1N1 PR8 virus and a live

attenuated version, were engineered to encode the H2-K<sup>d</sup> immunodominant CD8<sup>+</sup> T cell epitope, FAPGNYPAL, for the Sendai virus nucleoprotein (SenNP). Following intranasal (i.n.) inoculation with these constructs, a SenNP-specific CD8 T cell response was elicited in the respiratory tract, resulting in central memory, effector memory, and tissue resident memory T cells. Systemic immunization by intraperitoneal (i.p.) injection resulted in similar quantities of central and effector memory CD8 T cells subsets, but no tissue resident memory T cells in the lung or airways. Interestingly, i.p. infection did generate tissue resident memory T cells in the nasal cavity, but significantly fewer than those within i.n. infected mice. It is important to note that immunization with these vectors did not result in any Sendai-specific B cells responses or CD4 T cells. After these immunized contact mice were rested to memory, they were then co-housed with an index mouse infected with the transmissible Sendai virus. A firefly luciferase encoded in the Sendai virus would emit a bioluminescent flux from infected cells when treated with a luciferin substrate. This enabled tracking the course of viral transmission from the index mouse and potential infection of the contact mice through *in vivo* imaging.

Our findings show that TRM can prevent infection from transmission by significantly reducing the probability of infection. Additionally, the handful of animals that did become infected had significantly lower viral burdens than controls. While T cell mediated immunity is not sterilizing and requires cells to become infected to present antigen on MHC-I (excluding possible cross presentation), TRM extinguished any initial infection events to prevent the establishment of a full-scale infection, as detectable by our analytical methods. Interestingly, i.p. primed mice were not protected against transmission and had no difference in viral burden or probability of infection compared to the vector control, indicating that central and effector memory CD8 T cells did not contribute to the reduction in transmission in our model.

After demonstrating that CD8 TRM protect against respiratory virus transmission, we asked which CD8 TRM effector mechanisms were responsible. We evaluated the contributions of Perforin/Granzyme mediated cellular cytotoxicity, Fas-FasL cell death, and IFN- $\gamma$  signaling. While cytolytic capacity from Perforin/Granzyme and Fas-FasL was dispensable, IFN- $\gamma$  signaling was required. These findings align with a recent publication demonstrating that T cell secreted IFN- $\gamma$  mediated protection against heterologous SARS-CoV-2 aerosolized infection<sup>9</sup>. To investigate how TRM-secreted IFN- $\gamma$  was impacting the local cellular microenvironment during transmission, we turned to a peptide dosing model where *WT* and *Ifng*<sup>-/-</sup> mice were dosed intranasally with SenNP peptide to activate resident T cells. RNA sequencing results revealed that IFN- $\gamma$  signaling induced antiviral transcriptional programs associated with the induction of interferon stimulated genes and increased antigen presentation in nasal cavity epithelial cells. These findings were confirmed at the protein level by flow cytometry, illustrating a stark increase of MHC-I and MHC-II expression that was dependent on IFN- $\gamma$ . Taken together, these data demonstrate that respiratory tract TRM rapidly produce IFN- $\gamma$  which initiates antiviral programming in the nasal microenvironment to prevent respiratory virus transmission. As such, IFN- $\gamma$  could serve as a potential biomarker of vaccine efficacy for transmission prevention.

When assessing the potential of a T cell mediated vaccine, an important question to consider is the durability of the response. Previous studies have shown that TRM in the lung and BAL decline over time, resulting in a loss of heterosubtypic immunity<sup>10,11</sup>. Interestingly, TRM numbers in the nasal cavity remain relatively stable over time, a finding corroborated by this study<sup>12</sup>. To assess the durability of TRM-mediated protection against transmission, cohorts of mice were primed with various -SenNP expressing vectors, rested for 6 months, and challenged with Sendai-Luciferase transmission. After influenza vector based -SenNP immunization, protection against

transmission declined between 1 month and 6 months but did not reach control levels of transmission. In contrast, adenoviral vector -SenNP vaccinated mice were completely protected against transmission at both 1 month and 6 month timepoints. This was attributed to the ability of adenoviral vector immunization to maintain TRM populations throughout the respiratory tract over time. Previous studies from the lab have demonstrated that intranasal delivery of adenoviral vectors results in long-lived antigen depot formation in alveolar macrophages which provides necessary TCR stimulation to maintain TRM in the BAL and lung<sup>13, 14</sup>. To develop a T cell-based vaccines for humans, selecting the appropriate immunization that enables maintenance of TRM populations over time is critical. These findings demonstrate that protection against transmission is dependent on the number of TRM present in the respiratory tract, and that intranasal vaccine induced TRM have the potential to provide long-lasting protection against viral transmission. Not only did the data presented in this chapter illustrate that CD8 TRM can prevent the establishment of infection during respiratory virus transmission, but this data also showed that this protection was dependent on IFN- $\gamma$  and durable for at least 6 months. Overall, the data in this chapter highlight the importance of mucosal T cell responses against respiratory viruses and support the continued development of T cell-mediated vaccines to prevent respiratory virus transmission among populations.

In Chapter III, we investigate the localization of the T cell response during respiratory virus transmission and identify which anatomical TRM populations are required to prevent transmission. When designing an intranasal vaccine for human use, it is necessary to understand which immune cell populations should be generated to induce maximal protection against transmission. While many intranasal vaccine studies have focused on the lung as a site of protection, many raise concerns over the feasibility of generating lung resident T cells in humans. Unlike other tissue

sites, lung TRM formation requires local antigen delivery, which may necessitate administration of large liquid volumes to human vaccine recipients and subsequent discomfort. The role of upper respiratory tract (URT) or nasal cavity TRM has been understudied, but recent evidence has highlighted their importance in SARS-CoV-2 immunity. Here, we seek to investigate which TRM populations are necessary to prevent respiratory virus transmission by first identifying the location of T cell activation during transmission. Using Nur77<sup>GFP</sup> reporter mice and EdU labelling, we demonstrate that antigen-specific TRM in the nasal cavity, but not the lung or the BAL, become activated and proliferate in response to transmitted Sendai-Luc. Supporting these findings, we show that nasal cavity TRM transition to activated effector states and adopt antiviral transcriptional programs using single cell RNA sequencing and RNA velocity approaches. These findings suggested that the nasal cavity was an important site involved in the immune response to transmission. To test whether nasal cavity TRM alone were sufficient to protect against transmission, we used a low volume infection approach with our adenoviral vector to generate solely nasal cavity TRM, without eliciting SenNP-specific lung or BAL responses, and challenged the mice with Sendai-Luciferase transmission. Nasal cavity TRM alone were largely sufficient to protect against transmission, with a small number of breakthrough infections localizing in the trachea region. Overall, these findings establish the nasal cavity, or URT, as an essential site for immune surveillance to prevent the establishment of infection in a transmission model. Future intranasal vaccine strategies should focus on generating URT resident memory CD8 T cells to prevent infection, with lung TRM as a secondary consideration for severe disease prevention.

## Outstanding Questions

### *Loss of Nasal Cavity TRM Functionality*

One interesting observation from the 6-month timepoint transmission experiment was that while nasal cavity TRM numbers did not decline over time, the protection against transmission was reduced (with the exception of adenoviral vector immunization). There are several potential explanations for this discrepancy that should be addressed in future studies to better understand the requirements for TRM-mediated protection against transmission. It is well known that T cells can become “exhausted” under chronic antigenic stimulation and lose functional capacity, characterized by the expression of *Tox*, *Tcf1*, PD-1, TIM-3, and LAG-3<sup>15-17</sup>. Interestingly, TRM share some of these features with exhausted cells, particularly PD-1 expression<sup>18,19</sup>. Whether nasal cavity TRM can become exhausted and lose functionality over time has not been explored. If nasal cavity TRM resist apoptosis and do not re-circulate, they may be subject to undergoing exhaustion from chronic signals in the tissue. In the single cell RNA sequencing data presented in Chapter III, a cluster of SenNP+ CD8 T cells expressing *Tox* and *Tcf1* was identified, suggesting that a subset of nasal cavity T cells may be adopting an exhaustion-like transcriptional program. A decrease in nasal cavity TRM functionality could explain why protection against transmission declined over time, while TRM numbers remained relatively stable.

### *Nasal Cavity TRM Maintenance*

Potential exhaustion of nasal cavity TRM over time raises questions regarding the maintenance of TRM at this site. TRM can be maintained either by prolonged survival without apoptosis, self-proliferation, or by an influx and subsequent differentiation of circulating CD8 T cells into TRM, depending on the local microenvironment and factors required for TRM

establishment<sup>20, 21</sup>. Previous studies from the lab demonstrated that adenoviral vector immunization facilitated TRM maintenance by providing sufficient persistent antigen to draw circulating T cells into the lung and promote their proliferation and differentiation into TRM, balancing out the rate of apoptosis at that site<sup>13, 14</sup>. Without sources of antigen for this continual recruitment, lung and airway TRM underwent metabolic starvation and apoptosis, resulting in an overall decline in cell numbers<sup>10</sup>. In contrast, skin TRM, which do not require local antigen recognition for formation and do not decline in number over time, seem to largely resist apoptosis and persist through continual fatty acid oxidation and IL-23 and IL-15 cytokine stimulation<sup>22-24</sup>. The mechanisms and signals that enable nasal cavity TRM cell maintenance are largely unknown, although one study shows that nasal cavity TRM persist with minimal replenishment from circulating cells<sup>12</sup>. It would also be interesting to determine how nasal cavity TRM maintenance differs under various vaccine scenarios, for example whether adenoviral vector vaccination maintains nasal cavity TRM by the same mechanisms as influenza vectored vaccination. Whether antigen sources or depots exist and persist in the nasal cavity, potentially providing chronic antigenic stimulation for exhaustion, is also unknown. One preliminary experiment using a Cre recombinase expressing adenovirus vaccination in Ai14 reporter mice did not illuminate a source of antigen persistence in the nasal cavity (data not shown). However, further experimentation is needed. Understanding how nasal cavity TRM are maintained would inform effective vaccine design for long-lived nasal cavity TRM-mediated protection against transmission.

#### *Localization of T Cells within Nasal Cavity*

Another unexplored hypothesis relevant to this dissertation is that TRM in different compartments of the nasal cavity may behave differently. The nasal cavity is highly heterogenous, consisting of the nasal turbinates, septum, maxillary sinuses, and nasal associated lymphoid tissue,

as well as separate regions of respiratory and olfactory epithelium<sup>25-27</sup>. Where specifically TRM form within the nasal cavity is largely unknown, although one study identified adoptively transferred OT-I cells throughout the nasal tissue of influenza infected mice<sup>12</sup>. It is possible that TRM responding to transmission are localized closer to the conducting airways where they are more likely to encounter inhaled virus particles. Due to the unique microenvironment and lower temperature caused by exposure to air, TRM at these sites may have different qualities than those lodged deeper within the tissue in terms of their longevity, maintenance, and function. Future studies should utilize microscopy and spatial transcriptomics approaches to identify the specific locations of nasal cavity TRM activation during respiratory virus transmission and investigate any differences in their functions.

#### *Nasal Cavity TRM from Systemic vs. Intranasal Vaccination*

Data presented in Chapter II assessed the protection against transmission induced by systemic intraperitoneal (i.p.) vaccination and mucosal intranasal (i.n.) vaccination. I.p. vaccination did not provide any significant level of protection as seen by total viral burden or probability of infection compared to the control group. On the other hand, the i.n. infection group had few breakthrough infections with lower viral burden. This finding was surprising given the antigen-specific T cell responses induced by each route of vaccination. While i.p. vaccination did not generate any lung or BAL TRM as expected, both routes generated TRM in the nasal cavity, albeit the cell number was significantly less in the i.p. group than the i.n. group. The data in Chapter III illustrates that the nasal cavity is the principal site of the T cell response to transmission. Based on these findings, we would expect an intermediate level of protection against transmission afforded by the number of nasal cavity TRM generated by i.p. vaccination. This raises several interesting questions regarding nasal cavity TRM generated by i.p. immunization. Do TRM

elicited by i.n. and i.p. vaccination differ in their functional profiles, their ability to secrete cytokines, especially IFN- $\gamma$ , proliferation capacity, or ability to eliminate infected cells by cytotoxic activity? Do they have a similar antigenic threshold for activation? Could nasal cavity TRM from i.p. immunization be located in different regions of the nasal cavity tissue, perhaps those located further away from the conducting airways, as opposed to those from i.n. immunization? Are nasal cavity TRM from i.p. and i.n. infection primed similarly in terms of which secondary lymphoid organs and antigen presenting cells are involved, and the signals they impart during CD8 T cell activation? These are all important questions to address for future studies.

#### *CD8 TRM Effector Mechanisms Under Different Vaccination Scenarios*

In Chapter II, we demonstrated that IFN- $\gamma$  signaling was required to prevent transmission, as IFN- $\gamma$  induced antiviral transcriptional programming and increased antigen presentation in nasal cavity epithelial cells. These findings were based off of LAIV-SenNP vaccination which induced a significantly lower number of -SenNP specific TRM throughout the respiratory tract compared to Ad-SenNP or PR8-SenNP immunization. When *Ifng*<sup>-/-</sup> mice were vaccinated with Ad-SenNP and challenged with Sendai-Luc transmission, they were completely protected from transmission and no breakthrough infections were observed (data not shown). This suggests that when a sufficiently large number of TRM are present, other effector mechanisms, likely cytotoxic cell death pathways, are able to compensate for the loss of IFN- $\gamma$ . We hypothesize that when a large number of TRM are present and lining the respiratory mucosa, TRM are able to immediately eliminate any infected cells, negating the need for IFN- $\gamma$  mediated activation of neighboring epithelial cells in preparation of an amplifying infection. However, when TRM are sparser throughout the respiratory mucosa, IFN- $\gamma$  is needed to “bide time” for the existing TRM to proliferate and migrate to infected cells, or for an influx of circulating effector CD8 T cells to

eliminate the breakthrough infection. It will be interesting for future studies to confirm experimentally which CD8 TRM effector mechanisms are required to prevent transmission and which effectors mechanisms can compensate for others when varying levels of TRM are present in the respiratory tract.

### **Implications for Vaccines to Prevent Respiratory Virus Transmission**

Adenoviral vector vaccination emerged as a highly attractive vaccine platform for the prevention of respiratory virus transmission from the work presented in this thesis. We showed that intranasal adenoviral vector immunization elicits a high number of antigen-specific tissue resident memory CD8 T cells and maintains these cellular populations throughout the respiratory tract for an extended period of time, providing prolonged protection. Several intramuscularly administered Ad-vectored vaccines were produced and approved by international regulatory bodies during the SARS-CoV-2 pandemic. Although these Ad-vectored vaccines were effective at preventing severe disease from SARS-CoV-2, they were ultimately removed from the market due to extremely rare incidents of vaccine-induced thrombotic thrombocytopenia<sup>28, 29</sup>. While the adenoviral vector SARS-CoV-2 vaccines did induce spike-spike specific IgG and T cell responses in the blood, one study showed that this only marginally decreased lung pathology and respiratory tract viral titers in SARS-CoV-2 challenged nonhuman primates<sup>30, 31</sup>. In contrast, intranasal delivery of Ad-vectored vaccines elicited robust antigen-specific IgA and IgG responses as well as tissue resident memory B and T cells in both the upper and lower respiratory tract of nonhuman primates<sup>32, 33</sup>. Immune responses and protection from infection was superior when a SARS-CoV-2 Ad-vectored vaccine was administered intranasally as opposed to intramuscularly<sup>34-36</sup>. Of course, to bring intranasal Ad-vector vaccines to the clinic, more research is needed on possible

adverse events and strategies to prevent their occurrence. In combination with the data presented in this thesis, these studies highlight the potential for intranasally administered adenoviral vectored vaccines to provide durable immunity and prevent respiratory virus transmission, supporting their continued investigation and development.

Respiratory virus transmission in humans can occur by direct contact, fomite, droplet or aerosol routes<sup>4</sup>. The study in this thesis used a mouse model of direct, continuous contact, where transmission could occur by any of the aforementioned routes<sup>37</sup>. However, our experiments suggest that the localization of the immune response may differ depending on the mode of transmission. It will be important for future studies to discern not only which tissue locations require immune surveillance given a particular route of viral transmission, but also which immune correlates of protection or memory responses are associated with each route of transmission. Several groups have been performing controlled human influenza challenge and transmission studies to address these questions<sup>38, 39</sup>. One recent study identified tissue resident memory CD8 T cells and class switched germinal center B cells in nasal swabs of human SARS-CoV-2 vaccine recipients<sup>27</sup>. Such nasal swab sampling strategies in humans challenge and transmission studies will be particularly illuminating into the immune responses induced by vaccination and infection at this critical and understudied site of immune surveillance.

The ideal outcome of vaccination is neutralizing antigen-specific IgG or IgA antibodies that prevent viral particles from entering and infecting cells, while CD8 T cell mediated immunity generally requires that a handful of cells become infected and present antigen on MHC-I to activate those CD8 T cells. As this thesis focuses on tissue resident memory CD8 T cells, further research is needed to decipher the contributions of tissue resident memory CD4 T cells and resident memory B cells (BRM), particularly in the nasal mucosa, to protection against viral transmission. Although

less is known about respiratory tract CD4 TRM, key studies have demonstrated their capacity to regulate lung barrier immunity and secrete cytokines to aid B cell class switching<sup>40-42</sup>. A recent preprint identifies influenza specific CD4 TRM in the nasal mucosa of mice and humans, and illustrates their ability to provide heterosubtypic influenza protection through cytokine secretion<sup>43</sup>. Similarly, resident memory B cells capable of producing IgA have been identified in human and mouse respiratory tract tissues and are protective in influenza virus and bacterial challenge models<sup>27, 44-46</sup>. More studies are needed to assess the roles of CD4 TRM and BRM in preventing respiratory virus transmission and to evaluate the interplay between these cellular populations with CD8 TRM.

The work presented in this thesis demonstrates that intranasal vaccine induced tissue resident memory CD8 T cells can provide sufficient immune surveillance to prevent infection from natural respiratory virus transmission. This has been a long-standing and elusive question in the respiratory virus field due to the lack of an appropriate model system. Not only does this work introduce a novel experimental mouse model and demonstrate the ability of intranasal T cell mediated vaccines to protect against transmission, but it also characterizes this protection in terms of its durability, localization, and requisite effector mechanisms. Engaging the T cell arm of the immune response is essential to complement B cell mediated neutralizing antibody responses. These findings hold significant translational impact for the development of vaccines that provide cross protection against mutating and emerging viral strains and prevent the spread of respiratory viruses on the population level.

## References

1. Slutter B, Pewe LL, Kaech SM, Harty JT. Lung airway-surveilling CXCR3(hi) memory CD8(+) T cells are critical for protection against influenza A virus. *Immunity*. 2013;39(5):939-48. doi: 10.1016/j.immuni.2013.09.013. PubMed PMID: 24238342; PMCID: PMC3872058.
2. Zheng MZM, Wakim LM. Tissue resident memory T cells in the respiratory tract. *Mucosal Immunol*. 2022;15(3):379-88. Epub 20211020. doi: 10.1038/s41385-021-00461-z. PubMed PMID: 34671115; PMCID: PMC8526531.
3. Wu T, Hu Y, Lee YT, Bouchard KR, Benechet A, Khanna K, Cauley LS. Lung-resident memory CD8 T cells (TRM) are indispensable for optimal cross-protection against pulmonary virus infection. *J Leukoc Biol*. 2014;95(2):215-24. Epub 20130904. doi: 10.1189/jlb.0313180. PubMed PMID: 24006506; PMCID: PMC3896663.
4. Leung NHL. Transmissibility and transmission of respiratory viruses. *Nat Rev Microbiol*. 2021;19(8):528-45. Epub 20210322. doi: 10.1038/s41579-021-00535-6. PubMed PMID: 33753932; PMCID: PMC7982882.
5. Bouvier NM, Lowen AC. Animal Models for Influenza Virus Pathogenesis and Transmission. *Viruses*. 2010;2(8):1530-63. doi: 10.3390/v20801530. PubMed PMID: 21442033; PMCID: PMC3063653.

6. Pan T, Chen R, He X, Yuan Y, Deng X, Li R, Yan H, Yan S, Liu J, Zhang Y, Zhang X, Yu F, Zhou M, Ke C, Ma X, Zhang H. Infection of wild-type mice by SARS-CoV-2 B.1.351 variant indicates a possible novel cross-species transmission route. *Signal Transduct Target Ther.* 2021;6(1):420. Epub 20211214. doi: 10.1038/s41392-021-00848-1. PubMed PMID: 34907154; PMCID: PMC8669038.
7. Bao L, Gao H, Deng W, Lv Q, Yu H, Liu M, Yu P, Liu J, Qu Y, Gong S, Lin K, Qi F, Xu Y, Li F, Xiao C, Xue J, Song Z, Xiang Z, Wang G, Wang S, Liu X, Zhao W, Han Y, Wei Q, Qin C. Transmission of Severe Acute Respiratory Syndrome Coronavirus 2 via Close Contact and Respiratory Droplets Among Human Angiotensin-Converting Enzyme 2 Mice. *J Infect Dis.* 2020;222(4):551-5. doi: 10.1093/infdis/jiaa281. PubMed PMID: 32444876; PMCID: PMC7313959.
8. Zhang C, Cui H, Li E, Guo Z, Wang T, Yan F, Liu L, Li Y, Chen D, Meng K, Li N, Qin C, Liu J, Gao Y, Zhang C. The SARS-CoV-2 B.1.351 Variant Can Transmit in Rats But Not in Mice. *Front Immunol.* 2022;13:869809. Epub 20220428. doi: 10.3389/fimmu.2022.869809. PubMed PMID: 35572504; PMCID: PMC9095975.
9. Fumagalli V, Rava M, Marotta D, Di Lucia P, Bono EB, Giustini L, De Leo F, Casalgrandi M, Monteleone E, Mouro V, Malpighi C, Perucchini C, Grillo M, De Palma S, Donnici L, Marchese S, Conti M, Muramatsu H, Perlman S, Pardi N, Kuka M, De Francesco R, Bianchi ME, Guidotti LG, Iannaccone M. Antibody-independent protection against heterologous SARS-CoV-2 challenge conferred by prior infection or vaccination. *Nat Immunol.*

2024;25(4):633-43. Epub 20240314. doi: 10.1038/s41590-024-01787-z. PubMed PMID: 38486021; PMCID: PMC11003867.

10. Hayward SL, Scharer CD, Cartwright EK, Takamura S, Li ZT, Boss JM, Kohlmeier JE. Environmental cues regulate epigenetic reprogramming of airway-resident memory CD8(+) T cells. *Nat Immunol.* 2020;21(3):309-20. Epub 20200117. doi: 10.1038/s41590-019-0584-x. PubMed PMID: 31953534; PMCID: PMC7044042.

11. Slutter B, Van Braeckel-Budimir N, Abboud G, Varga SM, Salek-Ardakani S, Harty JT. Dynamics of influenza-induced lung-resident memory T cells underlie waning heterosubtypic immunity. *Sci Immunol.* 2017;2(7). Epub 20170106. doi: 10.1126/sciimmunol.aag2031. PubMed PMID: 28783666; PMCID: PMC5590757.

12. Pizzolla A, Nguyen THO, Smith JM, Brooks AG, Kedzieska K, Heath WR, Reading PC, Wakim LM. Resident memory CD8(+) T cells in the upper respiratory tract prevent pulmonary influenza virus infection. *Sci Immunol.* 2017;2(12). doi: 10.1126/sciimmunol.aam6970. PubMed PMID: 28783656.

13. Lobby JL, Uddback I, Scharer CD, Mi T, Boss JM, Thomsen AR, Christensen JP, Kohlmeier JE. Persistent Antigen Harbored by Alveolar Macrophages Enhances the Maintenance of Lung-Resident Memory CD8(+) T Cells. *J Immunol.* 2022;209(9):1778-87. Epub 20220926. doi: 10.4049/jimmunol.2200082. PubMed PMID: 36162870; PMCID: PMC9588742.

14. Uddback I, Cartwright EK, Scholler AS, Wein AN, Hayward SL, Lobby J, Takamura S, Thomsen AR, Kohlmeier JE, Christensen JP. Long-term maintenance of lung resident memory T cells is mediated by persistent antigen. *Mucosal Immunol.* 2021;14(1):92-9. Epub 20200609. doi: 10.1038/s41385-020-0309-3. PubMed PMID: 32518368; PMCID: PMC7726002.
  
15. Cardenas MA, Prokhnevskaya N, Sobierajska E, Gregorova P, Medina CB, Valanparambil RM, Greenwald R, DelBalzo L, Bilen MA, Joshi SS, Narayan VM, Master VA, Sanda MG, Kissick HT. Differentiation fate of a stem-like CD4 T cell controls immunity to cancer. *Nature.* 2024. Epub 20241023. doi: 10.1038/s41586-024-08076-7. PubMed PMID: 39443797.
  
16. Blank CU, Haining WN, Held W, Hogan PG, Kallies A, Lugli E, Lynn RC, Philip M, Rao A, Restifo NP, Schietinger A, Schumacher TN, Schwartzberg PL, Sharpe AH, Speiser DE, Wherry EJ, Youngblood BA, Zehn D. Defining 'T cell exhaustion'. *Nat Rev Immunol.* 2019;19(11):665-74. Epub 20190930. doi: 10.1038/s41577-019-0221-9. PubMed PMID: 31570879; PMCID: PMC7286441.
  
17. Khan O, Giles JR, McDonald S, Manne S, Ngiow SF, Patel KP, Werner MT, Huang AC, Alexander KA, Wu JE, Attanasio J, Yan P, George SM, Bengsch B, Staupe RP, Donahue G, Xu W, Amaravadi RK, Xu X, Karakousis GC, Mitchell TC, Schuchter LM, Kaye J, Berger SL, Wherry EJ. TOX transcriptionally and epigenetically programs CD8(+) T cell exhaustion. *Nature.* 2019;571(7764):211-8. Epub 20190617. doi: 10.1038/s41586-019-1325-x. PubMed PMID: 31207603; PMCID: PMC6713202.

18. Wang Z, Wang S, Goplen NP, Li C, Cheon IS, Dai Q, Huang S, Shan J, Ma C, Ye Z, Xiang M, Limper AH, Porquera EC, Kohlmeier JE, Kaplan MH, Zhang N, Johnson AJ, Vassallo R, Sun J. PD-1(hi) CD8(+) resident memory T cells balance immunity and fibrotic sequelae. *Sci Immunol.* 2019;4(36). doi: 10.1126/sciimmunol.aaw1217. PubMed PMID: 31201259; PMCID: PMC7458867.
19. Hombrink P, Helbig C, Backer RA, Piet B, Oja AE, Stark R, Brassler G, Jongejan A, Jonkers RE, Nota B, Basak O, Clevers HC, Moerland PD, Amsen D, van Lier RA. Erratum: Programs for the persistence, vigilance and control of human CD8(+) lung-resident memory T cells. *Nat Immunol.* 2017;18(2):246. doi: 10.1038/ni0217-246d. PubMed PMID: 28102212.
20. Yenyuwadee S, Sanchez-Trincado Lopez JL, Shah R, Rosato PC, Boussiotis VA. The evolving role of tissue-resident memory T cells in infections and cancer. *Sci Adv.* 2022;8(33):eabo5871. Epub 20220817. doi: 10.1126/sciadv.abo5871. PubMed PMID: 35977028; PMCID: PMC9385156.
21. Schenkel JM, Masopust D. Tissue-resident memory T cells. *Immunity.* 2014;41(6):886-97. Epub 20141206. doi: 10.1016/j.immuni.2014.12.007. PubMed PMID: 25526304; PMCID: PMC4276131.
22. Zaid A, Mackay LK, Rahimpour A, Braun A, Veldhoen M, Carbone FR, Manton JH, Heath WR, Mueller SN. Persistence of skin-resident memory T cells within an epidermal niche.

Proc Natl Acad Sci U S A. 2014;111(14):5307-12. Epub 20140324. doi:

10.1073/pnas.1322292111. PubMed PMID: 24706879; PMCID: PMC3986170.

23. Whitley SK, Li M, Kashem SW, Hirai T, Igyarto BZ, Knizner K, Ho J, Ferris LK, Weaver CT, Cua DJ, McGeachy MJ, Kaplan DH. Local IL-23 is required for proliferation and retention of skin-resident memory T(H)17 cells. *Sci Immunol.* 2022;7(77):eabq3254. Epub 20221111. doi: 10.1126/sciimmunol.abq3254. PubMed PMID: 36367947; PMCID: PMC9847353.

24. Pan Y, Tian T, Park CO, Lofftus SY, Mei S, Liu X, Luo C, O'Malley JT, Gehad A, Teague JE, Divito SJ, Fuhlbrigge R, Puigserver P, Krueger JG, Hotamisligil GS, Clark RA, Kupper TS. Survival of tissue-resident memory T cells requires exogenous lipid uptake and metabolism. *Nature.* 2017;543(7644):252-6. Epub 20170220. doi: 10.1038/nature21379. PubMed PMID: 28219080; PMCID: PMC5509051.

25. Pizzolla A, Wang Z, Groom JR, Kedzierska K, Brooks AG, Reading PC, Wakim LM. Nasal-associated lymphoid tissues (NALTs) support the recall but not priming of influenza virus-specific cytotoxic T cells. *Proc Natl Acad Sci U S A.* 2017;114(20):5225-30. Epub 20170501. doi: 10.1073/pnas.1620194114. PubMed PMID: 28461487; PMCID: PMC5441821.

26. Sobiesk JL, Munakomi S. Anatomy, Head and Neck, Nasal Cavity. *StatPearls.* Treasure Island (FL)2024.

27. Ramirez SI, Faraji F, Hills LB, Lopez PG, Goodwin B, Stacey HD, Sutton HJ, Hastie KM, Saphire EO, Kim HJ, Mashoof S, Yan CH, DeConde AS, Levi G, Crotty S. Immunological memory diversity in the human upper airway. *Nature*. 2024;632(8025):630-6. Epub 20240731. doi: 10.1038/s41586-024-07748-8. PubMed PMID: 39085605.
28. Mendonca SA, Lorincz R, Boucher P, Curiel DT. Adenoviral vector vaccine platforms in the SARS-CoV-2 pandemic. *NPJ Vaccines*. 2021;6(1):97. Epub 20210805. doi: 10.1038/s41541-021-00356-x. PubMed PMID: 34354082; PMCID: PMC8342436.
29. Greinacher A, Thiele T, Warkentin TE, Weisser K, Kyrle PA, Eichinger S. Thrombotic Thrombocytopenia after ChAdOx1 nCov-19 Vaccination. *N Engl J Med*. 2021;384(22):2092-101. Epub 20210409. doi: 10.1056/NEJMoa2104840. PubMed PMID: 33835769; PMCID: PMC8095372.
30. Ryan FJ, Norton TS, McCafferty C, Blake SJ, Stevens NE, James J, Eden GL, Tee YC, Benson SC, Masavuli MG, Yeow AEL, Abayasingam A, Agapiou D, Stevens H, Zecha J, Messina NL, Curtis N, Ignjatovic V, Monagle P, Tran H, McFadyen JD, Bull RA, Grubor-Bauk B, Lynn MA, Botten R, Barry SE, Lynn DJ. A systems immunology study comparing innate and adaptive immune responses in adults to COVID-19 mRNA and adenovirus vectored vaccines. *Cell Rep Med*. 2023;4(3):100971. Epub 20230217. doi: 10.1016/j.xcrm.2023.100971. PubMed PMID: 36871558; PMCID: PMC9935276.

31. Lambe T, Spencer AJ, Thomas KM, Gooch KE, Thomas S, White AD, Humphries HE, Wright D, Belij-Rammerstorfer S, Thakur N, Conceicao C, Watson R, Alden L, Allen L, Aram M, Bewley KR, Brunt E, Brown P, Cavell BE, Cobb R, Fotheringham SA, Gilbride C, Harris DJ, Ho CMK, Hunter L, Kennard CL, Leung S, Lucas V, Ngabo D, Ryan KA, Sharpe H, Sarfas C, Sibley L, Slack GS, Ulaszewska M, Wand N, Wiblin NR, Gleeson FV, Bailey D, Sharpe S, Charlton S, Salguero FJ, Carroll MW, Gilbert SC. ChAdOx1 nCoV-19 protection against SARS-CoV-2 in rhesus macaque and ferret challenge models. *Commun Biol.* 2021;4(1):915. Epub 20210726. doi: 10.1038/s42003-021-02443-0. PubMed PMID: 34312487; PMCID: PMC8313674.
32. Gagne M, Flynn BJ, Andrew SF, Marquez J, Flebbe DR, Mychalowych A, Lamb E, Davis-Gardner ME, Burnett MR, Serebryanny LA, Lin BC, Ziff ZE, Maule E, Carroll R, Naisan M, Jethmalani Y, Pessaint L, Todd JM, Doria-Rose NA, Case JB, Dmitriev IP, Kashentseva EA, Ying B, Dodson A, Kouneski K, O'Dell S, Wali B, Ellis M, Godbole S, Laboune F, Henry AR, Teng IT, Wang D, Wang L, Zhou Q, Zouantchangadou S, Van Ry A, Lewis MG, Andersen H, Kwong PD, Curiel DT, Roederer M, Nason MC, Foulds KE, Suthar MS, Diamond MS, Douek DC, Seder RA. Mucosal adenovirus vaccine boosting elicits IgA and durably prevents XBB.1.16 infection in nonhuman primates. *Nat Immunol.* 2024;25(10):1913-27. Epub 20240903. doi: 10.1038/s41590-024-01951-5. PubMed PMID: 39227514; PMCID: PMC11436372.
33. Moliva JI, Andrew SF, Flynn BJ, Wagner DA, Foulds KE, Gagne M, Flebbe DR, Lamb E, Provost S, Marquez J, Mychalowych A, Lorag CG, Honeycutt CC, Burnett MR, McCormick

L, Henry AR, Godbole S, Davis-Gardner ME, Minai M, Bock KW, Nagata BM, Todd JM, McCarthy E, Dodson A, Kouneski K, Cook A, Pessaint L, Ry AV, Valentin D, Young S, Littman Y, Boon ACM, Suthar MS, Lewis MG, Andersen H, Alves DA, Woodward R, Leuzzi A, Vitelli A, Colloca S, Folgori A, Raggiolli A, Capone S, Nason MC, Douek DC, Roederer M, Seder RA, Sullivan NJ. Durable immunity to SARS-CoV-2 in both lower and upper airways achieved with a gorilla adenovirus (GRAd) S-2P vaccine in non-human primates. *bioRxiv*. 2023. Epub 20231122. doi: 10.1101/2023.11.22.567930. PubMed PMID: 38076895; PMCID: PMC10705562.

34. Afkhami S, D'Agostino MR, Zhang A, Stacey HD, Marzok A, Kang A, Singh R, Bavananthasivam J, Ye G, Luo X, Wang F, Ang JC, Zganiacz A, Sankar U, Kazhdan N, Koenig JFE, Phelps A, Gameiro SF, Tang S, Jordana M, Wan Y, Mossman KL, Jeyanathan M, Gillgrass A, Medina MFC, Smaill F, Lichty BD, Miller MS, Xing Z. Respiratory mucosal delivery of next-generation COVID-19 vaccine provides robust protection against both ancestral and variant strains of SARS-CoV-2. *Cell*. 2022;185(5):896-915 e19. Epub 20220209. doi: 10.1016/j.cell.2022.02.005. PubMed PMID: 35180381; PMCID: PMC8825346.

35. Hassan AO, Kafai NM, Dmitriev IP, Fox JM, Smith BK, Harvey IB, Chen RE, Winkler ES, Wessel AW, Case JB, Kashentseva E, McCune BT, Bailey AL, Zhao H, VanBlargan LA, Dai YN, Ma M, Adams LJ, Shrihari S, Danis JE, Gralinski LE, Hou YJ, Schafer A, Kim AS, Keeler SP, Weiskopf D, Baric RS, Holtzman MJ, Fremont DH, Curiel DT, Diamond MS. A Single-Dose Intranasal ChAd Vaccine Protects Upper and Lower Respiratory Tracts against

SARS-CoV-2. *Cell*. 2020;183(1):169-84 e13. Epub 20200819. doi: 10.1016/j.cell.2020.08.026.

PubMed PMID: 32931734; PMCID: PMC7437481.

36. van Doremalen N, Purushotham JN, Schulz JE, Holbrook MG, Bushmaker T, Carmody A, Port JR, Yinda CK, Okumura A, Saturday G, Amanat F, Krammer F, Hanley PW, Smith BJ, Lovaglio J, Anzick SL, Barbian K, Martens C, Gilbert SC, Lambe T, Munster VJ. Intranasal ChAdOx1 nCoV-19/AZD1222 vaccination reduces viral shedding after SARS-CoV-2 D614G challenge in preclinical models. *Sci Transl Med*. 2021;13(607). Epub 20210727. doi: 10.1126/scitranslmed.abh0755. PubMed PMID: 34315826; PMCID: PMC9267380.

37. Burke CW, Bridges O, Brown S, Rahija R, Russell CJ. Mode of parainfluenza virus transmission determines the dynamics of primary infection and protection from reinfection. *PLoS Pathog*. 2013;9(11):e1003786. Epub 20131121. doi: 10.1371/journal.ppat.1003786. PubMed PMID: 24278024; PMCID: PMC3836739.

38. Killingley B, Enstone JE, Gretores J, Gilbert AS, Lambkin-Williams R, Cauchemez S, Katz JM, Booy R, Hayward A, Oxford J, Bridges CB, Ferguson NM, Nguyen Van-Tam JS. Use of a human influenza challenge model to assess person-to-person transmission: proof-of-concept study. *J Infect Dis*. 2012;205(1):35-43. Epub 20111130. doi: 10.1093/infdis/jir701. PubMed PMID: 22131338.

39. Nguyen-Van-Tam JS, Killingley B, Enstone J, Hewitt M, Pantelic J, Grantham ML, Bueno de Mesquita PJ, Lambkin-Williams R, Gilbert A, Mann A, Forni J, Noakes CJ, Levine

MZ, Berman L, Lindstrom S, Cauchemez S, Bischoff W, Tellier R, Milton DK, Consortium E. Minimal transmission in an influenza A (H3N2) human challenge-transmission model within a controlled exposure environment. *PLoS Pathog.* 2020;16(7):e1008704. Epub 20200713. doi: 10.1371/journal.ppat.1008704. PubMed PMID: 32658939; PMCID: PMC7390452.

40. Shenoy AT, Lyon De Ana C, Arafa EI, Salwig I, Barker KA, Korkmaz FT, Ramanujan A, Etesami NS, Soucy AM, Martin IMC, Tilton BR, Hinds A, Goltry WN, Kathuria H, Braun T, Jones MR, Quinton LJ, Belkina AC, Mizgerd JP. Antigen presentation by lung epithelial cells directs CD4(+) T(RM) cell function and regulates barrier immunity. *Nat Commun.* 2021;12(1):5834. Epub 20211005. doi: 10.1038/s41467-021-26045-w. PubMed PMID: 34611166; PMCID: PMC8492657.

41. Son YM, Cheon IS, Wu Y, Li C, Wang Z, Gao X, Chen Y, Takahashi Y, Fu YX, Dent AL, Kaplan MH, Taylor JJ, Cui W, Sun J. Tissue-resident CD4(+) T helper cells assist the development of protective respiratory B and CD8(+) T cell memory responses. *Sci Immunol.* 2021;6(55). doi: 10.1126/sciimmunol.abb6852. PubMed PMID: 33419791; PMCID: PMC8056937.

42. Oja AE, Piet B, Helbig C, Stark R, van der Zwan D, Blaauwgeers H, Remmerswaal EBM, Amsen D, Jonkers RE, Moerland PD, Nolte MA, van Lier RAW, Hombrink P. Trigger-happy resident memory CD4(+) T cells inhabit the human lungs. *Mucosal Immunol.* 2018;11(3):654-67. Epub 20171115. doi: 10.1038/mi.2017.94. PubMed PMID: 29139478.

43. Mathew N, Gailleton, R., Scharf, L., Schon, K., Stromberg, A., Lycke, N., Bemark, M., Tang, K., Angeletti, D. . Nasal tissue-resident memory CD4<sup>+</sup> T cells persist after influenza A virus infection and provide heterosubtypic protection. bioRxiv. 2024. doi: <https://doi.org/10.1101/2024.07.06.602325>.
44. Barker KA, Etesami NS, Shenoy AT, Arafa EI, Lyon de Ana C, Smith NM, Martin IM, Goltry WN, Barron AM, Browning JL, Kathuria H, Belkina AC, Guillon A, Zhong X, Crossland NA, Jones MR, Quinton LJ, Mizgerd JP. Lung-resident memory B cells protect against bacterial pneumonia. *J Clin Invest*. 2021;131(11). doi: 10.1172/JCI141810. PubMed PMID: 34060477; PMCID: PMC8159694.
45. Oh JE, Song E, Moriyama M, Wong P, Zhang S, Jiang R, Strohmeier S, Kleinstein SH, Krammer F, Iwasaki A. Intranasal priming induces local lung-resident B cell populations that secrete protective mucosal antiviral IgA. *Sci Immunol*. 2021;6(66):eabj5129. Epub 20211210. doi: 10.1126/sciimmunol.abj5129. PubMed PMID: 34890255; PMCID: PMC8762609.
46. Tan HX, Juno JA, Esterbauer R, Kelly HG, Wragg KM, Konstandopoulos P, Alcantara S, Alvarado C, Jones R, Starkey G, Wang BZ, Yoshino O, Tiang T, Grayson ML, Opdam H, D'Costa R, Vago A, Austin Liver Transplant Perfusionist G, Mackay LK, Gordon CL, Masopust D, Groom JR, Kent SJ, Wheatley AK. Lung-resident memory B cells established after pulmonary influenza infection display distinct transcriptional and phenotypic profiles. *Sci Immunol*. 2022;7(67):eabf5314. Epub 20220128. doi: 10.1126/sciimmunol.abf5314. PubMed PMID: 35089815.